Chalmers Tekniska Högskola
Institutionen för Vattenbyggnad

Department of Hydraulics Chalmers
University of Technology

Seepage through Earth-fill Dams and Stability Analysis of Downstream Embankment

by

Nahidh Hamid Sharif

Submitted to the School of Civil Engineering, Chalmers University of Technology in partial fulfillment of the degree of Licentiate.

Report Series A:27
ISSN 0348-1050
Address: Department of Hydraulics
Chalmers University of Technology
412 96 Göteborg, Sweden

Göteborg 1997

Tel.: +31 772 10 00
Fax: +31 772 21 28

Seepage through Earth-fill Dams and Stability Analysis of Downstream Embankment

Nahidh Hamid Sharif
Chalmers University of Technology
Department of Hydraulics

Abstract

A two-dimensional fluid-dynamics model is applied to analyze seepage through selected isothermal, saturated porous media. Confined flow domain simulations are treated in order to predict the velocity vector for constant and varied cross-section areas. Darcy-Brinkman and Forchheimer-Brinkman models are applied for selected flow domains. Both the uncoupled and the fully coupled solver methods are used to solve the system of equations for the flow field by using the fluid dynamics analysis package FIDAP (Fluid Dynamics Analysis Package, 1996). The FIDAP 7.61 is a computer program using a discretization method based upon the finite element method (FEM). The numerical solution of the unconfined flow is beyond the scope of this study.

A new analytical solution (Sharif's equation) with the incorporation of the nonlinear flow equation (Forchheimer's equation) is proposed for free surface unconfined flow in porous medium. The solution is compared with the available analytical solutions for free surface flow in a simple rectangular earth dam.

Seepage stability analysis of the soil particles is done in order to make a comparison of the effects of linear and nonlinear flow equations on the formulation of the relationship between the flow velocity and the hydraulic gradient in confined and unconfined flow domains.

Analytical solutions are also used for the chosen flow domains in order to estimate the accuracy of the numerical solutions. No significant differences were observed between the analytical and numerical solutions of the Darcy and Forchheimer models. However, a comparison of the theories of Dupuit and Polubarinova-Kochina showed different analytical solutions for the selected unconfined flow face with phreatic surface. The results of the proposed analytical solution (Sharif's equation) for the free surface were in good agreement with recent work. The effect of the nonlinear resistance term of the proposed solution was obviously in predicting the value of the hydraulic gradient at turbulent flow state. The resultant hydraulic gradient by the new solution differ from that by the available analytical solutions.

For confined flow problems no differences are found between the Darcy-Brinkman and Forchheimer- Brinkman models in numerical solutions for low flow velocities (laminar). However, where a turbulent state dominates the flow domain, for which Darcy's law is not valid, significant differences are found between the linear and

Seepage through Earth-fill Dams and Stability Analysis of Downstream Embankment

Nahidh Hamid Sharif
Chalmers University of Technology
Department of Hydraulics

Abstract

A two-dimensional fluid-dynamics model is applied to analyze seepage through selected isothermal, saturated porous media. Confined flow domain simulations are treated in order to predict the velocity vector for constant and varied cross-section areas. Darcy-Brinkman and Forchheimer-Brinkman models are applied for selected flow domains. Both the uncoupled and the fully coupled solver methods are used to solve the system of equations for the flow field by using the fluid dynamics analysis package FIDAP (Fluid Dynamics Analysis Package, 1996). The FIDAP 7.61 is a computer program using a discretization method based upon the finite element method (FEM). The numerical solution of the unconfined flow is beyond the scope of this study.

A new analytical solution (Sharif's equation) with the incorporation of the nonlinear flow equation (Forchheimer's equation) is proposed for free surface unconfined flow in porous medium. The solution is compared with the available analytical solutions for free surface flow in a simple rectangular earth dam.

Seepage stability analysis of the soil particles is done in order to make a comparison of the effects of linear and nonlinear flow equations on the formulation of the relationship between the flow velocity and the hydraulic gradient in confined and unconfined flow domains.

Analytical solutions are also used for the chosen flow domains in order to estimate the accuracy of the numerical solutions. No significant differences were observed between the analytical and numerical solutions of the Darcy and Forchheimer models. However, a comparison of the theories of Dupuit and Polubarinova-Kochina showed different analytical solutions for the selected unconfined flow face with phreatic surface. The results of the proposed analytical solution (Sharif's equation) for the free surface were in good agreement with recent work. The effect of the nonlinear resistance term of the proposed solution was obviously in predicting the value of the hydraulic gradient at turbulent flow state. The resultant hydraulic gradient by the new solution differ from that by the available analytical solutions.

For confined flow problems no differences are found between the Darcy-Brinkman and Forchheimer- Brinkman models in numerical solutions for low flow velocities (laminar). However, where a turbulent state dominates the flow domain, for which Darcy's law is not valid, significant differences are found between the linear and

Chalmers Tekniska Högskola
Institutionen för Vattenbyggnad

Department of Hydraulics Chalmers
University of Technology

Seepage through Earth-fill Dams and Stability Analysis of Downstream Embankment

by

Nahidh Hamid Sharif

Submitted to the School of Civil Engineering, Chalmers University of Technology in partial fulfillment of the degree of Licentiate.

Report Series A:27 **Göteborg 1997**
ISSN 0348-1050

Address: Department of Hydraulics
Chalmers University of Technology
412 96 Göteborg, Sweden

Tel.: +31 772 10 00
Fax: +31 772 21 28

Acknowledgments

This research work has been carried out at the Department of Hydraulics, School of Civil Engineering, Chalmers University of Technology, under the supervision of Professor Lars Bergdahl, Head of the Department.

The author sincerely thanks Professor Bergdahl for his highly regarded supervision and encouragement. His guidance and advice have provided valuable discussion during the course of this work.

I would also like to thank my colleagues at the Department of Hydraulics for numerous helpful discussions and assistance. Special thanks go to Jens Uwe Friemann for his assistance with the numerical simulations. Special thanks are directed to Dr. Gustavo Perrusquía for his proof reading and suggestions on language.

Finally, I would like to thank my parents and my family for their endless support and encouragement in everything I undertake.

Göteborg, February 1997

Nahidh Hamid Sharif

nonlinear models in both analytical and numerical solutions. Hence, the results verified that Darcy's law is not applicable beyond the limit of $Re > 10$.

Keywords: Porous medium, Seepage, Free surface, Stability analysis, Finite element modeling

Summary

Fluid flow in porous media is a fundamental fluid mechanics problem that is of interest to scientists and researchers in many research fields. Nowadays there is a growing interest in fluid flow through porous media, due to heat transfer and pollutant transport problems (Casamitjana and Roget, 1988; Yu *et al.*, 1991; Mendoza and Zhou, 1992).

An accurate description of the flow field is essential to the design of earth-fill and rock-fill dams. Filter criteria is formulated in terms of the properties of the flow domain. The stability of the downstream slope for an earth-fill dam stipulate a comprehensive study of the seepage flow, position of the phreatic-line and the exit point. Knowledge of the flow field in porous media is also essential to research on environmental problems associated with heat transfer and pollutant transport.

Many studies have been conducted to describe the flow of water through porous media in general. The solution of an appropriate equation, recently published, makes it possible to obtain estimates of pore-water pressure and seepage quantities in practical circumstances.

The finite element method (FEM) has been the main and most widely used numerical procedure in solving seepage problems in porous media, for the past ten years (Desai, 1971). Before the FEM became the most powerful method for solving such partial differential equations, much works had been done in terms of the finite difference method (Desai, 1971; Remson, 1971).

A two-dimensional fluid dynamic model was applied in this work to analyze seepage through selected isothermal, saturated porous media. Confined flow domain simulations were treated in order to predict the velocity vector for constant and varied cross-section areas. Darcy-Brinkman and Forchheimer-Brinkman models were applied for a selected flow domain. Both the uncoupled and the fully coupled solver methods were applied to solve the system of equations for the flow field by using the fluid dynamics analysis package FIDAP [FluId Dynamic Analysis Package, (1996)]. The FIDAP 7.61 is a computer program using a discretization method based upon the finite element method (FEM).

A new analytical solution for free surface unconfined flow in porous medium with the incorporation of the nonlinear Forchheimer equation was proposed in this study to predict the shape of the phreatic line and the exit hydraulic gradient.

Seepage stability analysis of the pore particles was done in order to make a comparison of the effects of linear and nonlinear flow equations on the formulation of the relationship between the flow velocity and the hydraulic gradient in confined and unconfined flow domains.

The flow domain of interest is assumed to be homogeneous and isotropic. The fluid and the solid are in thermal equilibrium. Two averaged quantities are introduced to derive the porous flow equations. In order to maintain consistent boundary conditions at fluid and porous media boundaries, the equations for both the fluid and the porous media are solved in terms of volume averaged quantities. Input files were used for two-dimensional linear, steady-state analysis.

Analytical solutions were formulated for the chosen flow domains in order to estimate the accuracy of the numerical solutions. No significant differences were recognized between the analytical solution and the numerical solution of the Darcy and Forchheimer models.

In comparison between analytical solutions for the unconfined flow with phreatic surface, the results differ for different theories (Dupuit and Polubarinova-Kochina solutions). The results of the proposed solution was in good agreement with recent work. The proposed solution (Sharif's equation), showed obviously the effect of the nonlinear resistance term at different flow states. The predicted exit hydraulic gradient by the proposed solution differ from that of the available analytical solution.

No differences were found between the Darcy-Brinkman and Forchheimer- Brinkman models in numerical solutions for low flow velocities (laminar). However, where a turbulent state dominates the flow domain, for which Darcy's law is not valid, significant differences were found between the linear and nonlinear equations in both analytical and numerical solutions. Hence, the results verified that Darcy's law is not applicable beyond the limit of $\boldsymbol{Re} > 10$. The predicted exit point of the phreatic line was also obtained in the simulation.

CONTENTS Page No.

List of Symbols

Roman letter

A	cross section area
A	a parameter to compensate for the viscosity value in the numerical model of the finite element method
A_c	cross section area of the flow domain
a	a constant in the Forchheimer equation
a_c	a parameter in the Polubarinova-Kochina solution
a	a parameter in the Polubarinova-Kochina solution and has a value between 0-0.5
$\mathbf{B}$	boundary of the descritized domain
B	inertia coefficient in the numerical model
b	a constant in the Forchheimer equation
$\mathbf{b}$	height of the rectangular flow domain
b	a parameter in the Polubarinova-Kochina solution and has a value between 0-0.5
C	a parameter in the Polubarinova-Kochina solution
C	a constant in the cylindrical flow equations
C_1	a constant in the Forchheimer equation for the cylindrical flow domain
C_2	a constant in the Forchheimer equation for the cylindrical flow domain
C_i	experimental coefficient in the Hazan equation
C_p	packing coefficient in the Stokes equation
C_s	product of the packing coefficient in the Stokes equation with experimental coefficient in the Hazan equation
c	a constant in the Forchheimer equation
c_g	constant of the ideal gas
c	a parameter in the Polubarinova-Kochina solution and has a value between 0-1.0
c'	constant of the integration in the general Darcy law
c_1	constant of the integration for the proposed nonlinear free surface flow equation (Sharif's equation)
D	exact solution of the difference equations
D_{15f}	size of the filter particles that hold the base-soil
D_{15b}	size of the base soil particles that filter seeping water
D_{85b}	size of the base soil particles that subjected to seepage force
d	grain diameter
d_t	significant particle size in Solvik formulation for the turbulent hydraulic conductivity
d_{10}	sieve opening diameter where 10% of the tested materials would pass
d_{50}	sieve opening diameter where 50% of the tested materials would pass
E	electric potential
e	void ratio
F	a vector term that includes the effect of the body forces and boundary

	conditions in the solved nonlinear algebraic equations.
F_t	total seepage force in confined saturated flow
F	flow function in the Engelund solution of the nonlinear equation
F	function in the Polubarinova-Kochina solution for a simple rectangular earth dam
F_B	buoyancy force term in the force balance equation for unconfined flow
F_D	drag force term in the force balance equation for unconfined flow
F_f	friction force term in the force balance equation for unconfined flow
F_G	gravity force term in the force balance equation for unconfined flow
F_s	seepage force term in the force balance equation for unconfined flow
f	body force vector term in the numerical model
f_i	body force tensor term in the numerical model
g	gravitational acceleration
g	gravity vector term in the numerical model
G_s	specific gravity of the soil in the stability criteria, ($G_s = \gamma_s/\gamma_w$)
H	total hydraulic head in the Darcy law
H	upstream boundary condition in the Polubarinova-Kochina solution
h	piezometric head in the incompressible Navier-Stokes equation for fluid flow in porous medium
h	elevation above the reference level in the Solvik equation
h	downstream boundary condition in the Polubarinova-Kochina solution
h_1	upstream water head
h_2	downstream water head
h_D	falling head in the Darcy law for the confined flow
h_d	falling head in the Dupuit approximation for the free surface unconfined flow
h_F	falling head in the Forchheimer equation for the confined flow
h_l	falling head in the proposed solution at laminar state
h_P	falling head in the Polubarinova-Kochina solution for the free surface flow in a simple rectangular earth dam
h_S	falling head in the proposed nonlinear solution for the free surface unconfined flow
h_0	exit point elevation of the phreatic line above downstream water level in the Polubarinova-Kochina solution
h_t	falling head in the proposed solution at turbulent state
i	imaginary root of the hodograph function in the Polubarinova-Kochina solution
J	negative hydraulic gradient in the Darcy law
J	hydraulic gradient vector in the general Darcy law
J_e	current density in the flow of electricity equation in a conducting medium
J_D	negative hydraulic gradient in the Darcy solution for the confined radial flow
J_F	negative hydraulic gradient in the Forchheimer solution for the confined radial flow
J_l	negative hydraulic gradient in the proposed solution for the free surface

	unconfined flow at laminar state
J_t	negative hydraulic gradient in the proposed solution for the free surface unconfined flow at turbulent state
J_S	negative hydraulic gradient in the proposed solution for the free surface unconfined flow
J_{exit}	negative exit gradient in the unconfined saturated flow
$J_{critical}$	negative critical hydraulic gradient in the confined saturated flow
$\mathbf{j}$	unit vertical vector in the stability criteria for the confined and unconfined saturated flow
K	hydraulic conductivity or coefficient of permeability for the confined and unconfined free surface flow equations
K_x	hydraulic conductivity in the x-direction
K_y	hydraulic conductivity in the y-direction
K_z	hydraulic conductivity in the z-direction
K_e	electrical conductivity in flow of electricity equation in a conducting medium
K_t	turbulent hydraulic conductivity in the Solvik equation
$\boldsymbol{K_p}$	matrix form of the linear part of equation system in the numerical model
$\boldsymbol{K_{D\text{-}F}}(\mathbf{u})$	matrix form of the nonlinear part of equation system in the numerical model
$K(\xi)$	complete elliptic integral of the first kind in the Polubarinova-Kochina solution for a simple rectangular earth dam
k	physical or intrinsic permeability in the confined and unconfined flow equations
k_x	intrinsic permeability in the x-direction
k_y	intrinsic permeability in the y-direction
k_z	intrinsic permeability in the z-direction
$\boldsymbol{k}$	intrinsic permeability vector in the general Darcy law
k_i	intrinsic permeability tensor in the numerical model
k	a parameter in the Polubarinova-Kochina solution for a simple rectangular earth dam
L	length of the flow domain
l	length of the base of the dam in the Polubarinova-Kochina solution
$\boldsymbol{M}$	matrix form of the inertia terms in the numerical model
$\mathbf{m}$	slope inclination ratio in the Solvik equation
$\boldsymbol{m}$	power of the Forchheimer term in the numerical model
m	power of the quadratic resistance term in the confined and unconfined flow equations
N	number of the nodes in the finite difference method
N	numerical solution of the difference equations
n	porosity
n	number of the iterations in the finite element solution
$\boldsymbol{n}$	power of the nonlinear resistance term in the Missbach equation
$\boldsymbol{P}_1$	water pressure at the inflow side of a volume sand
$\boldsymbol{P}_2$	water pressure at the outflow side of a volume sand

P_1	applied boundary stress at the inflow elements in the finite element simulation for the rectilinear flow problem
P_2	applied boundary stress at the outflow elements in the finite element simulation for the rectilinear flow problem
P_{N1}	applied normal boundary stress at the inflow side in the finite element simulation for the radial flow problem
P_{N2}	applied normal boundary stress at the outflow side in the finite element simulation for the radial flow problem
p	dynamic pressure term in the Navier-Stokes equation for flow in porous medium
p_1	upstream dynamic pressure in the Darcy equation for steady state flow without free surface in porous medium
p_2	downstream stream dynamic pressure in the Darcy equation for steady state flow without free surface in porous medium
p_o	dynamic pressure inside a well
$p_{(x=0)}$	boundary condition pressure at x = 0
$p_{(x=L)}$	boundary condition pressure at x = L
$p_{,i}$	fluid pressure tensor in the numerical model
Q	total discharge flow through a cross sectional area of a porous medium
Q	discharge per unit length of the well in the Engelund solution for the nonlinear flow equation
Q_D	discharge per unit width obtained from the Darcy equation for the rectangular and cylindrical flow domain
Q_d	discharge per unit width obtained from the Dupuit approximation for the simple rectangular earth dam
Q_F	discharge per unit width obtained from the Forchheimer equation for the rectangular and cylindrical flow domains
Q_H	discharge per unit width at the inflow boundary obtained from the Polubarinova-Kochina solution for a simple rectangular earth dam
Q_h	discharge per unit width at the outflow boundary obtained from the Polubarinova-Kochina solution for a simple rectangular earth dam
Q_{h_o}	discharge per unit width at the separation height obtained from the Polubarinova-Kochina solution for a simple rectangular earth dam
Q_S	discharge per unit width obtained from the proposed nonlinear solution for the free surface unconfined flow
$\overline{Q}$	applied fluid flux in the steady state three-dimensional equation
Q_s	specific discharge in the Solvik equation at the toe of a dam
Q_T	total outflow at the toe of the dam
Q_x	total discharge through vertical surface
$\boldsymbol{q}$	discharge vector per unit area (flow velocity vector)
q	discharge per unit area (flow velocity)
q_D	discharge per unit area (flow velocity) obtained from the Darcy equation for the rectangular and cylindrical flow domains
q_F	discharge per unit area (flow velocity) obtained from the Darcy equation for the rectangular and cylindrical flow domains

q_d	discharge per unit area (flow velocity) obtained from the Dupuit approximation for the free surface unconfined flow
q_l	discharge per unit area (flow velocity) obtained from the proposed solution for the free surface unconfined flow at laminar state
q_p	discharge per unit area (flow velocity) obtained from the Polubarinova-Kochina solution for a simple rectangular earth dam
q_t	discharge per unit area (flow velocity) obtained from the proposed solution for the free surface unconfined flow at turbulent state
q_x	discharge per unit area in the x-direction (flow velocity)
q_y	discharge per unit area in the x-direction (flow velocity)
q_0	discharge per unit area for a steady state flow without free surface
$\boldsymbol{Re}$	Reynolds number for flow in porous medium
R_1	Radial distance from a well
R_0	radius of a cylindrical well
$\mathbf{R}$	flow domain in the finite difference method
$\mathbf{R}(\mathbf{u}_i)$	residual vector in the finite element solution
$\mathbf{R}_0$	reference vector in the finite element solution
r	radial distance in the cylindrical flow domain
r_1	inner radius of the cylindrical flow domain
r_1	outer radius of the cylindrical flow domain
S	exact solution of the differential equation in the finite difference method
s	distance measured in the direction of the resultant velocity
T	temperature
T_0	reference temperature in the numerical model of the finite element method
t	time
t'	increment time step
$\boldsymbol{U}$	global vector of the unknowns (velocities and pressures) in the equation system of the finite element method
U	local average seepage velocity
U_x	local average seepage velocity in the x-direction
U_x	horizontal component of the velocity in the two-dimensional numerical model for rectangular flow domain
U_y	vertical component of the velocity in the two-dimensional numerical model for rectangular flow domain
U_N	normal component of the velocity in the two-dimensional numerical model for cylindrical flow domain
$\mathbf{u}_i$	unknown vectors of the global matrix in the equation system of the finite element method
u	complex velocity in the x-direction of the hodograph transformation
$u_{i,jj}$	Eulerian fluid velocity components in the numerical model
V	volume of the soil element
V	volume of rigid porous with viscous incompressible fluid in the numerical model of the finite element method
V_f	volume occupied by the fluid in the numerical model of the finite element

	method
V_s	volume occupied by the solid in the numerical model of the finite element method
υ	complex velocity in the y-direction of the hodograph transformation
X	horizontal coordinate of the free surface in the Polubarinova-Kochina solution
x_i	coordinates of the nodal points on the free surface
$\dot{x}_i$	rate of change of x_i in the finite element method
x	Cartesian coordinate
Z	function in the Polubarinova-Kochina solution for simple rectangular earth dam
z	Cartesian coordinate
z	complex number
Y	vertical coordinate of the free surface in the Polubarinova-Kochina solution
y	Cartesian coordinate

Greek letters

α	slope angle of rock surface in the direction of the flow in the Solvik equation
α	a parameter in the Polubarinova-Kochina solution
α_1	a variable postulated by Crank for the hodograph transformation
α	slope angle of the downstream embankment
β	angle of the dam slope in the Solvik equation
β	a parameter in the Polubarinova-Kochina solution
β_0	shape factor of the grain in the Solvik equation
β_T, β_{cn}	volume expansion coefficients in the general Navier-Stokes equation of the numerical model
$\varepsilon_{\mathbf{u}}$	tolerance factor of the convergence criteria in the solution of finite element method
ϕ	potential function
ϕ	piezometric head
ϕ'	effective angle of friction in the Solvik equation
φ	dependent variable in the finite difference method
Φ	velocity potential
Φ_e	flow rate of electricity
γ	weight density of the fluid
γ_w	weight density of the water in the stability criteria for confined saturated flow
γ_s	weight of solid in the stability criteria for confined saturated flow
γ_f	buoyancy weight in the stability criteria for confined saturated flow
γ_b	submerged unit weight in the stability criteria for confined saturated flow

γ_t	total weight in the stability criteria for confined saturated flow
λ	tortuosity coefficient
μ	dynamic viscosity for a fluid
$\tilde{\mu}$	effective dynamic viscosity
ν	kinematic viscosity of a fluid
θ	angle between the velocity vector q and the x-axis in the Engelund solution for the nonlinear flow equation in porous medium
θ	angle of the curvature in the cylindrical flow domain
θ	slope angle of the free surface in the exit gradient criteria for unconfined saturated flow
ρ	density of a fluid
ρ_0	constant density of a fluid in the general Navier-Stokes equation of the numerical model
ψ	stream function
ψ	parameter of the integral in the Polubarinova-Kochina solution
∇	Nabla operator
Δ	Laplace operator
χ	parameter of the incompressible fluid
τ_c	critical shear stress according to the Shields limits
τ	a postulated parameter in the Polubarinova-Kochina solution for a simple rectangular earth dam
Ω	flow domain in the numerical model of the finite element method
Ω_f	fluid region in the numerical model of the finite element method

List of Figures **Page No.**

List of Tables **Page No.**

1. Introduction

A good understanding of fundamental seepage and drainage principles will help engineers avoid serious mistakes in selecting the best kinds of systems to control seepage and groundwater. Generally, in describing fluid flow through porous media the Newton's law of friction together with the classical Navier-Stokes equations of hydrodynamics, provide a basis for studying the behavior of liquids under motion in porous media. Unfortunately the resulting equations become so complex that their solutions are impracticable. Recognizing these problems, Darcy (1856) resorted to experimental study of the flow of water through a sand filter and developed a semi-empirical representation of the behavior of fluids flowing through porous media.

Traditionally, most water flow problems have been solved on the assumption of Darcy's linear relation between head loss and velocity

$$\boldsymbol{q} = -K \frac{\partial H}{\partial \boldsymbol{s}} = |K\boldsymbol{J}| \tag{1.1}$$

in which $\boldsymbol{q}$ is the vector of Darcy velocity (superficial or average seepage velocity); K is the hydraulic conductivity or the coefficient of permeability in the s direction which depends on properties of the fluid and the medium; H is the total fluid head; $\boldsymbol{s}$ is the distance measured in the direction of the resultant velocity at the point under consideration; and $\boldsymbol{J}$ is the negative vector of total head gradient $(-\partial H / \partial s)$. The total head is equal to the sum of the piezometric and velocity heads.

The flow conditions described by Eq. (1.1) provided the velocities are small. Darcy's law is usually considered applicable to what is known as creeping flows or Stokes flow in porous media. However, since the last century (Slichter, 1898), it has been realized that Darcy's Law fails to hold for high flow velocities. Thus, while many of the practical problems of flow through porous materials can be solved accurately by the assumption of Darcy's Law, various situations have arisen in which a more accurate relation between head loss and velocity must be employed to obtain realistic solutions. Such situations include flow in the area adjacent to a pumping well in a coarse-grained aquifer and flow through rock- fill dams and banks (Volker, 1969).

The limited validity of Darcy's Law has led to the suggestion of relations that would be accurate for all flow ranges encountered. Forchheimer (1901) suggested replacing Darcy's law by the nonlinear equation

$$J = aq + bq^2 \tag{1.2}$$

in which a and b are constants determined by the properties of the fluid and medium. Although Forchheimer later added a third order term, cq^3, to make the equation fit the experimental results more accurately, his original expression given as Eq. (1.2), has

become known as the *Forchheimer* equation, the term by which it will be referred to here.

Many researchers have confirmed this relation on the basis of experimental evidence (Volker, 1969). The *Forchheimer* equation has been derived theoretically for certain flow conditions. Ergun and Orning (1949) derived both a hyperbolic and a parabolic equation on the basis of the second term in Eq. (1.2) for unconfined flow. Some solutions, e.g. the free surface flow in earth-fill and rock-fill dams, are complicated. The problem of predicting the exit point of the phreatic line (the surface of the water table), then the nonlinearity of the surface line itself introduces another difficulty to a possible explicit solution for the nonlinear flow equation in unconfined aquifer.

In an isotropic homogenous porous medium, for flow satisfying Darcy's Law, the application of the continuity relation yields the Laplace differential equation:

$$\nabla^2 H = 0 \tag{1.3}$$

Because the velocity head is negligible, the total head H can be set to the piezometric head h so that Eq. (1.3) becomes

$$\nabla^2 h = \Delta h = 0 \tag{1.4}$$

The solution of this equation for various boundary conditions has been widely reported in the literature. Analytic solutions are available for many simple common problems, e.g. as outlined by Polubarinova-Kochina (1962) and Harr (1962). Numerical finite difference solutions to various problems including free surface flows are also well documented: (Shaw and Southwell, 1941; Thom and Apelt, 1961); Boulton, 1954; and Jeppson, 1968). For the past ten years, the method of finite elements has been applied to the solution of seepage problems (Zienkiewicz, Mayer and Ceung, 1966). The advantages of the finite element method are the ability in dealing with complex boundaries and with the properties of anisotropy and non-homogeneity of the media. This method has also applied to the analysis of "free surface" problems including two-dimensional flow (Finn, 1967) and axisymmetric flow (Taylor and Brown, 1967).

Analytical solution of the free surface with the application of the nonlinear relation is not generalized in the literature, though several numerical solutions are worked out for simple flow case. The complex differential equations obtained from the nonlinear flow equation have been too difficult to solve by analytical mathematics. Analysis of such flow is, however, essential for seepage problems in practical applications.

Objective

Since ancient times, dams have been constructed to make use or to economize water resources. Dams regulate and store water, and water head applied for hydropower generation systems. However, a dam also constitutes a danger to downstream valley areas. Thus, dam safety demands control of the seepage and filtration of water inside the core of the dam and understanding of the flow methodology within the pores. Also to prevent any erosion inside the dam or at the embankments in various flow conditions. In most cases when the flow exceeds the laminar limit ($Re > 10$) and maintain a turbulent state , the estimation of the flow discharge by the linear relation (between the hydraulic gradient and the flow velocity) cause a deviation from the correct solution. When accurate flow relations are taken into consideration in predicting flow quantity and the phreatic line position, it will decrease the risks of the loss of lives, the dam failure, and damage to property and the environment. This study was undertaken in order to apply the nonlinear relation between the hydraulic gradient and flow velocity in porous media (non-Darcy flow) and with the aim of making a stability analysis of the porous material in common earth-fill and rock-fill dams specifically the stability of the downstream side of the dams. This study is divided into three parts:

1. An estimation of the quantity of seepage using a nonlinear relationship,
2. A formulation of governing flow domain equations (for confined and unconfined flow), and
3. A stability analysis related to a critical gradient (filter criteria and exit gradient).

2. Review of literature

2.1. Description of porous media

In order to study the flow of fluids through porous media, it is essential to identify and understand the terms denoting the two materials involved: fluids and porous media. A porous medium has been defined in the literature as a solid body that contains pores (this assumes that it is quite clear what the pore means). However, it is difficult to give an exact geometrical definition to the word pore from the appearance of shape. But to call a medium porous, the pores must be void spaces that are distributed more or less regularly through the material of the medium. Very small voids in a solid are often called molecular interstices, while very large ones are called caverns. Pores are defined as void spaces intermediate in size between caverns and molecular interstices; hence the description of their size is relative.

The pores in porous systems may be *interconnected* or *non-interconnected.* Flow of intersticial fluid is possible only if at least part of the pore space is interconnected. The interconnected part of the pore system is known as the *effective* pore space of the porous medium.

According to the preceding description, beds formed of sand, granules, porous rocks (such as limestone, pumice, dolomite, filter paper, etc.), as well as catalytic particles containing extremely fine micropores, are examples of porous media. Hence, the term porous media encompasses a very wide variety of substances. Because of this, it is desirable to classify porous media (into several classes) according to the types of pore spaces which they contain. A porous medium, of course, is not restricted to only one class of pore spaces and, thus may have pore spaces belonging to several classes. A classification of pore space was devised by Manegold (1937, 1941). He divided pore space into voids, capillaries, and force spaces: *voids* are characterized by the fact that their walls have only an insignificant effect upon hydrodynamic phenomena in their interior; in *capillaries*, the walls do have a significant effect upon hydrodynamic phenomena in their interior, but do not, however, bring the molecular structure of the fluid into evidence; *in force space* the molecular structure of the fluid is brought into evidence. In addition, pore spaces have also been classified according to whether they are *ordered* or *disordered*, and according to whether they are dispersed or connected.

Thus, a porous medium is characterized by a variety of geometrical properties. First of all, the fraction of void to total volume is important. This fraction is commonly known as the porosity. when the calculation of the porosity is based upon the interconnected pore space, instead of the total pore space, the resulting value is termed *effective* porosity. Second, another well-defined geometrical quantity of a porous medium is its *specific internal area.* This is the ratio of internal area to bulk volume and it is therefore expressed as a reciprocal length (Scheidegger,1960).

It would be most desirable to be able to define a geometrical quantity that characterizes the size of the pores in a given porous medium. Unfortunately, the pore system of a porous body forms a very complicated surface, geometrically difficult to describe. Theoretically, it is possible to give an analytical equation for it, however there are practical difficulties in quantification. It is natural that one would like to define the size of a pore; a convenient measure of the size would be diameter. However, the term diameter makes sense geometrically only if all the pores are of uniform spherical shape, otherwise more specifications are necessary (Muskat, 1946).

In an actual flow of fluids through pores, the limitation of assuming the pores to be of uniform spherical shape only is not appropriate description, because the porosity will not have the effect that it is supposed to have. Usually the analogy of flow in pipes is used to describe the geometry of the pores. The pipes supposed to be of circular cross-section, of certain diameter. But this kind of analogy of the pores to the flow in pipes, is definitely not correct because the pores are not in general of circular type, and that makes the matters worse. The pores do not even have a uniform cross-section since the walls diverge and converge irregularly. Thus, one can not speak about the largest or the smallest diameter of the pipe at any one (Harr, 1983).

Actually, by employing the term *porous medium*, and by considering *flow of fluids through a porous medium*, we can take a basic and important step towards defining the concepts of flow phenomena in porous media.

Summary of the above descriptions, and definitions of a porous medium is depicted in Figure 2.1, (Bear, Zaslavsky and Irmay 1968) and discussed below:

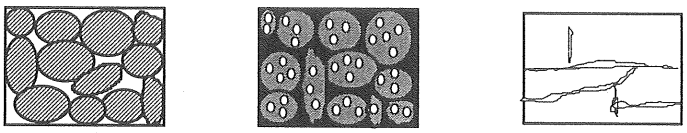

(a) (b) (c)

Figure 2.1. Diagram showing several types of rock interstices (Bear, 1972)

Figure 2.1a shows a portion of space occupied by *heterogeneous or multiphase* matter. At least one of the phases comprising this matter is not *solid*. This may be a gaseous or liquid phase. The solid phase is called the *solid matrix*. The space within the porous medium domain that is not part of the solid matrix is referred to as *void space* (or pore space).
Figure 2.1b shows that the solid phase should be distributed throughout the porous medium within the domain occupied by a porous medium; solids must be present inside each representative elementary volume. An essential characteristic of a porous medium is that the *specific surface* of a solid matrix is *relatively high*. In many respects, this characteristic dictates the behavior of the fluids in porous media. Another basic feature of a porous medium is that the various openings comprising the void space are *relatively narrow*.

Figure 2.1c shows the at least some of the pores comprising the void space should be interconnected. The interconnected pore space is sometimes termed the *effective pore space*. As far as flow through porous media is concerned, *unconnected pores* may be considered as part of the solid matrix. Certain portions of the interconnected pore space may, in fact, also be ineffective as far as flow through the medium is concerned. For example, pores may be of a type known as *dead-end pores* or blind pores, i.e. pores or channels with only a narrow single connection to the interconnected pore space, so that almost no flow occurs through them. Bear (1972) found another way to define this porous medium characteristic by the requirement that any two points within the effective pore space may be connected by a curve that lies completely within the pore space. Moreover, except for special cases, any two such points may be connected by curves of an arbitrary maximal distance. He also stated that for a finite porous medium domain, this maximum distance is dictated by the dimensions of the domain. The features described above have been concluded in the literature to be comparative, rather than absolute.
Rideal (1958) also indicates the various characteristics of porous materials, emphasizing the difficulty in arriving at an exact definition still sufficiently general to be applied to the wide variety of porous media. It is this difficulty, defining a geometry of the solid surface which acts as a boundary to the flow in the void space, that forces us to the introduction of the continuum approach as a tool for handling phenomena in porous media (Scott, 1969). Another characteristic that is introduced to understand porous media, is the concept of a *continuum medium*, which is common to most branches of physics.

The same difficulties are encountered, when one deals with the fluid or fluids contained in the void space, in phenomena associated with both liquid and gas, such as motion, mass transport, etc. The concept of the fluid itself requires some further careful work. Actually, fluids are composed of a large number of molecules that move about, colliding with each other and with the solid walls of the container in which they are placed. According to theories of classical mechanics, when we can get a full description of a given system of molecules, e.g. as given by Bear (1972), with the initial positions of the molecules in space and their momenta, then we can predict their future positions. Although this seems to be simple, it is difficult problem to predict the path of the flow of even as few as three molecules. With the advent of high speed digital computers, the many body problem (*many molecules*) can be attacked in principle numerically (Landau and Lifschitz, 1958). In addition, because the number of molecules is so large, their initial positions and momenta cannot be determined simply by observation.
Landau and Lifschitz (1958) introduced another concept to the motion of fluids in porous media by adopting a *statistical approach* in nature, in order to derive information regarding the motion of a system composed of a many molecules. Statistical mechanics is an analytical science by which statistical properties of a very large number of molecules (or particles in general) may be determined from laws governing the motion of individual molecules (Bear,1987).

Since the ultimate objective of this study is to handle phenomena in porous media, the need for a general method of treating fluids in porous medium can be met by averaging phenomena in the fluid continuum filling the void space. Consequently, the microscopic scale has been chosen for reference to the fluid continuum level, that is one can regard the actual or molecular structure of a fluid as a continuum. Scheidegger (1960) concluded, in his comprehensive study of the continuum of fluids, that the concept of a *particle* was essential for this analysis. He stated that, although particle size is much larger than the mean free path of a single molecule and the particles should be sufficiently small, in comparison with molecules. In this way, a value relevant to the description of bulk fluid properties may be obtained. These values are then related to a centroid. Then at every point in the domain occupied by a fluid, there can be a particle possessing definite dynamic and kinematic properties.

In the literature there are several physical phenomena of fluids, observed on a macroscopic scale, which are in fact the based on the theory of molecular motion. Among these there are *mass transport by molecular diffusion, heat transfer*, and *momentum transfer* which manifest themselves in the form of internal friction or viscosity. In each of these cases, because the transfer phenomena are not treated on a molecular level, thus by averaging the transport production of individual molecules and passing it to a higher level, as referred to above for the fluid continuum, we can describe various transfer phenomena. Actually *transfer coefficients* are needed in such studies are the molecular diffusivity, thermal diffusivity, kinematic viscosity, hydraulic conductivity, etc.(Bear, 1972). In describing a flow in porous media, we have a fluid continuum enclosed by a solid surface and the solid surface of the porous medium. At any point in this fluid continuum we can define the specific physical, dynamic and kinematic properties of a fluid particle. We need to know how we can solve a flow problem in a porous medium at this level. From the theory of fluid mechanics, we can derive the details of a fluid's behavior within the void space. For example, we can use the Navier-Stokes equations for the flow of a viscous fluid to determine the velocity distribution of the fluid in the void space by satisfying specific boundary conditions, such as zero velocity at all fluid-solid interfaces. However, it is often difficult to define the boundary conditions themselves. Thus, by adopting the continuum approach, we can reduce the difficulties; our approach can be facilitated by averaging to the macroscopic level. This also can be seen as a *continuum approach.*

2.2. Creeping flow in porous medium (Stokes' motion)

To obtain a full description of the motion of a Newtonian fluid in porous medium, when the fluid is regarded as a continuum (cf. 2.1), the motion of the fluid can be described if the position of every material point of the fluid is known at every time-instant. There are three kinds of physical conditions which determine such motion. The first, is the continuity condition, the second is the rheological equation of state

and the third is the classical Newton law of motion (Daily, 1966). These physical conditions are expressed mathematically as a system of differential equations. An additional set of initial and boundary conditions is needed to determine the problem completely. For example, it should be specified whether or not the particular fluid sticks to the walls of a container. Different combinations of rheological equations and boundary conditions are needed depending on whether the fluid is a liquid or gas, whether it is viscous or non-viscous, etc. (Scheidegger, 1960). The *continuity conditions* and *Newton's law* of motion are well known; for example, Lamb (1968) expressed them in a representation suitable to the description of a continuous medium. The rheological condition expressed here is the relation between the stresses and the strains in the fluid (and their time derivatives). In the case of an ideal fluid, it is assumed that there are no shear stresses applied and that the fluid is incompressible, however generally fluids are viscous and compressible.

Finally, the initial and boundary conditions mentioned above represent the following: first, the shape and walls of the container of the fluid; second, the external condition such as the pressure drop; and third; the type of interaction between the fluid and walls. When the fluid is viscous, it is generally assumed that it sticks to the walls (Scheidegger, 1960).

The set of conditions outlined above can be combined to form various differential equations which are applicable to different kinds of fluids. The best known of these equations is that of Navier and Stokes (see e.g. Lamb, 1968). It is applicable to incompressible viscous fluids. The Navier-Stokes equation has been re-stated in the literature many times because of its fundamental importance. The compressible Navier-Stokes equation has the following structure:

$$\rho \boldsymbol{g} - \nabla p + \mu \nabla^2 \boldsymbol{q} + \frac{\mu}{3} \nabla (\nabla \cdot \boldsymbol{q}) = \rho \frac{\partial \boldsymbol{q}}{\partial t} + \rho (\boldsymbol{q} \cdot \nabla) \boldsymbol{q}. \tag{2.1}$$

For incompressible fluids, $\nabla \cdot \boldsymbol{q} = 0$ and the Navier-Stokes equation become

$$\rho \boldsymbol{g} - \nabla p + \mu \nabla^2 \boldsymbol{q} = \rho \frac{\partial \boldsymbol{q}}{\partial t} + \rho (\boldsymbol{q} \cdot \nabla) \boldsymbol{q}. \tag{2.2}$$

The structure of the Navier-Stokes equation and the boundary conditions make the analytical solution of equation (2.2) very difficult. Naturally many attempts have been done to find an approximation of this equation which would enable an easier analytical treatment. Thus, an attempt to eliminate the inertia terms of the incompressible Navier-Stokes equations for flow in a gravity body-force field have led to the following simplified form:

$$\mu \nabla^2 \boldsymbol{q} = -\rho \boldsymbol{g} + \nabla p. \tag{2.3}$$

The equation above must be solved together with the constant-density continuity equation, $\nabla \cdot \boldsymbol{q} = 0$. This has become known as the creeping motion of fluids. The entire system of equations above must satisfy the same boundary conditions as must be satisfied for the full Navier-Stokes equations, namely the vanishing of the normal and tangential components of the relative velocity on the surface of the rigid boundaries.

Stokes (1851) gave the first known solution for a case of creeping motion. He used the approximation presented above to solve the creeping motion case of flow past a fixed sphere and its counterpart: the case of a solid sphere falling through a highly viscous infinite fluid. In addition to the modified Navier-Stokes equations, the continuity equation and the usual boundary condition of vanishing relative velocity at the surface of the sphere were satisfied.

In this study, for low Reynolds number flow through certain porous medium, such as flow of water, oil, and other fluids through filter beds, surface soil, and porous rock, the approximation of the creeping motion is very helpful in describing the seepage through a porous medium.

With the Stokes approximation for the creeping motion and omitting the inertia terms from the full Navier-Stokes equation (Daily, 1966), equation (2.3) for creeping motion in porous media becomes:

$$\nabla (p + \gamma h) = \mu \nabla^2 \boldsymbol{q}. \tag{2.4}$$

With the continuity equation $\nabla \cdot \boldsymbol{q} = 0$, and taking the divergence of both sides of equation (2.4), (Harr, 1968) :

$$\nabla^2 (p + \gamma h) = 0. \tag{2.5}$$

Equation (2.5) is the well-known Laplace equation and its solution for particular boundary conditions yields the spatial distribution of $(p+\gamma h)$. The Laplace equation for incompressible fluids can be satisfied by a velocity potential function (Streeter, 1978). This can be shown in many cases where laminar flow holds and where, for zero inertia effects, the velocities and the flow rate are linearly proportional to the gradient of $(p+\gamma h)$. Hence, the analogy of liquid flow in tubes in a given direction gives a mean velocity of

$$q_x = -\frac{const}{\mu} \frac{\partial (p + \gamma h)}{\partial x}. \tag{2.6}$$

where the constant of proportionality depends on the flow-passage geometry.
For porous-media flow where the average discharge velocities are of interested rather than the local velocities in pores, the Laplace equation is also applicable, i.e. for

laminar flow through small irregular pore passages. The analogy with flow through tubes, for a liquid (or a gas under small pressure differentials so that its density does not vary), the velocity can be written as

$$q_x = -\frac{k_x}{\mu}\frac{\partial(p+\gamma h)}{\partial x} \tag{2.7}$$

where q_x is the *superficial* or *discharge velocity* defined as the local flow rate averaged over a finite area of the porous medium and k_x is the *intrinsic permeability* in x-direction (Daily, 1966). Thus, for a given cross-sectional area ΔA of porous material through which ΔQ is flowing, the superficial or discharge velocity is

$$q_x = \frac{\Delta Q}{\Delta A}. \tag{2.8}$$

For ΔA, finite but of the order of several pore channels, q_x approaches a local- average value. When a local-average velocity is used in the equations, the physical system is replaced by a mathematical continuum. In the literature, the term *local average seepage velocity* through the pores has been defined as

$$U_x = \frac{\Delta Q}{n\Delta A} \tag{2.9}$$

where n, the porosity, is the ratio of the volume of the voids to the total volume of the porous medium and the voids. The factor k_x which is called the *intrinsic* or *physical permeability*. It has the dimension of length squared, and assumes saturated conditions. It depends on the flow geometry, on the type of porous medium, and on the density, shape, and arrangement of the pores. Thus it is constant if the medium is incompressible and isotropic.

In 1856, Darcy published an relation equivalent to Eq.(2.7) based on experiments in connection with water supplies for the fountains of the city of Dijon. He put together the intrinsic permeability and the density of the liquid with the kinematics viscosity as one hydraulic conductivity (coefficient of permeability):

$$K = \frac{k\gamma}{\mu}. \tag{2.10}$$

The coefficient K has the units of a velocity under saturated conditions. It is found to be a function of the flow geometry (type of medium and pore characteristics) and also of the fluid specific weight and viscosity. Thus, it is constant for a given fluid at a fixed temperature if the porous medium is incompressible and isotropic. The isotropic medium is the one that has the same hydraulic conductivity in all flow directions, therefore the flow in three directions is (Scott, 1963)

$$q = -\frac{k}{\mu}\nabla(p + \gamma h) \tag{2.11}$$

where q is the vector superficial velocity. Equation (2.11) is the well-known Darcy law in the literature. As shown above, the Darcy law is a linear relationship between the velocity and the gradient $(p + \gamma h)$ used in seepage-flow equations. This relationship holds as long as the flow remains laminar and inertia effects remain unimportant. From many experiments with sand, a Reynolds number $Re \approx 10$ was shown to be an upper limit for the Darcy law. This Reynolds number may be exceeded in rock aquifers and in the vicinity of well casings. The evidence from sand beds is that for $Re > 10$, departure from Darcy's law occurs due to fluid acceleration causing inertia effects while the flow is still laminar. The transition from laminar flow to turbulence is gradual, somewhere between $Re = 60$ and $Re = 600$. The flow resistance seems to become independent of Reynolds number at about $Re = 1000$ (Daily, 1966). Hence, another form for the relation of the velocity with the gradient is needed to cover the nonlinear flow in a porous medium.

2.3. Flow field equations (linear and nonlinear)

The steady flow of a viscous, incompressible and chemically inactive fluid through a saturated, homogeneous, isotropic and geometrically stable porous medium, in the absence of compressible free gases at low Reynolds numbers ($Re = qd/\nu$) and at constant temperature, obeys the Darcy law (Darcy, 1856; Irmay, 1946, 1947)

$$q = -K \nabla h = K J \tag{2.12}$$

where H is the piezometric head and J is the negative hydraulic gradient.

Darcy's law has been extended to non-homogeneous media (Boussinesq, 1904; Irmay, 1953), and then to non-isotropic media (Irmay, 1951). Jacob (1950) and Florin (1948) have applied the Darcy law to unstable media; it has also been applied to unsteady flow (Boussinesq, 1904; Irmay, 1951, Polubarinova-Kochina, 1962). Darcy's law has been extended to apply to compressible fluids by Muskat, (1946), and then to unsaturated media by Richards (1931) and Irmay (1956). A detailed review of the various theories is given in the literature (Muskat, 1946, 1949; Polubarinova-Kochina, 1951, 1962; Scheidegger, 1960; Bear, 1972).

At larger Reynolds numbers, Forchheimer (1901) suggested replacing equation (2.12) by the nonlinear formula which bears his name:

$$J = a\, q + b\, q^2. \tag{2.13}$$

This formula has been suggested also by Lindquist (1933). At low Reynolds numbers ($Re < 1$), the second term may be omitted, and the linear Darcy formula (2.12) is obtained. Here $a = 1/K$ *is* the hydraulic resistivity of a porous medium (see Figure 2.2).

For Reynolds numbers ($Re \approx 1$) the second term is of the same order as the first term. This is the case for a nonlinear viscous flow (Irmay, 1958). Irmay (1956) has shown that there is no reason in general to expect a linear solution of the fundamentally nonlinear *Navier-Stokes* equations. The linear *Poiseuille* solution in straight tubes is an exception caused by vanishing curvature, however, in the flow through porous media it is clearly predicted that flow paths are strongly curved.

At larger Reynolds numbers ($Re > 100$) the flow becomes turbulent, as was experimentally shown by the injection of dyes (Schneebeli, 1955). Equation (2.13) remains valid, but with different values of a and b. At very large Reynolds numbers $a = 0$ (analogous with rough turbulent flow).

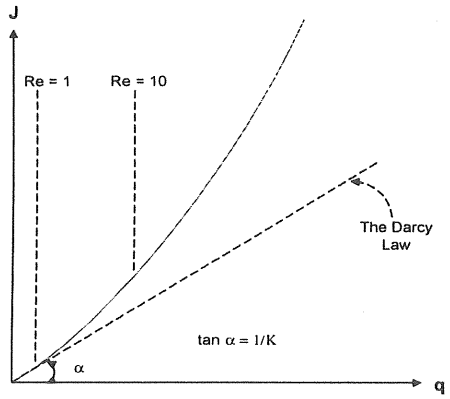

Figure 2.2. Schematic curve representing experimental relationship between flux and hydraulic gradient (Bear, 1972).

Missbach (1937) has suggested a different relationship:

$$J = a\, q^n \qquad (1 < n < 2) \qquad (2.13a)$$

while Polubarinova-Kochina (1962) suggested the same as Forchheimer the following form

$$J = a\, q + b\, q^2 + c\, q^3. \qquad (2.13b)$$

It has been shown in the literature that the Forchheimer formula is the only one that has a wide empirical basis (Irmay, 1956). Forchheimer applied the operator ∇ to the vectorial equation (2.12) obtaining

$$\nabla q = -\nabla \cdot (K \nabla h) = 0. \tag{2.14}$$

In homogeneous media K is constant, and

$$\nabla \cdot \nabla h = \nabla^2 h = \frac{\partial^2 h}{\partial x^2} + \frac{\partial^2 h}{\partial y^2} + \frac{\partial^2 h}{\partial z^2} = 0. \tag{2.15}$$

This is the well-known equation of the *Laplace potential.* In media of non-uniform K variable in space, equation (2.14) becomes (Boussineq, 1904):

$$\nabla \cdot (K \nabla h) = K \nabla^2 h + \nabla h \cdot \nabla K = 0 \tag{2.16}$$

or

$$\nabla^2 h + \nabla h \cdot \nabla \ln K = 0 \tag{2.16a}$$

which is a type of *Poisson* equation (Irmay, 1953). However, Scheidegger (1960) thinks that equation (2.12) should perhaps be replaced by

$$q = -\nabla (K h) \tag{2.12a}$$

which, instead of (2.16a), gives

$$\nabla^2 (K h) = K \nabla^2 h + 2 \nabla h \cdot \nabla K + h \nabla^2 K = 0. \tag{2.16b}$$

Bear (1972) has pointed out that Eq. (2.16b) means for a domain without energy gradient there is a flow due to the differences in K, which is not logical without a source of energy. Accordingly, Bear (1972) found that it is important to generalize the Darcy law in terms of the piezometric head.

Many authors have tried to derive the Darcy law by means of various ingenious physical models and analogies. An excellent review is given by Scheidegger (1960). The models are the capillary tube analogies (Smith, 1932; Irmay, 1951); the hydraulic-radius theories (Terzaghi, 1925; Kozeny, 1927; Irmay, 1951); the drag theories by Emersleben (1924, 1925); and the turbulent-flow analogy by Yuhara (1954) and by direct derivation from the *Navier-Stokes* equations (Hall, 1956; Hubbert, 1956).

Irmay (1956) drew the conclusion that the above theories have weak points: they are mostly analogies, the applicability of which has not been proved, or they are based on the introduction of unspecified coefficients, which are somehow ignored in later developments. None of them lead towards Forchheimer's formula. Irmay derived both Darcy's law and Forchheimer's law easily, from the Navier-Stokes hydrodynamic equations, for viscous flow through a homogeneous isotropic incompressible saturated medium.

2.4. Analytical solutions

2.4.1. Solution of Darcy flow (linear flow)

Steady state flow without a free surface

The solutions to hydrodynamic problems concerning the flow of homogeneous fluids in porous media are obtained by solving the differential form of the Darcy equation (Scheidegger, 1960)

$$q_y = Q/A = -(k_y/\mu)(p_2 - p_1 + \rho g h)/h. \tag{2.17}$$

In this form, it applies to vertical flow in a horizontal bed of finite thickness h, being percolated by an incompressible liquid of (constant) density ρ. This form of the law has only a very restricted use. Scheidegger's aim is therefore to express Eq. (2.17) in differential form. It is shown in the literature (Harr, 1968; Scheidegger, 1960) that there is are different ways of doing this. Naturally, q will become a vector $\boldsymbol{q}$ which might be called the local seepage -velocity, or superficial velocity, and the pressure difference in Eq. (2.17) must be expressed by the pressure gradient.

A first possibility is to let h in Eq. (2.17) become infinitesimal,

$$\boldsymbol{q} = -(k/\mu)(\nabla p + \rho \boldsymbol{g}), \tag{2.18}$$

where $\boldsymbol{g}$ is a vector in the direction of gravity and of the magnitude of gravity. However, the Darcy experiment does not tell us what would happen if the hydraulic conductivity and viscosity are variables. Thus, the coefficients should be taken into the gradient:

$$\boldsymbol{q} = -\nabla(\boldsymbol{k}p/\mu) + k\rho\,\boldsymbol{g}/\mu. \tag{2.19}$$

Scheidegger (1960) concluded that the first possible solution to equation (2.18) is equivalent to the introduction of potential ϕ *(as a definition)* since the equation can be rewritten as follows (Hubbert, 1940):

$$\phi = gz + \int_{P_0}^{p} dp/\rho(p) \tag{2.20a}$$

$$\boldsymbol{q} = -(k\rho/\mu)\nabla\phi \tag{2.20b}$$

where z denotes the vertical coordinate. On the other hand Scheidegger (1960) showed that Eq. (2.18) can be equivalent to the introduction of a velocity-potential

(by *definition*) since as the equation can be rewritten as follows (Gardner, Collier and Farr, 1934):

$$\Phi = k\,p / \mu + \int_{z_0}^{z} \frac{k \rho g}{\mu} dz \tag{2.21a}$$

where

$$q = -\nabla \Phi. \tag{2.21b}$$

Both representations by potentials are valid only if the integrals are univalent (Scheidegger, 1960).

The majority of technical mathematical reports concluded that it is not possible to distinguish between the two differential representations of Darcy's law if the experiments are performed using only constant viscosity fluids and porous media of homogeneous intrinsic permeability. Hence a great uncertainty exists as to whether the differential form of Darcy's law given in equation (2.18) or that given in equation (2.19) is the correct one.

Hubbert (1940) set out to show that Eq. (2.20a) would be the only correct one because of thermodynamic considerations. This fact has been given in the literature by using the second principle, i.e. the entropy principle, of thermodynamics; however Hubbert's proof does not seem to be convincing (Scheidegger, 1960). Furthermore, even if it were to be shown that the velocity potential does not generally exist, the corresponding differential formulation (2.19) of Darcy's law would still be possible.

In general, the force potential form, equation (2.18), of Darcy's law has been preferred to equation (2.19) in the literature because it is easier to treat analytically. There is another indication of its correctness, however, in the fact that, when it is extended to immiscible multiple phase flow, it leads to the relative permeability concept. The relative permeability is actually variable through the porous medium during a flow experiment, which means that a distinction between equations (2.18) and (2.19) is important. The fact is that the relative permeability equations as generalized from (2.18), not from (2.19), lead to an adequate description of a force-potential.

Neither differential form of Darcy's law, (2.18) or (2.19), is sufficient to determine the flow pattern in a porous medium for given boundary conditions, as the equations contains three unknowns (q, p, ρ). Two additional equations are therefore required for the complete specification of a problem. One is the connection between ρ and p of the fluid (Scheidegger, 1960):

$$\rho = \rho\,(p) \tag{2.22}$$

while the other is the continuity conditions:

$$-n\frac{\partial \rho}{\partial t} = \nabla \cdot (\rho q) \tag{2.23}$$

where, as usual, n is the porosity and t is the time. With the help of these equations, one can eliminate all of the unknowns except p which leads to either of the following equations, according to whether a force-potential (a) or a velocity potential (b) is assumed:

(a) $$n\frac{\partial \rho}{\partial t} = \nabla \cdot [(\rho k / \mu)(\nabla p - \rho g)] \tag{2.23a}$$

(b) $$n\frac{\partial \rho}{\partial t} = \nabla \cdot [\rho\{\nabla (k p / \mu) - k\rho g / \mu\}] \tag{2.23b}$$

where g is a vector pointing downward.

In general, the differential equation in question seems to be very closely related to the equation of diffusion and to that of heat conduction. Thus, solutions obtained with the intention of solving the heat-conduction equation can often be taken over directly for the hydromechanics in porous media. The treatment of the differential equation resulting from Darcy's law is, actually, a discipline of mathematics and has very little to do with the physics of a problem. General methods that are applicable have been found in appropriate mathematical texts such as that by Courant and Hilbert (1943). Much of the mathematical material that is directly applicable to the flow in porous media has also been accumulated by Carslaw and Jaeger (1959) in connection with their study of heat conduction. This book is a comprehensive review of the methods that are applicable to the solution of the differential equation; these are a part of a study on the theory of functions and mathematical analysis. A review of physical conditions for which solutions have been achieved is given below.

The physical conditions of the flow for which solutions might be sought are: (a) confined steady state flow, (b) gravity flow with a free surface, and (c) unsteady state flow (transient flow). Of these, steady state flow solutions for incompressible fluids are the most easily obtained; they are simply represented by solving the Laplace equation. Except for a few other special cases, Darcy's law, however, leads to nonlinear differential equations. The analytical methods to deal with these have been well analyzed and specified for so long that efforts have been directed towards scaling these phenomena and also towards experimental representation by analogous effects (Scheidegger, 1960).

Polubarinova-Kochina (1962) gave a comprehensive review of solutions of ground water flow, which is also included in the book by Muskat (1946).

The steady state problem is always characterized by the vanishing of the partial time derivatives of the physical quantities such as the density, velocity, etc. Equation (2.23) thus reduces to

$$\nabla \cdot \left[\left(\frac{\rho k}{\mu} \right) (\nabla p - \rho g) \right] = 0 \tag{2.24}$$

(note that g is a vector pointing downward, but coordinates increase upward).

If the fluid is incompressible and the porous medium homogeneous, one has

$$\Delta p = 0 \tag{2.25}$$

where Δ denotes the Laplace operator. This is the well-known Laplace differential equation, applicable in many instances in physics, and the general methods to which this differential equation is amenable lead to valid solutions presented for many cases. Thus, if two-dimensional problems are considered, methods based upon the theory of functions of complex variables are applicable, as well as the technique of using Green's function (Bear, 1988). A review of such methods has been given also in the books of Muskat (1946) and of Polubarinova-Kochina (1962). Golubeva (1950) discussed the utility of curvilinear coordinates in two-dimensional motion, while Shaw and Southwell (1941) and Dykstra and Parsons (1951) applied relation methods to the same problem. Other general methods for the treatment of steady flow have been discussed by Polubarinova-Kochina and Falikovich (1947). Furthermore, Polubarinova-Kochina (1951) showed how steady-state solutions for anisotropic flow can be obtained by a simple coordinate transformation onto principal axes, and Oroveanu (1966) published a lengthy discussion of the methods applicable to the treatment of systems with non-homogeneous permeability.
A classic example of a steady-state solution is a two-dimensional radial flow of an incompressible fluid into a well that completely penetrates the fluid-bearing medium. Assuming that the well is a cylinder of radius R_0, with inside pressure p_0, and that the pressure at a distance R_1 from the well is p_1, it is easy to verify that the required solution is

$$Q = \frac{2\pi k}{\mu \ ln(R_1/R_0)} (p_1 - p_0) \tag{2.25a}$$

where Q is the total discharge per unit of time and unit of penetration length of the well, k is the intrinsic permeability of the medium and μ is the viscosity of the fluid.

If the fluid in motion is compressible, then equation (2.24) does not reduce to the Laplace equation. However, it has been pointed out by Leibenzon (1947) that in the case of gases it does reduce to the Laplace equation if the following substitution is made (Scheidegger, 1960):

$$\chi = \int_{p_0}^{p} \rho \, dp \tag{2.26}$$

which leads to

$$\Delta \chi - \nabla \cdot (\rho^2 g) = 0. \tag{2.26a}$$

for gases the second term is much smaller than the first and can therefore be omitted. This also holds for horizontal flow of compressible liquids. One thus obtains

$$\Delta \chi = 0. \tag{2.27}$$

The study of the steady flow of compressible fluids is thus reduced in most instances to the discussion of the same differential equation as that encountered in the study of the steady flow of incompressible fluids. One has, for instance, in the linear case (coordinate x) for an ideal gas ($c_g p = \rho$)

$$\chi = (c_g / 2) p^2 = c' + bx. \tag{2.28}$$

With the boundary conditions $p_{(x=0)} = p_0$ and $p_{(x=L)} = p_L$, one has

$$p^2 = p_0^2 + x(p_L^2 - p_0^2)/L. \tag{2.29}$$

If Darcy's law is now expressed at x = 0, one obtains

$$q_0 = -\left(\frac{k}{\mu}\right)\left(\frac{dp}{dx}\right)_0 = -(k/\mu)(p_L^2 - p_0^2)/(2p_0 L). \tag{2.30}$$

Considerable work has also been done on the study of seepage underneath engineering structures, especially dams (with and without sheet-piling). Again, Muskat (1946) and Polubarinova-Kochina (1962) gave reviews of a wide variety of solutions that have been obtained. Such problems have also been investigated by Girinskii (1937, 1941).

The Laplace equation (2.25) occurs in many contexts in physics. Therefore, solutions of that equation can be obtained by performing suitable experiments which are themselves governed by the Laplace equation. In this manner, it is often possible to set up an analogy to certain problems of steady flow through porous media and thus to avoid the tedious job of solving the Laplace equation analytically. A discussion of some possible analogies has been published by Scheidegger, (1960). It can be summarized as follows:

(a) The flow of electricity. The steady flow of electricity in a conducting medium is governed by Laplace's equation.

$$\Delta \Phi_e = 0 \tag{2.31}$$

with the equation for current

$$J_e = -\nabla \Phi_e \tag{2.32}$$

where $\Phi_e = K_e E$, E is the electric potential, K_e the conductivity, and J_e the current density.

(b) The flow of heat. The flow of heat in heat-conducting media is also governed by the Laplace equation; unfortunately it is not generally feasible to use this fact for constructing experimental analogies of the flow through porous matter, as it is quite difficult to measure heat flow accurately. However, many analytical solutions of the Laplace's equation have been developed in connection with the study of heat flow (Carslaw and Jaeger, 1959), and these can be applied to porous flow problems.

(c) The distribution of stresses. It has been suggested that it might be possible to duplicate the flow of line by stress lines in stressed materials and to examine the latter by means of experimental stress analysis.

(d) The flow of viscous fluids. Under certain circumstances, the Navier-Stokes equation can be reduced to a Laplace equation. It is therefore possible to use the phenomenon of viscous flow for a representation of steady flow in porous media. An arrangement which has attained considerable popularity is the method of modeling two-dimensional flow in porous media by flow between two parallel plates a small distance apart. This type of analogy is usually called the *Hele-Shaw model* after Hele-Shaw (1899) who introduced it.
(e) Mechanical scaling. It is possible to represent a large-scale flow phenomenon in porous media by a small-scale one. All that is necessary is to establish the geometrical dimensions and then, to scale the pressure which can be scaled in any desirable way since the Laplace equation of the pressure is zero if that of p vanishes. A series of experiments using such scaling has been discussed in Muskat book (1946).

Steady state flow with a free surface (gravity flow).

A strange and unusual special case of the determination of steady state flow with gravity occurs where a fluid has a "free" surface. In fact, this is a problem of multiple-phase flow: above the "free surface" there is another fluid. Nevertheless, if that other fluid is a gas, and the original fluid is liquid, one can disregard the motion of the gas with respect to that of the liquid and assume that the gas pressure is constant in its entire domain. Thus, one can express the assumption that there is a free interface

between the two fluids by the condition that on this free interface the liquid pressure is constant and that any streamline having one point in common with this free surface lies entirely within it. In truth, no such free interface actually exists, as there is always a finite region within the porous medium where saturation drops from 100% to zero. But one can see that sharp saturation discontinuities can exist and that the assumption of an actual free surface could be sensible. A further peculiar phenomenon may occur if the notion of a free surface is accepted. If this surface intersects an open boundary of the porous medium, i.e. a boundary that is open to the gas and upon which therefore the pressure is constant and equal to that of the gas (atmospheric pressure), then the liquid will seep out from the boundary below the intersection with the free surface. Such a boundary is termed "surface of seepage". The boundary condition for a surface of seepage is that the pressure in the fluid is constant and equal to that at the free surface (atmospheric). In contrast to the free surface, however, a surface of seepage need not be a streamline (Scheidegger, 1960). The physical picture of the free seepage has been analyzed on many occasions, for instance, by Hamel (1934), Laurent (1949), and Childs (1956).

Thus, the analytical conditions of a flow with a free surface are fully determined. To summarize, one has to find a solution of the Laplace equation (2.25) with the boundary conditions such that there is a "free surface" which define a streamline and on which the fluid pressure is constant. On open boundaries below the intersection with the free surface, the liquid pressure must be constant and equal to that on the free surface. On impermeable boundaries, of course, the condition is, as usual, that the normal component of the filter velocity vanishes (Scheidegger, 1960) .

It is needless to prove that finding an analytical solution is extremely difficult and tedious when conforming to the above boundary conditions. However, Muskat (1946) and, in particular, Polubarinova-Kochina (1962) reviewed some methods that have been applied successfully, notably one employing hodograph transformation. In a medium of homogeneous permeability, the formulation using the velocity potential may be used:

$$\Phi = (k / \mu)(p + \rho g z) \tag{2.33}$$

$$q = -\nabla \Phi \tag{2.34}$$

$$\Delta \Phi = 0. \tag{2.35}$$

In two dimensions (x horizontal, y vertical coordinates), this leads to the possibility of representing everything in terms of complex numbers with $z = x + iy$. The hodograph transformation is characterized by

$$u = \frac{\partial \Phi}{\partial x} \tag{2.36}$$

$$v = \frac{\partial \Phi}{\partial y} \tag{2.37}$$

which can be also represented on a complex plane.

The hodograph method has the advantage that the free surface, the shape of which is unknown in the original formulation of the problem, is determined in the hodograph: it is simply circles with known parameters. In addition, the surface of seepage is also determined prior to an actual analytical solution of the problem. Thus, the "floating" boundary condition of the original problem becomes a fixed boundary condition after a hodograph transformation has been made (Muskat, 1946).

The use of hodograph transformations in connection with the problems of seepage was developed chiefly by Hamel (1934). Further discussions of analytical attempts to solve the problem are found in the literature, Muskat (1946), and Polubarinova-Kochina (1962).

Owing to the difficulties of obtaining analytical solutions to the problem with a free surface flow, graphical methods have been tried (Harr, 1968). In the case of radial flow (vanishing azimuthal component of the velocity), the flow equation, using the notation of velocity potential (cf. Eq. 2.33) reduces to

$$\frac{\partial^2 \Phi}{\partial r^2} + \frac{1}{r}\frac{\partial \Phi}{\partial r} + \frac{\partial^2 \Phi}{\partial z^2} = 0. \tag{2.38}$$

It is known from the theory of the Laplace equation that one can introduce a stream function ψ, defined by two differential equations:

$$\frac{\partial \psi}{\partial z} = 2\pi r \frac{\partial \Phi}{\partial r} \tag{2.39}$$

$$-\frac{\partial \psi}{\partial r} = 2\pi r \frac{\partial \Phi}{\partial z}. \tag{2.40}$$

The stream function ψ, in turn, satisfies the differential equation

$$\frac{\partial^2 \psi}{\partial r^2} - \frac{1}{r}\frac{\partial \psi}{\partial r} + \frac{\partial^2 \psi}{\partial z^2} = 0 \tag{2.41}$$

(as can easily be verified). The lines Φ = const. represented in the r-z plane equipotential curves, and the lines ψ = const. represent streamlines. The streamlines and the equipotential lines form a net of orthogonal curves. Therefore, from equations (2.39 and 2.40) one can show that the differential of the potential can be expressed in terms of the differential of the stream function

$$d\psi = 2\pi r \frac{d\,n}{d\,s} d\Phi \tag{2.42}$$

where *dn* is the differential along a potential line and *ds* is the differential along a streamline.
Using differences (denoted by Δ), instead of differentials, with the postulation (Harr, 1968):

$$\Delta\psi = \Delta\Phi \tag{2.43}$$

we have

$$\Delta s = 2\pi r\, \Delta n. \tag{2.44}$$

This introduced the possibility of a graphical solution which is particularly suited to the gravity flow problem. We have to construct a net of orthogonal curves satisfying (2.44) and the boundary conditions. This can be done by the method of trial and error. From the above graphical method, it is only a short step to the solution of gravity flow problems by actual numerical calculations. Such calculations have been carried out, as reported in the literature (Stallman, 1956).

Because of the difficulties involved in obtaining rigorous solutions conforming to the assumptions basic to the present considerations, approximate procedures have been developed. The best known is that by Dupuit (1863) as modified by Forchheimer (1930). If it is assumed that, for small inclinations of the free surface of a gravity flow system, the flow may be taken as horizontal and, furthermore, that the corresponding velocities are proportional to the slope of the free surface, one readily arrives at the following differential equation for the height *h* of the free surface above the (horizontal) impermeable bed of the system (Muskat, 1946):

$$\Delta (h^2) = 0 \tag{2.45}$$

Unfortunately, the assumptions basic to this simple theory do not seem to be entirely warranted, so that the entire theory has been severely questioned (Muskat, 1946). The assumptions of the Dupuit-Forchheimer theory have also been used by Boussinesq (1904) to construct a theory of the time variations of the free surface. The latter author arrived at the equation

$$n \frac{\partial h}{\partial t} = \left(\frac{k\rho g}{\mu}\right) \nabla . (h \nabla h) \tag{2.46}$$

where the symbols have their usual meaning. This equation has been simplified for certain cases so as to become linear. However, since it is based on the Dupuit-

Forchheimer assumptions and, therefore, is subject to the same criticisms, further discussion seems unnecessary (Muskat, 1946).

It has been observed that the flux formulas obtained from the Dupuit-Forchheimer theory give much better results than the underlying assumptions might lead one to expect. Muskat (1946) showed that one can arrive at the Dupuit-Forchheimer *flux* formulas by another approximate theory which is free of the Dupuit assumptions.

The analytical difficulties of obtaining solutions to the gravity-flow problems have also prompted researchers to try experimental methods. Among these methods, electrical analogies once seemed to be helpful. However, the free surface cannot be duplicated in electrical models as there are no corresponding boundaries possible for electrical currents. Thus, the procedure is one of trial and error, of shaping the electrical model, in such a manner that its boundaries correspond to a free surface. Muskat (1946). The principle outlined above in connection with the description of free surface, and seepage has been applied to specific problems. Such specific applications are simply exercises in mathematics; they are not particular interest as far as the physical aspects of flow through porous media are concerned.

2.4.2. Solution of non-Darcy flow (nonlinear flow)

Compared with the number of solutions of the laminar (linear) equations available, only a few solutions of the various turbulent (nonlinear) flow equations have been investigated. In order to obtain analytical solutions for turbulent flow through porous media, the equations which are considered as basic have to be written first in a suitable analytical (vectorial) form. Assuming that the flow is linear (i.e. of Darcy-type) up to a "critical" Reynolds number, and above that Reynolds number, it is the nonlinear (i.e. of Forchheimer-type), Engelund (1953) proposed the following set of equations

$$-\nabla p = F(|\boldsymbol{q}|)\boldsymbol{q} \tag{2.47}$$

where

$$F(|\boldsymbol{q}|) = \begin{cases} \mu / k & for \quad \boldsymbol{Re} < \boldsymbol{Re}_{critical} \\ a + b|\boldsymbol{q}| & for \quad \boldsymbol{Re} > \boldsymbol{Re}_{critical} \end{cases}. \tag{2.48}$$

A suitable modification of (2.48) can be made to take account of gravity flow simply by introducing the "hydraulic head" H, instead of p, whereupon the equation above becomes

$$-\nabla H = F(|\boldsymbol{q}|)\boldsymbol{q} \tag{2.49}$$

where

$$H = z + h = z + \frac{p}{\rho g}.$$

It is quite hopeless to try to obtain analytical solutions of the system (2.48) in the general case of three-dimensional, non-steady state flow. However, a particular three-dimensional solution has been reported by Uchida (1952). Considering only the steady state case in two dimensions, the following solutions have been developed by Engelund (1953).

In two dimensions, the system (2.48) becomes (Cartesian coordinates x, y, z)

$$-\frac{\partial p}{\partial x} = F(q)q_x \qquad \text{and} \qquad -\frac{\partial p}{\partial y} = F(q)q_y. \tag{2.50}$$

The equation for continuity, is for the steady state,

$$\frac{\partial q_x}{\partial x} + \frac{\partial q_y}{\partial y} = 0 \tag{2.51}$$

which is automatically fulfilled by the stream-function ψ, introduced and defined by

$$q_x = -\frac{\partial \psi}{\partial y} \qquad \text{and} \qquad q_y = \frac{\partial \psi}{\partial x}. \tag{2.52}$$

From equation (2.50) it is evident that the gradients of p and $\boldsymbol{q}$ are oppositly directed vectors. Since the gradient of p is perpendicular to the surface p = const., the same must hold for the filter velocity vector $\boldsymbol{q}$, so that the filter streamlines cross the equipressure surface at right angles.
It is evident from equation (2.52) that the vector gradient ψ is perpendicular to $\boldsymbol{q}$, from which it follows that $\boldsymbol{q}$ is tangent to the curves ψ = const. From this, it can be concluded that these curves may be interpreted as streamlines.
Further it may be concluded from equation (2.52) that

$$|\nabla \psi| = |\boldsymbol{q}| = q. \tag{2.53}$$

Muskat (1946) found that the streamlines, ψ = const., and the contours, p = const. form an orthogonal system, just as in linear flow. Since equations (2.50) are not linear, they can not be solved directly; however, Engelund (1953) introduced new variables which made it possible to linearize the equations. Thus, with a convenient introduction of first coordinates s and n, denoting the length of the arc along curves ψ = const. and p = const., respectively, and next considering an *infinitesimal element* of

flow confined by two neighboring streamlines and two lines of constant pressure, the equation of continuity can then be written as

$$-\frac{1}{\Delta n}\frac{\partial(\Delta n)}{\partial s}=\frac{1}{q}\frac{\partial q}{\partial s}. \tag{2.54}$$

Since $\nabla\times(\nabla)=0$, the flow equations (2.50) can be rewritten as (Engelund, 1953):

$$\nabla\times\left[F(|\boldsymbol{q}|)\boldsymbol{q}\right]=0. \tag{2.55}$$

Applying Stokes' theorem to the equation above, Engelund (1953) expressed this condition by the vanishing of the circulation around any closed curve, i.e. around the element

$$-\frac{1}{\Delta s}\frac{\partial(\Delta s)}{\partial n}=\frac{1}{Fq}\frac{\partial}{\partial n}(Fq). \tag{2.56}$$

Engelund then proceeds to introduce, as more convenient independent variables, the flow velocity q and the angle θ between the velocity vector $\boldsymbol{q}$ and the x-axis. For the angle difference between the two streamlines of the element he obtained

$$\frac{\partial\theta}{\partial n}\Delta n=-\frac{1}{\Delta s}\frac{\partial(\Delta n)}{\partial s}\Delta s. \tag{2.57}$$

Furthermore, we have

$$\frac{\partial}{\partial s}\left(\frac{\pi}{2}-\theta\right)\Delta s=-\frac{1}{\Delta n}\frac{\partial(\Delta s)}{\partial n}\Delta n. \tag{2.58}$$

These expressions reduce to

$$\frac{1}{\Delta n}\frac{\partial(\Delta n)}{\partial s}=-\frac{\partial\theta}{\partial n}\quad\text{and}\quad\frac{1}{\Delta s}\frac{\partial(\Delta s)}{\partial n}=\frac{\partial\theta}{\partial s}. \tag{2.59}$$

Substitution into equations (2.54) and (2.55) yields

$$\frac{\partial\theta}{\partial n}=\frac{1}{q}\frac{\partial q}{\partial s} \tag{2.60}$$

and

$$-\frac{\partial\theta}{\partial s}=\frac{1}{qF}\frac{\partial}{\partial n}(qF)=\left(\frac{1}{q}+\frac{F'}{F}\right)\frac{\partial q}{\partial n} \tag{2.61}$$

where F' denotes the derivative dh/dq.
The quantities p and ψ can be introduced into these equations by the substitution of $\partial\theta/\partial n = (\partial\theta/\partial\psi)(d\psi/dn) = q(\partial\theta/\partial\psi)$, etc., (Engelund, 1953), and thus the equations (2.60) and (2.61) becomes:

$$\frac{\partial\theta}{\partial\psi}=-\frac{F}{q}\frac{\partial q}{\partial p} \tag{2.62}$$

and

$$\frac{\partial\psi}{\partial p}=\frac{1}{F}\left(\frac{1}{q}+\frac{F'}{F}\right)\frac{\partial q}{\partial\psi}. \tag{2.63}$$

These equations can be solved for q and θ as functions of p and ψ, However, Engelund (1953) has expressed in the same way the functions p and ψ in terms of q and θ, and substituted these into the flow equations. which then become

$$\frac{\partial\psi}{\partial\theta}=-\frac{q}{F}\frac{\partial q}{\partial p} \tag{2.64}$$

and

$$\frac{\partial\psi}{\partial q}=\frac{1}{F}\left(\frac{1}{q}+\frac{F'}{F}\right)\frac{\partial p}{\partial\theta}. \tag{2.65}$$

Furthermore, ψ can be eliminated from these equations by appropriate differentiation, which leads to

$$\frac{1}{q}\left(\frac{q}{F}\frac{\partial p}{\partial q}\right)+\frac{1}{F}\left(\frac{1}{q}+\frac{\partial F'}{\partial F}\right)\frac{\partial^2 p}{\partial\theta^2}=0. \tag{2.66}$$

Engelund arrived at a single partial differential equation for p, which describes linear as well as nonlinear steady state flow in porous media. He showed how it can be solved for particular cases.

In the extreme case of high Reynolds numbers, the quadratic term in equation (2.66) is preponderant (truly turbulent flow), and (2.66) can be reduced to

$$\frac{\partial^2 p}{\partial q^2}+\frac{2}{q^2}\frac{\partial^2 p}{\partial\theta^2}=0. \tag{2.67}$$

flow confined by two neighboring streamlines and two lines of constant pressure, the equation of continuity can then be written as

$$-\frac{1}{\Delta n}\frac{\partial(\Delta n)}{\partial s}=\frac{1}{q}\frac{\partial q}{\partial s}. \tag{2.54}$$

Since $\nabla\times(\nabla) = 0$, the flow equations (2.50) can be rewritten as (Engelund, 1953):

$$\nabla\times\left[F(|\boldsymbol{q}|)\boldsymbol{q}\right]=0. \tag{2.55}$$

Applying Stokes' theorem to the equation above, Engelund (1953) expressed this condition by the vanishing of the circulation around any closed curve, i.e. around the element

$$-\frac{1}{\Delta s}\frac{\partial(\Delta s)}{\partial n}=\frac{1}{Fq}\frac{\partial}{\partial n}(Fq). \tag{2.56}$$

Engelund then proceeds to introduce, as more convenient independent variables, the flow velocity q and the angle θ between the velocity vector $\boldsymbol{q}$ and the x-axis. For the angle difference between the two streamlines of the element he obtained

$$\frac{\partial\theta}{\partial n}\Delta n=-\frac{1}{\Delta s}\frac{\partial(\Delta n)}{\partial s}\Delta s. \tag{2.57}$$

Furthermore, we have

$$\frac{\partial}{\partial s}\left(\frac{\pi}{2}-\theta\right)\Delta s=-\frac{1}{\Delta n}\frac{\partial(\Delta s)}{\partial n}\Delta n. \tag{2.58}$$

These expressions reduce to

$$\frac{1}{\Delta n}\frac{\partial(\Delta n)}{\partial s}=-\frac{\partial\theta}{\partial n}\quad\text{and}\quad\frac{1}{\Delta s}\frac{\partial(\Delta s)}{\partial n}=\frac{\partial\theta}{\partial s}. \tag{2.59}$$

Substitution into equations (2.54) and (2.55) yields

$$\frac{\partial\theta}{\partial n}=\frac{1}{q}\frac{\partial q}{\partial s} \tag{2.60}$$

and

$$-\frac{\partial\theta}{\partial s}=\frac{1}{qF}\frac{\partial}{\partial n}(qF)=\left(\frac{1}{q}+\frac{F'}{F}\right)\frac{\partial q}{\partial n} \tag{2.61}$$

where F' denotes the derivative dh/dq.
The quantities p and ψ can be introduced into these equations by the substitution of $\partial\theta/\partial n = (\partial\theta/\partial\psi)(d\psi/dn) = q(\partial\theta/\partial\psi)$, etc., (Engelund, 1953), and thus the equations (2.60) and (2.61) becomes:

$$\frac{\partial\theta}{\partial\psi}=-\frac{F}{q}\frac{\partial q}{\partial p} \tag{2.62}$$

and

$$\frac{\partial\psi}{\partial p}=\frac{1}{F}\left(\frac{1}{q}+\frac{F'}{F}\right)\frac{\partial q}{\partial\psi}. \tag{2.63}$$

These equations can be solved for q and θ as functions of p and ψ, However, Engelund (1953) has expressed in the same way the functions p and ψ in terms of q and θ, and substituted these into the flow equations. which then become

$$\frac{\partial\psi}{\partial\theta}=-\frac{q}{F}\frac{\partial q}{\partial p} \tag{2.64}$$

and

$$\frac{\partial\psi}{\partial q}=\frac{1}{F}\left(\frac{1}{q}+\frac{F'}{F}\right)\frac{\partial p}{\partial\theta}. \tag{2.65}$$

Furthermore, ψ can be eliminated from these equations by appropriate differentiation, which leads to

$$\frac{1}{q}\left(\frac{q}{F}\frac{\partial p}{\partial q}\right)+\frac{1}{F}\left(\frac{1}{q}+\frac{\partial F'}{\partial F}\right)\frac{\partial^2 p}{\partial\theta^2}=0. \tag{2.66}$$

Engelund arrived at a single partial differential equation for p, which describes linear as well as nonlinear steady state flow in porous media. He showed how it can be solved for particular cases.

In the extreme case of high Reynolds numbers, the quadratic term in equation (2.66) is preponderant (truly turbulent flow), and (2.66) can be reduced to

$$\frac{\partial^2 p}{\partial q^2}+\frac{2}{q^2}\frac{\partial^2 p}{\partial\theta^2}=0. \tag{2.67}$$

According to the above equation, Engelund lists a set of specific solutions. As an illustrative example, one can reproduce here Engelund's solution for the symmetrical radial flow to a single well.
On account of symmetry, p is independent of θ and (2.67) becomes

$$\frac{\partial^2 p}{\partial q^2} = 0 \tag{2.68}$$

from which

$$p = c_1 q + c_2 \tag{2.69}$$

in this case p is a linear function of q. To see how p depends on the distance from the axis of the well, Scheidegger (1967) proposed

$$\frac{\partial p}{\partial r} = bq^2 = c_1 \frac{dq}{dr}. \tag{2.70}$$

The solution of this equation is

$$q = -\frac{c_1}{br} \quad \text{or} \quad c_1 = -2\pi qr\frac{b}{2\pi} = Q\frac{b}{2\pi} \tag{2.71}$$

where Q denotes the discharge per unit length of the well. Thus, p becomes

$$p = \frac{bQ}{2\pi} q + c_2 = \frac{Q^2 b}{4\pi^2 r} + c_2. \tag{2.72}$$

Solutions to the more general flow equation of Engelund (Eq. 2.66) are much more tedious to obtain. Engelund listed a variety of methods and applied them to a series of special cases which are of interest in the theory of groundwater flow into wells, drainage tubes, etc.

2.5. Influence of seepage on soil stability

One of the major concerns regarding the safety of embankment dams is the problem of internal soil stability when particles are subjected to drag forces resulting from reservoir seepage. This problem is particularly important when transverse cracking of the core occurs; this cracking is caused by differential settlement or hydraulic fracture, both of which can cause serious internal erosion resulting in catastrophic failure of dams. Numerous cases of near failure and total failure of dams, as a result of internal erosion, have been investigated and reported in detail in the literature

(Sherard, 1972). These studies have covered two aspects of the design of filters to prevent internal erosion. First, transverse cracking within the impervious core zone of dams is common and filters must, therefore, be capable of blocking internal erosion if such cracking should occur. Second, there has been recent recognition of the high erodibilty of dispersive soils (Sherard, 1974) and the need of increased knowledge for the design of the filters to block such erosion.

Seepage force can combine with soil weights to improve stability or worsen it, depending on the direction in which the forces act in relation to the geometric cross section; for example, if one considers an element where the flow acts downward, the drag force will act in the same direction as the weight of the soil particles, and tend to fix the particles in their positions. On the other hand, when the seepage force acts upward, the stability will depend on the weight of the particles compared with seepage forces (Cedergren, 1989).
The forces of seepage water often enter into calculations for the design of many different types of civil engineering works. When the forces acting on large earth masses are not in stable equilibrium, massive failures can take place. If the forces acting on individual soil particles are large and these particles are not firmly held in place, internal erosion and piping failures can take place. Dams and other important works influenced by seepage should be designed with suitable filters and drains (Harr, 1968).

Seeping water imparts a force to individual soil grains by friction. The force, F, acting on a given volume, V, of soil is equal to the volume in cubic meter multiplied by the unit weight of water, in newton per cubic meter and the hydraulic gradient; that is

$$F_l / V = \gamma_w J. \tag{2.73}$$

If the hydraulic gradient is 1.0, the seepage force per unit volume is equal to the unit weight of the water. Figure 2.3 shows a small volume of sand confined in a tube fitted with reservoirs on both sides. Head, h_1, presses on the sand at the left, while head, h_2, does so on the right. According to hydraulics, the water pressure force [N] on the left side of the sand is

$$P_1 = \gamma_w h_1 A \tag{2.74}$$

in which A is a cross-sectional area of the sand normal to the direction of flow. Likewise, the pressure force [N] on the right side is

$$P_2 = \gamma_w h_2 A. \tag{2.75}$$

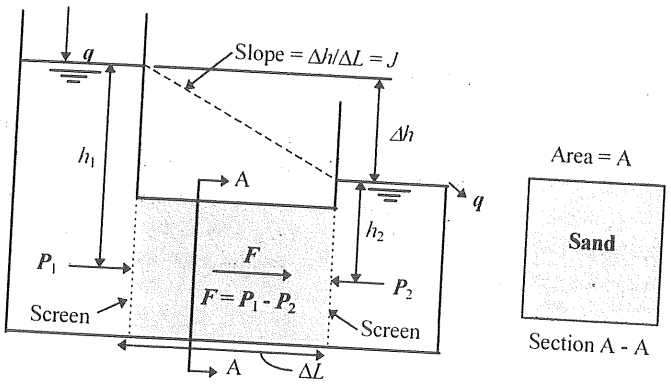

Figure 2.3. Seepage forces in soil

The resultant seepage force subjected by the flow on the soil is

$$P_1 - P_2 = \gamma_w A(h_1 - h_2). \tag{2.76}$$

Accordingly, the seepage force is proportional to the differential head and the cross-sectional area of the soil. Hence, seepage forces in earth masses can easily be determined when frictional force is expressed in relation to *hydraulic gradient J*, as in equation (2.73) This expression has been derived as follows.
The hydraulic gradient in the soil is

$$J = \frac{(h_1 - h_2)}{\Delta L} \tag{2.77}$$

which can also be expressed as $\Delta h/\Delta L$. The force exerted on the soil grains by friction must be equal to the difference in energy head between the upstream and downstream faces. The volume of soil is $V = A\,\Delta L$. Hence, equation (2.73) is already derived as

$$F_t = \Delta h \gamma_w A = \gamma_w \frac{\Delta h}{\Delta L} V. \tag{2.78}$$

The differential head Δh is always a measure of the loss in energy between two points. However, pressure difference can exist without seepage. The magnitude of the seepage force acting on a volume of soil must always be equal to that indicated in equation (2.73). In practice, this may be determined by either of two methods which require a flow net and give exactly the same result provided the work is carried out accurately.

(1) Calculate directly from equation (2.73), using hydraulic gradients measured in flow nets (gradient method).

(2) Determine graphically, using the boundary pressure method (Cedergren, 1989).

The amount of work required for determining seepage forces by the boundary pressure method is several times that required by the gradient method. For most applications, the gradient method is sufficiently accurate; however, in cases in which the gradient method can be applied only with difficulty, the boundary pressure method can always be used with confidence as the primary or referee method.

2.5.1. Seepage force in earth dams

It is generally assumed that when filters are provided there will be no need to concern for the magnitude of hydraulic gradients, because properly designed filters can provide 100% protection for gradients of any magnitude in earth dams. This requires, however, that every part of the impervious zone be protected with correctly designed filters. However it is generally known that not every contractor building dams and other works is aware of the difference between a properly constructed filter and one that can lead to failure. The importance of protecting every square meter of erodible zones cannot be overemphasized. With proper control of construction, there is no big problem in designing a dam with high internal gradients, however designs having high seepage gradients should offer substantial benefits. All other factors being equal, designs that hold internal gradients to low levels are safer than those that have exceptionally high gradients.

Under normal operating conditions, the downstream supporting embankments and the toe of dam are not to be exposed to seepage forces; often no requirements are specified for the drainage capacity of a dam. Some drainage capacity is, however, essential for the safety of the dam in case overtopping or big leaks should accidentally occur. This situation must be studied and constitutes a part of the overall risk analysis for a dam (Sherard, 1985).

Outflow of water at the toe of the dam is illustrated in Figure 2.4. Depending on the run-off intensity, the quantity of water exit on the slope at a certain level above the base can be determined by the hydraulic conductivity of the fill. The fill is subjected to seepage forces and pore water pressures which reduce the stability along potential sliding planes inside the fill. The overflowed part of the slope is also exposed to surface unraveling and erosion stone by stone.

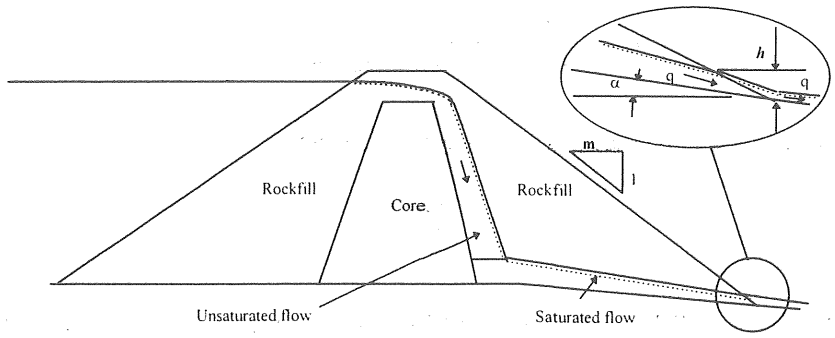

Figure 2.4. Outflow of water at the toe of a dam.

Flow through coarse rock fills is generally turbulent, and Darcy's law does not for this flow. Hence, the flow velocity is calculated as being (Solvik, 1976)

$$q = \sqrt{K_t \, J} \qquad (2.$$

where q is the flow velocity, K_t is the hydraulic conductivity at turbulent (m^2/sec^2), and J is the hydraulic gradient.

The turbulent hydraulic conductivity may roughly be estimated from the equation:

$$K_t = \frac{1}{\beta_0} \frac{n^3}{1-n} g \, d_t \qquad (2.$$

where β_0 is the grain shape factor ($\beta_0 = 3.6$ for quarried rock), n is the porosity o fill material, g is the acceleration of gravity, and d_t is the significant particle size.

In well-graded materials the significant particle size is approximated by $d_t = 1.7\, d_{10}$. For narrowly graded materials, $d_t = d_{50}$ is similarly used. The opening diameters d_{10} and d_{50} represent the sieve openings through which 10% 50%, respectively, of the materials would pass (by weight).

The porosity, n, may be in the range of 20-30% for well graded and well comp materials, and 35-40% for narrowly graded material. The hydraulic conductivit (m^2/sec^2), would be on the order of 0.1 d_{10} (m) for the rock-fill supporting sho and 0.2 d_{50} for the cover stones in the toe and the slope protection. The hydr conductivity of the rock-fill shoulder can easily be less than 1% of the hydr conductivity of the protective cover layer of large stones, and is substantially re with increasing content of fines. The water exits in the slope at an elevation, h, by the cross-sectional area required for the actual flow (Figure 2.4);

(2) Determine graphically, using the boundary pressure method (Cedergren, 1989).

The amount of work required for determining seepage forces by the boundary pressure method is several times that required by the gradient method. For most applications, the gradient method is sufficiently accurate; however, in cases in which the gradient method can be applied only with difficulty, the boundary pressure method can always be used with confidence as the primary or referee method.

2.5.1. Seepage force in earth dams

It is generally assumed that when filters are provided there will be no need to concern for the magnitude of hydraulic gradients, because properly designed filters can provide 100% protection for gradients of any magnitude in earth dams. This requires, however, that every part of the impervious zone be protected with correctly designed filters. However it is generally known that not every contractor building dams and other works is aware of the difference between a properly constructed filter and one that can lead to failure. The importance of protecting every square meter of erodible zones cannot be overemphasized. With proper control of construction, there is no big problem in designing a dam with high internal gradients, however designs having high seepage gradients should offer substantial benefits. All other factors being equal, designs that hold internal gradients to low levels are safer than those that have exceptionally high gradients.

Under normal operating conditions, the downstream supporting embankments and the toe of dam are not to be exposed to seepage forces; often no requirements are specified for the drainage capacity of a dam. Some drainage capacity is, however, essential for the safety of the dam in case overtopping or big leaks should accidentally occur. This situation must be studied and constitutes a part of the overall risk analysis for a dam (Sherard, 1985).

Outflow of water at the toe of the dam is illustrated in Figure 2.4. Depending on the run-off intensity, the quantity of water exit on the slope at a certain level above the base can be determined by the hydraulic conductivity of the fill. The fill is subjected to seepage forces and pore water pressures which reduce the stability along potential sliding planes inside the fill. The overflowed part of the slope is also exposed to surface unraveling and erosion stone by stone.

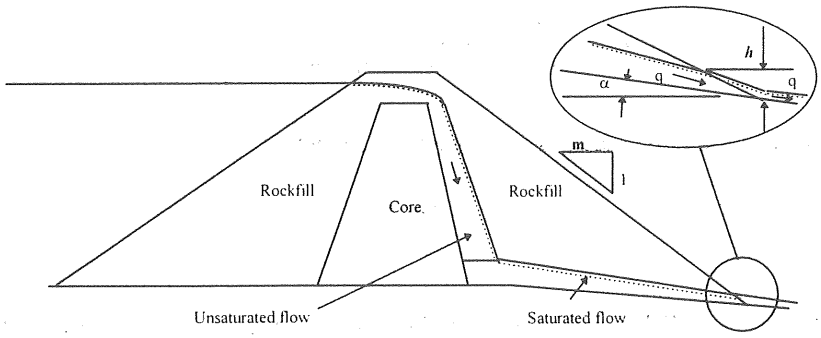

Figure 2.4. Outflow of water at the toe of a dam.

Flow through coarse rock fills is generally turbulent, and Darcy's law does not hold for this flow. Hence, the flow velocity is calculated as being (Solvik, 1976)

$$q = \sqrt{K_t J} \tag{2.79}$$

where q is the flow velocity, K_t is the hydraulic conductivity at turbulent flow (m^2/sec^2), and J is the hydraulic gradient.

The turbulent hydraulic conductivity may roughly be estimated from the equation:

$$K_t = \frac{1}{\beta_0}\frac{n^3}{1-n} g\, d_t \tag{2.80}$$

where β_0 is the grain shape factor ($\beta_0 = 3.6$ for quarried rock), n is the porosity of the fill material, g is the acceleration of gravity, and d_t is the significant particle size.

In well-graded materials the significant particle size is approximated by $d_t = 1.7\, d_{10}$. For narrowly graded materials, $d_t = d_{50}$ is similarly used. The sieve opening diameters d_{10} and d_{50} represent the sieve openings through which 10% and 50%, respectively, of the materials would pass (by weight).

The porosity, n, may be in the range of 20-30% for well graded and well compacted materials, and 35-40% for narrowly graded material. The hydraulic conductivity, K_t (m^2/sec^2), would be on the order of $0.1\, d_{10}$ (m) for the rock-fill supporting shoulder and $0.2\, d_{50}$ for the cover stones in the toe and the slope protection. The hydraulic conductivity of the rock-fill shoulder can easily be less than 1% of the hydraulic conductivity of the protective cover layer of large stones, and is substantially reduced with increasing content of fines. The water exits in the slope at an elevation, $\boldsymbol{h}$, given by the cross-sectional area required for the actual flow (Figure 2.4);

$$h = \frac{Q_s}{\sqrt{K_t\, J}} \frac{1}{(1 - \mathbf{m}\, tan\alpha)\, cos\alpha}. \qquad (2.81)$$

For the case where $\alpha = 0$, the above equation becomes

$$h = \frac{Q_s}{\sqrt{K_t\, J}} \qquad (2.82)$$

where h is the elevation above the reference level (m); Q_s is the specific flow of water (m^3/sec.m); $\mathbf{m}$ is the slope inclination ratio, $\mathbf{m} = \tan\beta$; α is the slope angle of the rock surface in the direction of the flow; and β is the angle of the dam slope.

When the surface of the dam above the tip of the toe and below elevation, h, overflowed. The specific flow, q, has a threshold value for the stability of the slope depending on the size and weight of the stones, the foundation inclination, α, the effective angle of friction, ϕ', and the slope inclination ratio, $\mathbf{m}$. For a given total outflow, Q_T, the specific flow, Q_s, is determined by the shape and width of the dam at the toe. The specific flow may be increased dramatically by narrowing gorge effects towards the toe.

Wörman and Olofsdotter (1991) stated in their analysis of the mechanism of interfacial erosion, that fluid flow through soil, will cause momentum transferring process from the fluid to the solid matrix. They found that when the exchange of momentum per unit time and area of solid matrix is sufficiently large, some grains that not locked in the solid matrix by inter-granular forces may become mobile. Hence, they concluded that this phenomenon can be pronounced in the contact surface between two materials of different grain size because the finer grains can pass through the pores of the coarser material. They also concluded that the transport rate depends on the forces applied by the fluid on individual, transported grains and the weight of the grains, which is also discussed in this study (see Section 2.5). Furthermore, they found that the transport and filtration of particles with a diameter below 100 μm is affected also by inter-granular forces due to electrostatic interaction between charged particles and London-Van der Waals forces between dipole-dipole, in which such electro-chemical forces result in cohesion within a medium, and in adhesion (and possibly adsorption) between the transported particles and transport medium (fluid) (Wörman and Olofsdotter, 1991). Hence, analysis of migration of clay core material in dams would require consideration of these phenomena. To prevent the transport of finer materials into the coarser one and to provide at the same time a draining capacity to reduce the possible excessive pore water pressure inside the embankments, a well-graded filter designed and placed carefully is necessary; consequently, filter criteria need to be taken into account in this study.

2.5.2. Filter importance and design criterion

For earth-fill and rock-fill dams, protective filters consisting of selected sands, gravel, or both, are usually installed within the cross section of the dam. The filters have two main functions: (1) to prevent internal erosion by blocking migration of particles from impervious core zones; and (2) to facilitate internal drainage of seepage flows, thus preventing excess hydrostatic pressure within the dam or foundation. In order to prevent internal erosion, the basic requirement of a filter is two-fold. First, it must have sufficiently small pore size to the prevent escape of core particles through the filter voids; second, its capacity for blocking migration of core particles must be continuous over the entire seepage surface, with no local discontinuities (Harr, 1968).

The current design practices for filters in earth-fill and rocks-fill dams is an outgrowth of a well-known concept proposed by Terzaghi (1922). His simple empirical criteria were: $D_{15f}/ D_{85b} < 4$ for hydraulic stability (D_{15f} is the size of filter particles that hold; D_{85b} is the size of the soil particles subjected to seepage force) and $D_{15f} / D_{15b} > 4$ to satisfy permeability requirements (D_{15b} is the size of particles of soil that filter seepage). These simple criteria do not give a unique filter gradation for a particular base-soil. The range of the 15% filter size, D_{15}, that the criteria allow increases progressively as the width of the base soil increases. For any D_{15f}, the void volume and permeability decrease as the width of gradation of the filter increases, and vice versa. Sand-gravel filter material that satisfies the D_{15f}/ D_{85b} ratio may be so widely graded that its hydraulic conductivity is not significantly different from that of the base material. This was the case at the Teton Dam (Casagrande, 1976). A widely graded sand-gravel filter can have two other serious defects. First, if it contains a significant percentage of fines passing the #200 sieve, then these fines, together with any interlocking effect due to the wide gradation, may impart sufficient cohesion for the filter to sustain a transverse crack. This would cause a discontinuity in the filter through which core material could be easily transported. Second, a widely graded filter material is difficult to place without segregation. This would result in discontinuity with the same consequences as before. Cedergren (1976, 1973) has emphasized the importance of these additional factors that should be considered in the selection of appropriate filter gradation within the limitation of the gradations that meet the Terzaghi criteria. Other investigators have sought to improve the Terzaghi filter design criteria by amplifying them in such a way that they yield a more specific gradation. In the author's opinion, the main effect of the amplifications of the Terzaghi criteria is that they permit the use of widely graded sand-gravel mixtures as filter materials.

However, consideration has not yet been given to the erodibilty characteristics of the core material in the design of protective filters. Many examples of gradations of the filter, shell and non-dispersive cohesive embankment or core material, which are based on Terzaghi criteria and are used in different dams have failed or nearly failed. It can be concluded that the gradation characteristics of the core fine alone do not yield enough information to determine whether or not a certain filter is suitable.

Consequently consideration of the erodibilty characteristics of the fine is also necessary in design of protective filters.

According to the above, it can be concluded that the idea of including deflocculated fines, which have a clogging tendency in core material, can give sufficient improvement to the filter performance. In fact, it is important to decide how much fine material is necessary to prevent the passage of eroded soil and at the same time, to block transverse crack (Sherman, 1978, 1979).

A variety of empirical tests has been used by different investigators to identify and classify soils with respect to their dispersion characteristics: the Crumb test (Emerson, 1954), the SCS dispersion ratio test (Decker, 1976), and the pinhole test (Sherard, 1976). These three tests are used mainly to identify dispersive clays; and even them are not suitable for all cases. The reasons that these tests are not suitable to identify the erosion characteristics of some soil types have been reported in the literature (Perry, 1976). It has been shown that the system of classification used in above tests is not able to predict piping performance. The author concludes that the reason for this incomplete classification is that it does not take into account important erosion factors, such as the chemistry of the soil and the composition of pore and eroding fluid.

2.5.3. Erodibility characteristics of soils

Soil erosion is a complex mechanism involving the soil and the nature of the interaction between the pore and eroding fluid at the surface. Because the critical shear stress, τ_c, is dependent on these factors, it can be used as a fundamental parameter to classify erodibilty characteristics. Hence, one of the accepted approaches for the evaluation of initiation and sustainability of particle motion or aggregation involves the calculation of the shear stresses caused by hydraulic flow. Any critical shear designation should indicate either: (1) a stress at which erosion begins; or (2) a stress that would cause a particular erosion rate. The critical shear stress which would cause a particular erosion resistance was defined by Shields (1936) as the value of the stress for zero sediment discharge that would be obtained by extrapolating a graph of observed erosion rate versus shear stress. Numerous results showing the influence of clay type and amount, pore and eroding fluid compositions, pH, temperature, and organic matter on τ_c, are reported in the literature. It can be concluded, based on these limited studies, that certain categories are proposed for the classification of core materials with respect to their erosion resistance (Arulanandan, 1973, 1976 and 1977). These categories, defined in term of critical shear stress, are:

1. Erodible soil, $\tau_c < 40$ N/m^2,
2. Moderately erodible fines, 40 N/m^2 $< \tau_c <$ 90 N/m^2, and
3. Erosion resistance soils, $\tau_c > 90$ N/m^2.

In addition to the previous requirements, there are two other considerations that are important in the evaluation of dam stability. The first is the concentration of suspended sediment and chemicals in eroding fluid (Reservoir water for existing dam and river water for proposed dam), which can have a major effect on the erodibilty of core material. Second, attention should be given to the permeability, crack resistance, and segregation characteristics of the filter material.

2.6. Field measurements

Experimental work has been done on the flow of water through different models of fill dams with different characteristics to verify the theoretical analysis of the flow equation. Linear and nonlinear equations have been applied to flow models found in the literature. Bear (1972) has published a detailed discussion of the work done for nonlinear flow equations. A comparison with a numerical finite element solution is also given in his conclusion.

Volker (1969) studied the seepage through a model of a gravel bank in an open flume. The flow conditions were then analyzed by the finite element method and checked against the experimental results. He used a flume 2.0 ft. wide and 2.0 ft. deep with one clear perspex side for viewing purposes. Drilled holes were made on the steel side to allow measurement of the piezometric heads.
No attempt was made in his experiments to model actual dam conditions, since the purpose of the investigation was simply to determine whether the numerical solution of the differential equations for nonlinear flow could predict accurately the position of the free surface and the quantity of discharge for known boundary conditions and material properties.
Volker also used a wire screen positioned at the toe of the gravel dam to prevent scour of material there. The flow ended in a vertical drop-off at the screen resulting in zero tailwater depth. No analysis of the stability of the gravel bank was considered in his applications.
His experimental work has shown that, provided the appropriate coefficients in the nonlinear flow equation are accurately measured and known, the finite element solutions agree well with observations of actual flow through coarse materials on a horizontal impervious base. Comparison of the results from two equations has shown that an equation of the Forchheimer type gives a small but significant improvement over one of the exponential type when calculating the discharge through coarse granular material. In view of the rational basis of the Forchheimer equation, one can realize from Volker's results that this improvement would become much more important when considering wider variations in flow range as in prototype rock-fill banks. He found also that there are some problems in obtaining solutions for flows with a cut-off wall, as this introduces singularities on the impermeable boundary which cause difficulties in the numerical analysis. Volker found that the nature of the flow passing over the cut-off wall cannot be represented exactly by the steady

continuous flow assumed in a theoretical analysis. Despite this, he concluded that discharge can be predicted to within about 10% of the observed value, which would normally be an acceptable result for engineering purposes.

Experiments have also been done by McCorquodale (1970) for steady and unsteady flow in rock-fill dams of rectangular section by applying non-Darcy flow equations. He followed also the work of Engelund (1953) by solving non-Darcy free-surface flow problems by finite-element analysis. Engelund (1953) gave the functional equation for turbulent and transitional two-dimensional flow. Hence, the purpose of McCorquodale's study was to present a modification of the functional equation used by Engelund (1953), which would be suitable for laminar, turbulent, and transitional two-dimensional flows. The finite element method was formulated and the solutions for non-Darcy free surface flows through the rectangular section were compared with their corresponding experimental flow fields. His experimental data were in good agreement with the finite-element solution.

Ching (1988) illustrated a boundary-element solution procedure which can be applied to the analysis of both steady-state and non-steady-state unconfined seepage problems. This analysis are performed for a laboratory model and prototype earth dams to determine the position of the free surface in steady-state conditions, as well as the movement of the free surface in a transient condition resulting from drawdown of the water level in a reservoir. The applicability of his method was evaluated by the means of comparison between the numerical solutions and measured laboratory and field data. The principles of the continuity of flow and Darcy's law were applied to formulate the boundary element problem with the utility of the kinematic boundary conditions proposed by Bear (1972). The final results showed that the boundary element method based on the described procedure is an efficient tool for the analysis of unconfined flow problems. He found that both steady and non-steady-state conditions can be solved by the same numerical algorithm which permits greater convenience.
The agreement between measured and predicted spatial variation of pore-pressure heads within a dam under both steady and non-steady state conditions has been found by Ching (1988) to be reasonable. He found that, under a drawdown condition, the rate of change in pressure heads depends not only on the drawdown rate of the pool level but also significantly on the locations where the pressure heads were measured within the dam. On the other hand he found that pore-pressure heads in the downstream side of the dam usually decrease at a much slower rate than those in the upstream side of the dam.

The effects of capillarity and change of hydraulic conductivity of the soil due to the change of soil skeleton were omitted in the formulation of the boundary element problem, although Ching did find a satisfactory correlation between the numerical solutions and laboratory and field observations. He has suggested that, for practical purposes, it may not be necessary to refine the analytic method to include the effects of capillarity and time-dependent hydraulic conductivity. He supposed that the

solution to the seepage problem can be considered adequate for the problems under consideration.

The author believes that the most important conclusion is about the controlling factor for seepage quantity, which is the hydraulic conductivity of the soil. Ching concluded that in most cases this can only be determined approximately in the laboratory. Therefore, there is an uncertainty in the predicted flow quantity. On the other hand, he found that the predicted pore-pressure heads are relatively insensitive to the hydraulic conductivity. Hence, the predicted pore pressure is more reliable, despite the degree of uncertainty, in the estimated hydraulic conductivities.

2.7. Numerical solutions

One can find that, in many cases, the partial differential equations governing flow through porous media cannot be solved by exact analytical methods. In certain cases, although a general analytical solution can be obtained, say in the form of an infinite series, it is very difficult and tedious to apply it to a specific problem. This is especially so when the boundaries of the flow domain have an irregular shape or, for free surface, gravity flow. In section 2.4 models and analogies are described that are used as tools for solving such problems. In the present section, some numerical techniques are outlined for the same purpose.

2.7.1. Method of finite differences

In most numerical methods of solving differential equations, the first step is to replace the differential equations by algebraic *finite difference equations*. These are relationships between the values of a dependent variable e.g. φ, at neighboring points of the x, y, z, t space. The numerical solution of the series of simultaneous equations thus obtained gives the values of the dependent variables at a predetermined number of discrete points (grid points) throughout the domain investigated. For simplicity most problems are limited mainly to two-dimensional flows.
In order to solve a problem in the xy plane, the flow domain **R** enclosed by a boundary **B** is divided by a mesh of grid lines as shown in Figure 2.5.

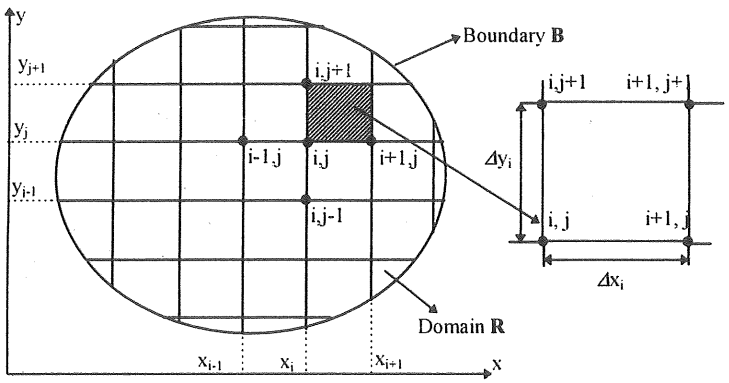

Figure 2.5. A grid for a numerical solution.

The distance between grid lines need not be constant throughout the flow domain. In some cases, when a specific need for a variable grid spacing arises, the spacing is often with $\Delta x_i = \Delta y_i = constant$. The grid lines then form a network of squares. For time-dependent problems, time is divided into increments Δt. In general, all time increments are chosen equal (Bear, 1979).

The differential equations are replaced by finite difference equations written in terms of the values of the dependent variables at the grid points. The solution of the difference equation, or the set of difference equations, is carried out numerically, by means of a high speed digital computer. If we denote the exact solution of the differential equation by S, the exact solutions of the difference equations by D, and the numerical solution of the difference equation by N, then we can call $|S - D|$ the truncation error, and $|D - N|$ the numerical, or the round-off error.

Trescott *et al.* (1976) suggest that, to avoid large truncation errors and possible convergence problems, one should use $\Delta x_i / \Delta x_{i-1} \leq 1.5$ whenever a variable grid is employed. Also they suggest that the grid should be oriented such that a minimum number of nodes are outside the aquifer domain considered. In an anisotropic aquifer, it is preferable to orient the grid with its axes parallel to the principal directions.
In general, the condition for convergence of the solution is that $|S - D| \rightarrow 0$ everywhere in the solution domain. The condition for stability is that everywhere in the solution domain $|D - N| \rightarrow 0$. The problem is to find N such that over the whole region of interest $|S - D|$ is smaller than the chosen error criterion. As $(S - N) = (S - D) + (D - N)$, the total error is made up of the truncation error and the round-off error. The truncation error, which is due to the arbitrary form selected for the finite difference equation, is often the larger part of the total error.
The finite difference equations can be obtained in two ways. The first, mathematical, approach is to approximate the derivatives appearing in the partial differential

equations. The second, physical, approach is to consider the water balance of an element of area $\Delta x_i \, \Delta y_i$. This is actually the first step in developing any continuity equation using the control box approach, before proceeding to the next step of letting Δt and the dimensions of the control box go to zero. This approach is also discussed in the literature in connection with a multiple-cell aquifer model (Bear, 1972).

2.7.2. Method of finite elements

Starting in the mid-1960s, a very powerful numerical technique-generally known as the finite element method–has been applied to numerous problems of flow through porous media, groundwater flow, multiphase flow, flow with a phreatic surface, hydrodynamic dispersion, consolidation, and heat and mass flow through porous media. This is a very powerful and extremely flexible method. It can handle any shape of the boundary and any combination of boundary conditions, inhomogeneous and anisotropic media, moving boundaries (by continuously changing the grid), free surface and interface, deformable media, etc.

In the finite element method, the objective is to transform the partial differential equation into an integral equation that includes derivatives of the first order only. Then the integration is performed numerically over elements into which the considered domain is divided.

The free surface in finite element solution

Boundary conditions in the form of prescribed heads and non-zero quantity of flow can be dealt with easily in the finite element formulation. More difficult circumstances arise when there is a free surface or under conditions of saturated-unsaturated flow.

Free surface for steady flow is usually determined by using iterative procedures, (Desai, 1972; Volker, 1969; Finn, 1967). The location of the free surface is first guessed and then modified successively on the basis of the values of fluid heads computed at each step of iteration. The boundary conditions of no flow across and of the total head equal to the head at the free surface are checked at each step, and an iterative procedure is carried out until the location of the free surface becomes essentially fixed. Hence, along the free surface we have

$$\frac{\partial \phi}{\partial n} = 0 \tag{2.82}$$

where

$$\phi = z(t). \tag{2.83}$$

On the other hand, the location of a transient free surface is relatively more difficult. Many procedures have been proposed. The procedure proposed by Desai, (1970, 1972) and Taylor *et al.* (1971) is based on the solution of the steady state version of the following equation,

$$\frac{\partial}{\partial x}\left(K_x \frac{\partial \phi}{\partial x}\right)+\frac{\partial}{\partial y}\left(K_y \frac{\partial \phi}{\partial y}\right)+\frac{\partial}{\partial z}\left(K_z \frac{\partial \phi}{\partial z}\right)+\overline{Q}=n\frac{\partial \phi}{\partial t} \tag{2.84}$$

where $\overline{Q}$ is the applied fluid flux.

The equation above is based on Darcy's law with a non-homogeneous porous medium.

At each time interval, the movements of the free surface (nodes) are obtained from computed values of nodal heads and velocities. The coordinates of the nodes on the free surface are then modified as

$$x_i^{t+\Delta t} = x_i^t + \Delta t\, \dot{x}_i(t') \tag{2.85}$$

where x_i denotes coordinates of nodal points on the free surface, i = 1,2...N, N is the number of the nodes on the free surface, t is the time, Δt is the time increment, the overdot denotes the rate of change of x_i, and t' is between t and $t+\Delta t$. In this case a possible difference scheme would be simply to use $t' = t$ which essentially yields a forward difference integration in time. It has been shown in the literature that it is usually necessary to use a small value of Δt in order to assure acceptable accuracy.

The foregoing scheme has been modified by Desai (1971) to include an iterative procedure in which alternative locations for computing $\dot{x}_i$ can be used. Based on what are known as Lipschitz's conditions, the size of Δt is increased or decreased automatically such that convergence and stability are assured at each time step.

Neuman and Witherspoon (1971) formulated the problem by using the variational principle. The resulting set of nonlinear differential equations was integrated in time by using the Crank-Nicolson procedure. From quantitative results, the scheme denoted above was considered to be unconditionally stable.
McCorquodale (1970) used the concept of Lagrangian coordinates for flow governed by a non-Darcy law (Forchheimer equation), and got a set of nonlinear equations that were solved by using the successive overrelaxation method. The stability of the procedure was found to depend on the size of Δt.
The concept of free surface is valid for many practical problems such as flow through silty, sandy and granular media. For certain situations, it is useful to look at the

problems as saturated-unsaturated flow and aim at determination of the zone of separation of the two regimes, rather than to try to find a distinct free surface.

Unsaturated or partially saturated flow problems using the FD method have been solved for the free surface by satisfying the conditions of zero pressure (Reisenauer, 1963; Taylor and Luthin, 1969). Desai (1970, 1971) used a procedure in which the fluid heads were computed in the entire flow domain and the free surface was located by finding those points where the total head equaled their elevation heads. The exit point on the free surface of seepage was located by an iterative procedure coupled with another method called fragments.

Neuman has proposed a general procedure, in which the free surface is located by finding points where the pressure head vanishes and the surface of the seepage is handled by a special iterative method. The advantage of these approaches is that we can avoid the necessity of deforming the finite elements mesh as required in the foregoing schemes. Alternative procedures based on the concept of space-time finite elements complete discretization with the well-known Galerkin's method (Desia, 1971; Oden, 1972; and FIDAP, 1996) have been proposed in many cases. General use of this concept will require further studies to evaluate it in the conventional semi discretization procedures.

3. Analysis of the problem

3.1. Problem to be solved

The investigation of seepage mechanisms in hydraulic structures and effects of piping problems requires a pre-study of the flow profile in various cases and for different degrees of freedom. In order to design and provide safe embankments for earth dams, the study presented here is based on numerical simulation of groundwater flow and flow through porous media with a gravity effect. Numerical experiments are done for various porous materials with incorporation of linear and nonlinear flow equations, in order to prove the need for a nonlinear relation between hydraulic gradient and the flow velocity

In most cases simulated with the experimental data, the analytical solutions are much more difficult to apply in those cases of gravity flow with a free surface. Polubarinova-Kochina (1958) and many others have proposed several transformations of the flow geometry using the hodograph solution methods. They solved both linear and nonlinear flow equations. However, these solutions are limited to a defined geometry. Hence, the numerical solution offers a better chance to solve cases with complicated flow domains.

Although mathematical solutions have been developed for particular cases of flow, the solutions are cumbersome and often approximate. Harr (1962) presents an interesting treatment of seepage theory, giving both rigorous and approximate mathematical solutions to seepage under weirs and other structures. He described, by conformal mapping, the velocity hodograph, and other special mapping techniques, such as the Zhukovsky functions and the Schwarz-Christoffel transformations.

In the current work, two-dimensional steady flow models are proposed. Two simulation problems of isothermal seepage through confined porous media were selected and solved analytically, then numerically by using the computer program (FIDAP, 1996). A problem of unconfined flow with a free surface was selected and solved by three different analytical methods.

3.1.1. Rectilinear confined flow

The domain for the problem simulated of a rectilinear confined flow is shown in Figure 3.1.

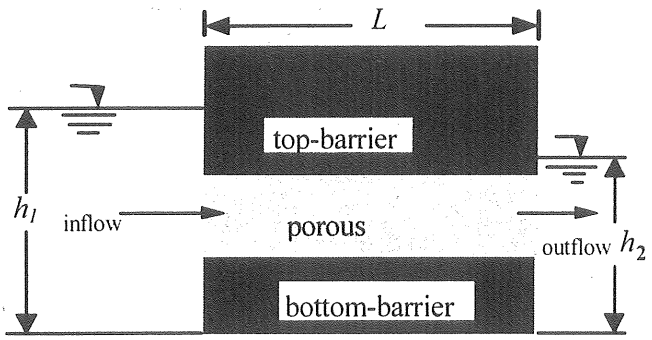

Figure 3.1. Schematic diagram of the rectilinear flow problem.

The flow domain is taken to be a homogeneous and isotropic, rectangular porous medium with a constant head difference between the upstream and downstream boundaries. Hence, we have a case without gravity effect where the flow is forced to be rectilinear. A case like this is expected to give an accurate solution when the Darcy law is applied (cf. 2.2). It is a simple case in which analytical solutions can easily be found for both linear and nonlinear relations (see Figure 2.2). Hence, an analytical solution is applied and a comparison with the numerical results is illustrated in this study, where linear and nonlinear relations are applied for laminar and turbulent states.

3.1.2. Radial confined flow

The complexity of the boundary configurations limits, in general, a broad application of exact mathematical methods for the solution of the flow in a porous medium. Some problems involving simple but practical boundaries have been solved in a closed form, yielding results of value both in the situation of immediate interest and in the interpretation of more complicated conditions. Hence, in this work we will consider the most elementary but, nevertheless, significant problem. A cylindrical flow domain is treated in this numerical presentation. In this simulation, the same degree of freedom as in the rectilinear case applies. The main difference between the cases is in the boundary configuration of the flow domain, which implies some changes in the boundary entity in order to meet the physical principle of the flow in such a domain. The geometry of the cylindrical flow domain is shown in Figure 3.2.

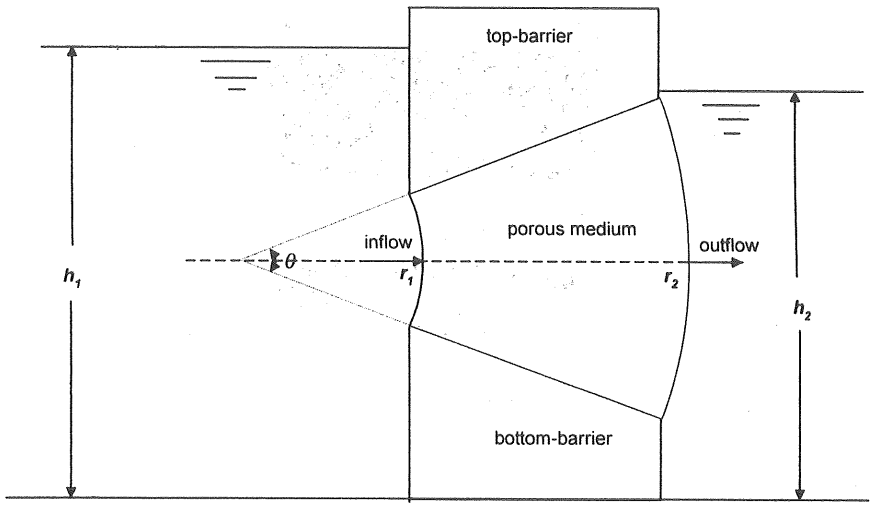

Figure 3.2. Schematic diagram of the radial flow problem

The cross-section area of the flow domain in this case varies with the radial distance. With this kind of geometrical shape, one can provide two directions for the flow velocity in x and y. In principle, the flow velocity is a function of the radial distance. The linear and nonlinear numerical models were also applied in this case, in order to make an accurate estimation of both equations for radial flow. At the same time, two forms of analytical solution for the radial flow were obtained and applied. A comparison of numerical solutions with the available analytical solutions was made. Different kinds of homogeneous isotropic porous media were specified in the numerical simulation which in turn provided two flow regimes (laminar and turbulent). The comparison gave a clear picture of the effect of the nonlinear term in the flow equation.

3.1.3. Free surface unconfined flow

When flow occurs through the medium of an earth dam, we are faced with an additional complexity: the top flow line must satisfy the requirement of being everywhere at atmospheric pressure; in other words, the total head at every point on the top flow line must be equal to the elevation head of the point. Although the mathematical solution is complicated by this condition, it can still be obtained by the methods of conformal mapping. Polubarinova-Kochina (1956) discussed the problem and supplied solutions (obtained by various mathematical devices) for seepage to and from a trapezoidal channel in a porous medium and seepage through an earth dam. Once again, the analytical solutions are of little practical utility because of the complexity inherent in the design of earth dams, which usually includes layers or zones of different permeabilities. In this type of application, a free surface flow with a

gravity effect is established here for a homogeneous isotropic earth-fill dam. The geometry of the flow domain is shown in Figure 3.3.

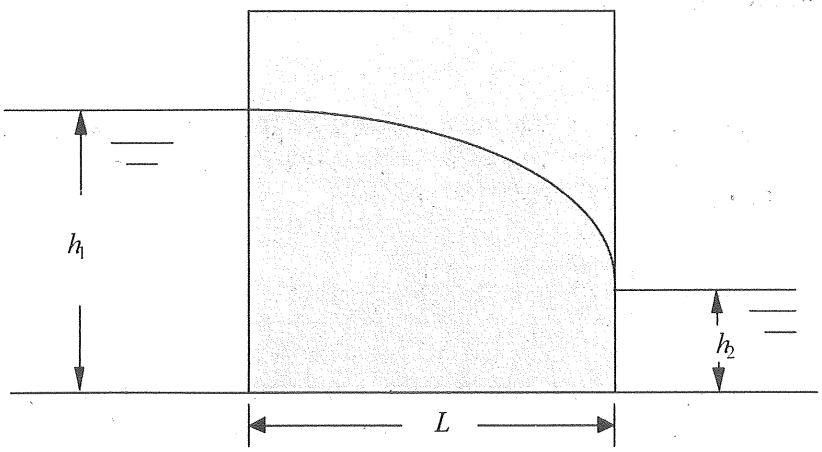

Figure 3.3. Schematic diagram of a rectangular earth dam

As a simple free surface flow problem, the example simulated is a steady state one and has a constant head difference between the upstream and downstream boundaries. The constant head difference provides inflow and exit points of the phreatic line. Therefore, the shape of the phreatic line can be found easily by applying the Dupuit-Forchheimer discharge approximation (analytical solution). However, many analytical solutions have been obtained for the phreatic line in a simple rectangular earth dam. The seepage stability analysis of the embankments of an earth dam at the exit gradient is also obtained using the gradient method (cf. sec. 3.4).

3.2. Governing equations

Numerical models

In **FIDAP** it is assumed that within the domain of interest, Ω, there is a region, V, containing rigid porous material saturated with a viscous incompressible fluid, as well as a region, Ω_f, occupied entirely by fluid. The saturating fluid in V is the same as in Ω_f, if the two regions share a common permeable interface; otherwise, the two fluids may be different. The porous medium is assumed to be homogeneous and isotropic, and the fluid and the solid are in thermal equilibrium. The equations describing the fluid motion and energy balance in the region V are formulated as follows. Within V, let V_f be the volume occupied by the fluid and V_s the volume occupied by the solid, where

$$V = V_f + V_s . \tag{3.1}$$

The porosity of the porous medium is defined by

$$n = V_f / V . \tag{3.2}$$

Two averaged quantities are introduced to derive the porous flow equations (Slattery, 1972; Bear, 1972). Accordingly, we have the following momentum equation to be solved in **FIDAP** (omitting temperature effects):

$$\frac{\rho}{n}\frac{\partial u_i}{\partial t} + \left(\frac{\rho \boldsymbol{B}}{\sqrt{k_i}} \|u_i\|^m + \frac{\mu}{k_i} \right) u_i = -p_{,i} + \tilde{\mu} u_{i,jj} + \rho f_i \tag{3.3}$$

where, ρ is the density of the fluid, $\boldsymbol{B}$ is the inertia coefficient, and μ is the dynamic viscosity of the fluid. Equation (3.3) is sometimes referred to as the *Forchheimer-Brinkman* model for porous flow .

By an appropriate selection of the various coefficients that appear in the above equation, different standard flow models can be derived. Thus, if $\tilde{\mu} = \boldsymbol{B} = 0$, the standard Darcy formulation is approached; while with $\boldsymbol{B} = 0$, $\mu = 10^{-3}$ Pa. s. and $\tilde{\mu} = 10^{-20}$, the Darcy-Brinkman model will be approached. If both $\boldsymbol{B}$ and $\tilde{\mu}$ are defined at the same time to be non-zero, the Darcy-Forchheimer model is approached and the flow equation applied will be definitely nonlinear.

In **FIDAP** the actual equation solved is

$$\frac{\rho}{n}\frac{\partial u_i}{\partial t} + \left(\frac{\rho \boldsymbol{B}}{\sqrt{k_i}} \|u\|^m + \frac{A\tilde{\mu}}{k_i} \right) u_i = -p_{,i} + \tilde{\mu} u_{i,jj} + \rho f_i . \tag{3.4}$$

Thus, in terms of input data to **FIDAP**

$$\mu = A\tilde{\mu} .$$

The term $\tilde{\mu} u_{i,jj}$ is the *Brinkman* term which is required to provide consistent boundary conditions between fluid and porous domains when both are present in a simulation. For the problem simulated here, the above mentioned models are approached by specifying certain values of the parameters that appear in the equation of motion, Eq. (3.4). Hence, the specified different degrees of freedom for the simulated cases are illustrated in Table 3.1:

Table 3.1. Specified flow domain characteristics for the numerical simulations.

Flow case	Flow state	Numerical model (FIDAP)	k_i Intrinsic permeability m^2	ρ Fluid density kg/m^3	$\tilde{\mu}$ Dynamic viscosity Pa.s	g Gravity m/sec^2	n Porosity	A ACOFF	B BCOFF	m POWER
Rectilinear flow	Laminar	Darcy	10^{-12}	1000	10^{-20}	-9.81	0.35	10^{+17}	0	1
		Forchheimer	10^{-12}	-//-	10^{-3}	-//-	0.35	1	0.55	1
	Turbulent	Darcy	10^{-08}	-//-	10^{-20}	-//-	0.56	10^{-17}	0	1
		Forchheimer	10^{-08}	-//-	10^{-3}	-//-	0.56	1	0.55	1
Radial flow	Laminar	Darcy	10^{-12}	1000	10^{-20}	-9.81	0.35	10^{+17}	0	1
		Forchheimer	10^{-12}	-//-	10^{-3}	-//-	0.35	1	0.55	1
	Turbulent	Darcy	10^{-08}	-//-	10^{-20}	-//-	0.56	10^{-17}	0	1
		Forchheimer	10^{-08}	-//-	10^{-3}	-//-	0.56	1	0.55	1
Free surface flow	Laminar	Darcy	10^{-12}	1000	10^{-20}	-9.81	0.35	10^{+17}	0	1
		Forchheimer	10^{-12}	-//-	10^{-3}	-//-	0.35	1	0.55	1
	Turbulent	Darcy	10^{-08}	-//-	10^{-20}	-//-	0.56	10^{-17}	0	1
		Forchheimer	10^{-08}	-//-	10^{-3}	-//-	0.56	1	0.55	1

It is necessary to mention here that in the radial flow simulation, the governing equation is reduced to the cylindrical coordinates. Hence the analytical solution of the radial flow requires the transformation of the flow equations to the cylindrical coordinates system.

3.3. The analytical solutions

3.3.1. Rectilinear flow

Applying Darcy's law and the continuity equation in the flow domain, a simple one-dimensional Laplace equation is yielded:

$$\frac{\partial^2 h}{\partial x^2} = 0. \tag{3.5}$$

The boundary conditions $h = h_1$ at $x = 0$ and $h = h_2$ at $x = L$, and integrating twice give

$$h_D(x) = h_1 - \left(\frac{h_1 - h_2}{L}\right)x \quad \text{or} \quad h_D(x) = h_1 - \left(\frac{\nu}{gk}\frac{Q}{A_c}\right)x \tag{3.6}$$

where A_c is the cross-section area of the flow domain, and D indicates the Darcy solution.

Equation (3.5) may be represented by two sets of curves that intersect at right angles to form a pattern of square figures known as a *flow net*. One set of lines is called the *streamlines* or *flow lines*; the other set is termed *equipotential lines*. The flow lines represent paths along which water can flow through a cross section. The equipotential lines are lines of equal energy level or head.

As the specific discharge Q increases, the relationship between the specific discharge Q and the hydraulic gradient J gradually deviates from the linear relationship expressed by Darcy's law [in the form given in Eq.(1.1)]. Practically all evidence indicates that Darcy's law is valid as long as the Reynolds number does not exceed a value between 1 and 10. In the range of validity of Darcy's law, $\boldsymbol{Re} < 10$, the viscous forces are predominant. As the velocity of the flow increases, a region of gradual transition is observed, from a laminar flow with predominant viscous forces, to laminar flow with inertial forces governing the flow. The value of $\boldsymbol{Re} = 100$ is often mentioned as the upper limit of this transition region in which Darcy's law is no longer valid. Some authors explain the deviation from the linear law by the separation of the flow from the solid walls of the solid matrix, caused at large $\boldsymbol{Re}$ by the inertial forces at (microscopic) points of the pore space where the flow diverges or is curved. At still higher values of $\boldsymbol{Re}$ ($150 > \boldsymbol{Re} > 300$), the flow becomes fully turbulent (Bear, 1972).

There is no universally accepted nonlinear equation of motion (that is, a relationship between J and Q) which is valid for $\boldsymbol{Re} > 10$. Many such relationships appear in the literature; most of them have the general form of Forchheimer equation (1901). For the purpose of accurate predictions in comparison with the linear Darcy equation, we apply the equation proposed by Ward (1964):

$$J = \frac{\nu}{gk}q + \frac{\boldsymbol{B}}{g\sqrt{k}}q^m \tag{3.7}$$

By substituting the total volume of the water flowing per unit of time, denoted as Q through a defined cross-sectional area normal to the direction of the flow and B as the inertia coefficient, the nonlinear differential equation becomes:

$$-\frac{\partial h}{\partial x}=\frac{\nu}{gk}\frac{Q}{A_c}+\frac{\boldsymbol{B}}{g\sqrt{k}}\left(\frac{Q}{A_c}\right)^m \tag{3.8}$$

To make an appropriate comparison with the numerical solution, the power m has been designated as equal to two. Thus the flow equation is of the second order.
If equation (3.7) is integrated with respect to x, the relation of the falling head with the distance is obtained as:

$$h_F(x)=h_1-\left(\frac{\nu}{gk}\frac{Q}{A_c}+\frac{\boldsymbol{B}}{g\sqrt{k}}\frac{Q^2}{A_c^{\,2}}\right)x. \tag{3.9}$$

where F indicates the Forchheimer solution.
A specific experimental data is available for the values of the inertia coefficient $\boldsymbol{B}$. Therefore the value of the inertia coefficient can be adopted from recent works to fit the properties of the selected porous media in this simulation.

3.3.2. Radial flow

For radial flow, Darcy's law with the continuity equation can be reduced to the cylindrical form

$$\frac{1}{r}\frac{\partial}{\partial r}\left(r\frac{\partial h}{\partial r}\right)=0. \tag{3.10}$$

For the current case of radial flow, we have to modify the flow equation with the applied boundary conditions. Thus, the linear flow equation becomes

$$Q=\frac{1}{\boldsymbol{C}}r\left(-K\frac{\partial h}{\partial r}\right) \tag{3.11}$$

where

$$\boldsymbol{C}=\frac{360^\circ}{2\pi\theta} \quad \text{and} \quad K=k\frac{g}{\nu}.$$

By integrating the above linear equation with respect to the radial distance "r"

$$\int_{r_1}^{r_2} Q\frac{1}{r}\,dr=-\frac{K}{\boldsymbol{C}}\int_{h_1}^{h_2} dh \tag{3.12}$$

and applying the boundary conditions (see Figure 3.2), the equation obtained for a finite porous medium with a constant head difference is

$$Q\,ln\left(\frac{r_2}{r_1}\right) = \frac{K}{C}(h_1 - h_2) \tag{3.13}$$

where r_1 and r_2 are the inflow and outflow radii of the flow domain.
Hence, by solving for Q from Eq. (3.13) we obtained

$$Q_D = \frac{K}{C}\frac{(h_1 - h_2)}{ln(r_2/r_1)} \tag{3.14}$$

where the sub-index, D, indicates the Darcy solution.

The falling head as a function of radius r can be written as

$$h_D(r) = h_1 + \frac{C}{K}Q_D\,ln\left(\frac{r_1}{r}\right) \tag{3.15}$$

for $r_1 \le r \le r_2$. The flow velocity in the flow domain that follows directly from the continuity is

$$q_D(r) = \frac{Q_D}{r}C. \tag{3.16}$$

The solution of the flow by nonlinear relation (Forchheimer equation) imposes the following modification of the flow equation in cylindrical coordinates. It has been shown in the rectilinear flow that the nonlinear relation takes the following form (Ward, 1964)

$$-\frac{\partial h}{\partial r} = \frac{\nu}{gk}q + \frac{B}{g\sqrt{k}}q^m. \tag{3.17}$$

As the cross-section area varies with "r", the differential equation in Eq.(3.17) becomes

$$-\frac{\partial h}{\partial r} = \frac{\nu}{gk}\frac{Q}{A_c} + \frac{B}{g\sqrt{k}}\left(\frac{Q}{A_c}\right)^m, \tag{3.18}$$

where Q, as mentioned above, is a volume flow rate per unit time through a unit cross-section area normal to the flow direction within the flow domain. Hence, by making the same formulation as above, the integrated equation obtained becomes

$$\int_{h_1}^{h_2} -dh = \int_{r_1}^{r_2} \left(C_1 \frac{1}{r} + C_2 \frac{1}{r^m} \right) dr \tag{3.19}$$

where

$$C_1 = C \frac{v}{g\,k} Q \qquad \text{and} \qquad C_2 = C^m \frac{B}{g\sqrt{k}} Q^m$$

and C is the same as in the linear equation. The power m is related to the Forchheimer equation and it has the limitation $1.6 \leq m \leq 2$. In Eq.(3.19), for the case where $m = 2$, the integration with respect to the radial distance gives the following relation in cylindrical coordinates:

$$h_1 - h_2 = \frac{\left(C_1 ln(r_2) r_2 - C_2\right)}{r_2} + \frac{\left(-C_1 ln(r_1) r_1 + C_2\right)}{r_1} \tag{3.20}$$

By solving Eq.(3.19) for the constant flow rate Q and integrating again equation (3.19), the falling head equation is obtained:

$$h_F(r) = h_1 + C_1 ln\left(\frac{r_1}{r}\right) + C_2\left(\frac{1}{r} - \frac{1}{r_1}\right) \tag{3.21}$$

Hence, the flow velocity can be obtained by simplifying equation (3.19) and substituting for the varied cross-section area in the flow equation

$$q_F(r) = \frac{Q_F}{r} C \tag{3.22}$$

where the sub-index F denotes the Forchheimer solution.

3.3.3. Free surface flow (unconfined aquifer)

The free surface flow problem has been described in Section 3.1.3; here, a flow bounded above by a phreatic surface is considered. This types of flow occurs in phreatic aquifers encountered in ground water hydrology. In many cases it is assumed for simplicity, that the thickness of the capillary zone above the phreatic surface is much smaller than that of the saturated domain below the phreatic surface.
The boundary conditions of a phreatic surface can be given in different ways depending on the governing equations. In most cases of free surface flow the main boundary condition is that the pressure on the free surface boundary is taken to be atmospheric, i.e., $P = 0$. In addition, the flow in the free surface is influenced by the

capillary zone above the free surface, which seems have been overlooked in the majority of the free surface flow simulations found in the literature.

The nonlinearity of the boundary conditions, together with the fact that the location of this boundary is unknown in advance and is, in fact, part of the required solution, makes an exact analytical solution of flow problems with such a boundary difficult, in all but a very limited number of cases. Some two-dimensional steady flow problems may be solved by the hodograph method (cf. Sec. 2.4). Numerical methods (cf. Sec. 2.7) are often employed.
A way to circumvent some of the difficulties is to derive analytically approximate solutions based on a linearization of the boundary conditions and/or the nonlinear continuity equations describing unconfined flows. Some of these methods are discussed and applied to the problem considered here.

The Dupuit approximation

The Dupuit approximation is among the most powerful tools for treating unconfined flows. In fact, it is the only simple tool available to most engineers and hydrologists for solving such problems.
Dupuit (1863) developed a theory based on several simplifying assumptions based on the observation that in most ground water flows the slope of the phreatic surface is very small. In steady two-dimensional unconfined flow without percolation in the vertical xy plane, the phreatic surface is a streamline. At every point along it, the pressure is zero and the flow velocity q is given by Darcy's law:

$$q = -K\frac{d\phi}{ds} = -K\frac{dy}{ds} = -K\sin\theta. \tag{3.23}$$

As the slope θ is very small, Dupuit suggested that $\sin\theta$ be replaced by the slope $\tan\theta = dh/dx$. The assumption of small θ is equivalent to assuming either that equipotential lines are vertical ($\phi = \phi(x)$ is independent of y) and the flow essentially horizontal, or there is simply a hydrostatic pressure distribution. Thus the Dupuit assumptions lead to the flow velocity expressed by

$$q_x = -K\frac{dh}{dx} \tag{3.24}$$

where $h = h(x)$ and then to the total discharge through any vertical surface of width b (see Figure 3.3)

$$Q_x = -K\,b\,h(x)\frac{dh}{dx}. \tag{3.25}$$

It may be noted here that all of these assumptions can be considered as good approximations in regions where θ is indeed small and the flow essentially horizontal. However, the application of Dupuit approximation is not warranted when turbulent flow dominates the flow domain. The nonlinear flow equation and the nonlinear water table of the free surface make it more complicated to rely on Dupuit's assumption.

The important advantage of the Dupuit assumptions is that the two independent variables of the original problem (x, y) have been reduced to one. In Eq (3.25), y does not appear as an independent variable. Hence, the Dupuit assumptions actually consist of omitting the vertical flow component q_y. The value of q_y varies from $q_y = 0$ along the horizontal impervious boundary to $q_y = -K \sin^2 \theta$ along the phreatic surface.

Equation (3.25) can be solved by direct integration for one-dimensional flows, as well as for radial converging or diverging flows. If one considers the case shown in Figure 3.3, the flow per unit width between the two reservoirs (vertical faces), following the Dupuit assumptions, the total discharge (per unit width) through a vertical cross-section is:

$$Q_d = q\,h(x) = -K\,h(x)\frac{dh}{dx}. \tag{3.26}$$

Integrating between $x = 0$ and any distance x, we obtain

$$Q_d\,dx = -K\,h(x)\,dh \qquad \text{and} \qquad Q_d \int_{x=0}^{x=L} dx = -K \int_{h=h_1}^{h=h_2} h(x)\,dh, \tag{3.27}$$

with the applied boundary conditions

$$Q_d = -K\frac{(h_1^2 - h_2^2)}{2L} \qquad \text{and} \qquad h_d(x) = \sqrt{h_1^2 - \frac{(h_1^2 - h_2^2)}{L}\,x}. \tag{3.28}$$

The Polubarinova-Kochina solution for a simple dam.

Polubarinova-Kochina (1951) and Risenkampf (1940) applied the theory of linear differential equations to some problems of ground water flow. A general treatment is given by Polubarinova-Kochina (1962) and applied to the problem of a simple rectangular dam and to other more difficult problems. The hodograph and complex potential planes are involved in these solutions, in addition to the solution of the hypergeometric equation. In this work attention is confine to the simple homogeneous rectangular dam problem which is depicted in Figure 3.4a, together with the hodograph $\widetilde{w}$-plane, the complex potential ζ-plane, and an auxiliary ξ-plane, shown

in Figures 3.4b,c and d, respectively. A review of the relevant properties mentioned by Polubarinova-Kochina for the hypergeometric equation (Crank, 1984; Bakker, 1997) is given in Appendix.

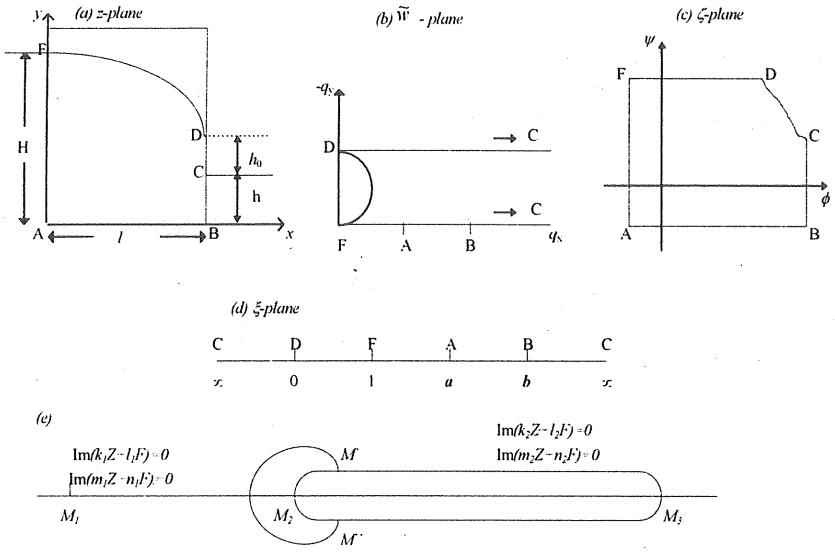

Figure 3.4. The Polubarinova-Kochina solution for a simple dam

The formulation of the solution by Polubarinova-Kochina yields the following set of integral equations:

$$l = \int_0^{\frac{\pi}{2}} \frac{K\left[\alpha + (\beta - \alpha)\sin^2(\psi)\right]}{\sqrt{\left[1 - \alpha - (\beta - \alpha)\sin^2(\psi)\right]}}\, d\psi \tag{3.29}$$

$$\mathrm{H} = C \cdot \int_0^{\frac{\pi}{2}} \frac{K\left[\beta + (1 - \beta)\sin^2(\psi)\right]}{\sqrt{\left[B - \alpha + (1 - \beta)\sin^2(\psi)\right]}}\, d\psi \tag{3.30}$$

$$\mathrm{h} = C \cdot \alpha^{\frac{1}{2}} \cdot \int_0^{\frac{\pi}{2}} \frac{K\left[\alpha\sin^2(\psi)\right] \cdot \sin(\psi)}{\sqrt{\left[\left(1 - \alpha\sin^2(\psi)\right) \cdot \left(\beta - \alpha\sin^2(\psi)\right)\right]}}\, d\psi \tag{3.31}$$

where $K(\xi)$ is the complete elliptic integral of the first kind.

The terms l, H and h, denote the length of the base of the rectangular earth dam specified with free surface flow, the boundary conditions at the upstream and downstream sides.

Crank (1984) put the expressions $1/(1-\xi) = cos^2\psi$, $\alpha_1 = 1-\alpha$, and $\beta_1 = 1-\beta$ in the integral for h_0 and obtained

$$h_0 = C \cdot \int_0^{\frac{\pi}{2}} \frac{K\left(cos^2(\psi)\right) sin(\psi) cos(\psi)}{\sqrt{\left[\left(1-\alpha_1 sin^2(\psi)\right)\left(1-\beta_1 sin^2(\psi)\right)\right]}} d\psi. \tag{3.32}$$

The height of the separation point above the dam base is $h_s = h + h_0$. Cryer (1976) pointed out errors in equations (3.30) and (3.31) from Polubarinova- Kochina (1962), and his corrections have been included here. The equation of the free surface is found by separating the real and it is imaginary parts of the functions introduced by Polubarinova-Kochina. Thus, it is shown

$$X = l - C \int_0^{\psi} \frac{K\left[sin^2(\psi)\right] \cdot sin(\psi)}{\sqrt{\left[\left(1-\alpha\, sin^2(\psi)\right) \cdot \left(1-\beta\, sin^2(\psi)\right)\right]}} d\psi \tag{3.33}$$

$$Y = h + h_0 + C \int_0^{\psi} \frac{K\left[sin^2(\psi)\right] \cdot sin(\psi)}{\sqrt{\left[\left(1-\alpha sin^2(\psi)\right) \cdot \left(1-\beta sin^2(\psi)\right)\right]}} d\psi \tag{3.34}$$

where

$$0 \le \psi \le \frac{\pi}{2}.$$

The parameters α, β and C in the above equations can be solved implicitly for the given boundary conditions H, h and l, where the complete elliptic integral mentioned above takes the following form:

$$K(\zeta) = \int_0^{\frac{\pi}{2}} \frac{d\psi}{\sqrt{1-\zeta\, sin^2(\psi)}}. \tag{3.35}$$

The solution of Polubarinova-Kochina is different from that obtained by the Dupuit approximation, since the exit point of the phreatic line lies above the tail water level. The results of Polubarinova-Kochina solution are very reasonable and in a good agreement with the experimental results of recent work on rectangular earth dams. Polubarinova-Kochina also treated several problems of ground water flow including the free surface flow in earth-fill dams with inclination at up- and downstream sides; she also found a solution for an earth dam with a filter at the dam toe.

Solution of the Forchheimer equation for free surface flow

The Forchheimer equation describes a nonlinear relation between the hydraulic gradient and the flow velocity; with the nonlinear free surface equation the partial differential equation obtained becomes too difficult to solve in closed form. Since the free surface position $s(x,y)$ is not known in advance, several simplifications have to be made to solve it. In the current analytical solution, the author solves the nonlinear problem by applying the Dupuit approximation. For a rectangular earth dam, Figure 3.3, by using the Forchheimer equation and s as the distance along the free surface, the gradient along the free surface is

$$-\frac{dh}{ds} = aq + bq^m . \tag{3.36}$$

Furthermore, for this two-dimensional flow we introduce the Dupuit assumption that the slope of the free surface is small ($\sin\theta = \tan\theta$). This is a matter of solution accuracy which will be discussed in Section 6. However, the approximation yields the equation:

$$-\frac{dh(x)}{dx} = a\frac{Q_S}{h(x)} + b\left(\frac{Q_S}{h(x)}\right)^m \tag{3.37}$$

where

$$a = \frac{\nu}{gk} \quad \text{and} \quad b = \frac{\boldsymbol{B}}{g\sqrt{k}}$$

while Q is a specific discharge per unit width of the dam. Since equation (3.37) is one-dimensional function which can be easily solved for the dependent variable $h(x)$, the solution is

$$-\frac{1}{2}\frac{h(x)^2}{Q_S a} + \frac{h(x)b}{a^2} - \frac{Q_S b^2 ln[a h(x) + bQ_S]}{a^3} + x = -c_1 \tag{3.38}$$

where c_1 is the constant of integration and can be found by applying the specified boundary conditions up- and downstream. By expanding the solution of the differential equation (3.38) in a Taylor series to the third order, one can obtain the following closed form for the phreatic line (Sharif's equation):

$$h_S(x) = h(0) - \frac{Q_S(a h(0) + bQ_S)}{h(0)^2}x - \frac{1}{2}\frac{Q_S^2(a h(0) + bQ_S)(a h(0) + 2bQ_S)}{h(0)^5}x^2 + O(x^3) \tag{3.39}$$

where $O(x^3)$ is the error order in the Taylor series.

The free surface equation (3.39) can be solved by applying again the specified boundary conditions and then finding the corresponding specific discharge Q_S. Because this equation is based on the Dupuit approximation, we do not expect to get a separated exit point at the downstream side; this is different from the Polubarinova-Kochina solution. On the other hand, this solution can be compared with the Dupuit solution which is based on Darcy's law in the case of a rectangular earth dam.

3.4. Stability analysis (seepage force)

3.4.1. Confined saturated flow

In flow in a porous medium at saturated conditions, the viscous friction exerted by the water flowing through the soil pores, constitutes an energy transfer from the water to the soil. A measure of this transfer is the head loss (Δh) between the points under consideration (Δl), shown in Figure 3.5.

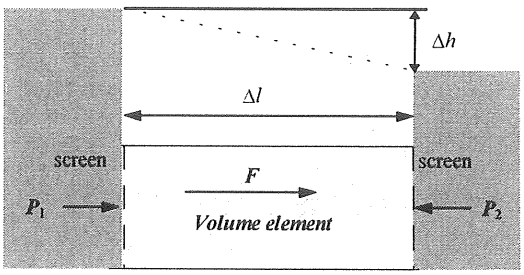

Figure 3.5. Seepage force in confined flow

The energy transfer corresponds to the seepage force. The seepage force is responsible for the phenomenon known as quicksand (Terzaghi, 1943) and it is of importance in the stability analysis of earth structures subject to the action of seepage. The first rational approach to the problem was presented by Terzaghi (1922); it forms the basis of all subsequent studies. The theory is presented in a somewhat modified form.

One starts by considering all of the forces acting on a unit volume of soil through which rectilinear seepage occurs.

1. The weight of the solid phase per unit volume is

$$\gamma_s = \frac{G_s \cdot \gamma_w}{1+e} \tag{3.40}$$

where e is the void ratio, G_s is the specific gravity of the soil material, and γ_w is the unit weight of water. If we define unit vertical vector **j** as positively directed upwards, we have for γ_s

$$\gamma_s = -\mathbf{j}\frac{G_s \cdot \gamma_w}{1+e} \tag{3.41}$$

2. The second force γ_f is the buoyancy, which corresponds to the weight of water per unit volume displaced by the soil particles:

$$\gamma_f = \mathbf{j}\frac{\gamma_w}{1+e}. \tag{3.42}$$

The summation of Eq.(3.41) and Eq.(3.42),

$$\gamma_b = -\mathbf{j}\frac{\cdot \gamma_w (G_s - 1)}{1+e}, \tag{3.43}$$

is called the submerged unit weight.

3. The total weight per unit volume of the soil-water mass γ_t is

$$\gamma_t = -\mathbf{j}\frac{\cdot \gamma_w (G_s + e)}{1+e}. \tag{3.44}$$

The difference between Eq.(3.43) and Eq.(3.44) is simply $-\mathbf{j}\ \gamma_w$. These results are plotted on a vertical axis in Figure 3.6 below.

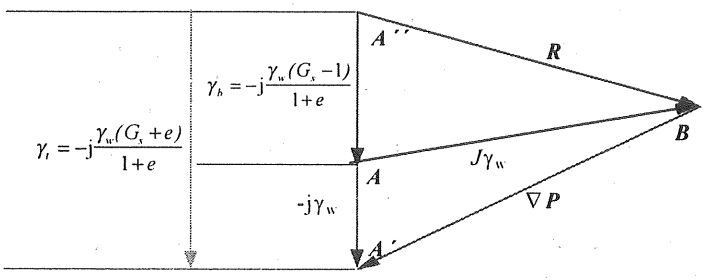

Figure 3.6. Forces polygon in confined flow through saturated porous medium

The forces represent the hydrostatic forces per unit volume acting within the flow medium. For a complete analysis, one has to include the hydrodynamic forces. The piezometric head can be written as

$$h = \frac{P}{\gamma_w} + z. \tag{3.45}$$

The gradient of both sides of Eq.(3.45) yields

$$\frac{\nabla P}{\gamma_w} = \nabla h - \mathbf{j} \tag{3.46}$$

where **j** is a unit vector, as before. Simplification of the above equation and replacing the gradient of h by $-J$ yields the vector form

$$\nabla P = -J\gamma_w - \mathbf{j}\gamma_w. \tag{3.47}$$

Equation (3.47) is represented by the triangle $AA'B$ in Figure 3.8. The term $J\gamma_w$ (AB) represents the seepage force per unit volume of fluid , the direction of which is normal to the equipotential lines, while R ($A''B$) represents the magnitude and direction of the resultant force (per unit volume) acting within the pore water at a point in the soil. Hence if R = 0, it appears from Figure 3.6 that a critical condition (quicksand) is defined by

$$J_{critical} = \frac{G_s - 1}{1 + e} = \frac{\gamma_b}{\gamma_w}. \tag{3.48}$$

For a porous medium with $K = 10^{-5}$ m/sec. (sandy silt soil), the typical values of the specific gravity G_s = 2.11 and void ratio e = 0.538 (see Table 3.1), we can see that the value of the critical gradient obtained is

$$J_{critical} = 0.721.$$

It is usual to take the value of the critical gradient as unity when information is lacking about the specific gravity and void ratio. Equation (3.48) provides the basis for stability determinations of the factor of safety against a quick condition (called piping).

The procedure above requires the determination of the maximum hydraulic gradient along the discharge boundary, called the exit gradient, which will yield the minimum resultant force (R_{min}) at this boundary. This can be done analytically or graphically by means of a flow net. In recent work the numerical solution offers a good chance to compute the gradient for complicated geometry and different boundary conditions.

Under quick conditions there is no intergranular pressure, the soil exhibits no shearing strength and has the properties of a fluid with density given by the following equation (Scatt, 1963)

$$\gamma_t = \frac{1+n}{1+e}\gamma_s. \tag{3.49}$$

It is of interest to note that the critical gradient from Eq.(3.48) depends only on the specific gravity of soil grains and the void ratio of the soil, while the equation does not says anything about the grain size of the soil. Therefore, the reaction occurs independently of the grain size. Scatt (1963) drew the conclusion that a quick condition is possible in all types of soil, and provided that there are no cohesive or adhesive forces between soil grains, such forces would resist the separation of soil particles. This implies that we can expect quick conditions in soils with grain sizes ranging upward from that of silt. In these soils, the properties are typically such that the right hand side of Eq. (3.48), and hence, $J_{critical}$, are close to unity.

There is some uncertainty about the nature of cohesive forces in very fine-grained soils, and it is probable that a critical gradient in a cohesive soil would eventually cause a quick condition if maintained at a critical level for a long enough time. This behavior is related to the change of the pore pressure which, in a cohesive soil, constitutes a transient or non steady-state flow problem because of its compressibility and low hydraulic conductivity, and to the fact that considerable time is usually involved in the progressive change of the pore pressures or hydraulic gradient in cohesive materials. This means that, although a quick condition may not be impossible in cohesive soils, it is unlikely in practice that a boundary water-pressure condition would exist for a long enough time to give rise to a critical gradient through an entire layer of soil (Bear, 1972).
In soils consisting of larger grain sizes, such as gravel, the quantity of water that would be required to maintain a critical gradient through the soil would be very large; in practice it is extremely unlikely flows of water sufficient to maintain gravel in a quick condition would be encountered. Hence, we have a process with a practical limitation on both sides of the granular-size scale.
In the confined flow case we have under consideration two flow states which are related to the stability of the boundary materials at the inflow and outflow side (sand and coarse gravel). The linear and nonlinear flow equations are incorporated in the estimation of the incipient motion of the porous material. However, the critical gradient obtained from both linear and nonlinear relations is reviewed here. First, for the linear Darcy's law we have

$$\nabla P = -J_D\gamma_w - \mathbf{j}\gamma_w. \tag{3.50}$$

In order to have a stable boundary material, the hydraulic gradient according to linear Darcy flow should be less than the critical gradient maintained at quick condition. Bear (1972) reported an empirical relation between the intrinsic permeability and the grain diameter (Hazan equation) as

$$k = 6.54 \times 10^{-4} d^2 \tag{3.51}$$

where d is the grain diameter and k is the intrinsic permeability.

The actual gradient can then be formulated as

$$-J_D = \frac{q\,\mu}{6.54 \times 10^{-4} d^2 \rho\, g} \tag{3.52}$$

which must be less than the critical gradient $J_{critical}$. Hence, the stability condition became

$$J_{critical} \geq \frac{q\,\mu}{6.54 \times 10^{-4} d^2 \rho\, g}. \tag{3.52a}$$

By solving d from Eq. (3.52a), the required grain diameter can be obtained for the stability condition in confined flow.
For nonlinear flow (Forchheimer) the hydrodynamic forces in confined flow can be written as

$$\nabla P = -J_F \gamma_w - \mathbf{j}\gamma_w. \tag{3.53}$$

By introducing the gradient in the form proposed by Ward (1964),

$$-J_F = \left(\frac{\nu}{g \cdot k} q + \frac{0.55}{g \cdot \sqrt{k}} q^2 \right), \tag{3.54}$$

at critical condition, one can obtain

$$J_{critical} \geq \left(\frac{\nu}{g \cdot 6.54 \times 10^{-4} d^2} q + \frac{0.55}{g \cdot \sqrt{6.54 \times 10^{-4} d}} q^2 \right). \tag{3.55}$$

These equations for linear and nonlinear confined flow can be used to predict the stability of the porous material at the discharge or exit boundary.

3.4.2. Unconfined saturated flow

Previous researchers on transport processes in porous media have treated the magnitude and direction of the seepage force vector as independent variables. Muniram (1996) found that the magnitude and direction of the seepage vector are strongly related at the seepage face. Muniram also found that seepage parallel to the slope face results in the minimum stable seepage slope. However, it is stated in the

literature that the seepage force is independent of either the hydraulic conductivity or the flow velocity: it depends only on the hydraulic gradient (Ghislain, 1986). Thus, the seepage force can be the same in a medium of very low hydraulic conductivity, where the velocity of the flow is almost negligible, and in a coarse medium, where the velocity is very high.

For the case of unconfined flow, the seepage exit face through a simple rectangular earth dam is studied. The destabilizing forces acting on an individual soil particle situated at the interface, between the porous medium and the surface flow produced by seepage at the exit point, are sketched in Figure 3.7 below.

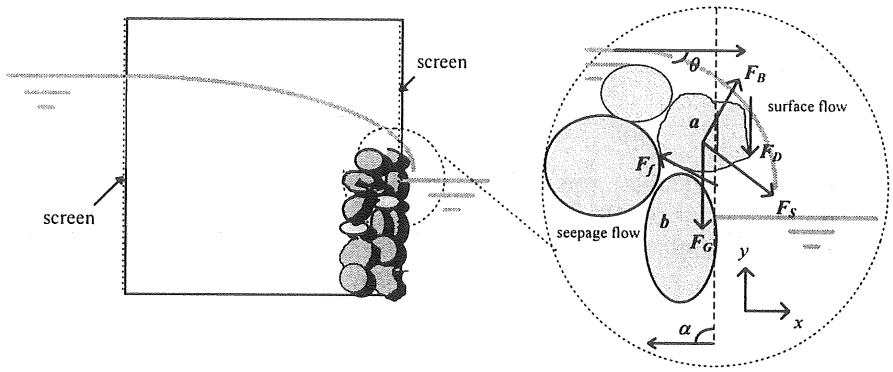

Figure 3.7. Flow field and forces on an individual particle at the downstream face

Bear (1972) defined destabilizing forces by applying the concept of the representative elementary volume (REV) which distinguishes between the macroscopic scale and the microscopic scale. However, the porosity is used as the REV in defining destabilizing forces, where F_D is the drag force due to the momentum exchanged between the surface flow and the particle, F_B is the buoyancy force due to the pressure field around the individual particle, and F_S is the seepage force of the momentum exchanged between the individual particle and the seepage flow. Furthermore, F_G is the gravity force downward.
At quick condition, the individual particle, ***a*** is nearly to move on the sub particle, ***b***, with a friction force, $\mathbf{F}_f$. When a critical condition at the uppermost layer is incipient, the force balance equation of a unit volume can be set to

$$(F_f + F_S + F_D + F_B + F_G) \cdot \mathbf{j} = \mathbf{0} \qquad (3.56)$$

where **j** is a unit vector in the direction of the surface flow. The seepage force acting on a single grain in linear laminar seepage flow may be expressed as (Rumer and Drinker, 1966)

$$F_S = \lambda \, \mu \, \mathrm{U} d \qquad (3.57)$$

where λ is a tortuosity coefficient that takes into account the effect of neighboring particles, μ is the dynamic viscosity of the fluid, d is the grain diameter and U is local average (seepage) velocity. The coefficient λ reaches a limiting value of 3π for a single sphere in an infinite fluid (Stokes, 1850), so that for an average particle (Howard and Mclane, 1988)

$$\lambda = C_p 3\pi \tag{3.58}$$

where C_p is a packing coefficient that expresses the effect of the geometry of the pore system upon local streamline configurations around the particle.
The flow velocity that may be expressed depends on whether a linear or nonlinear seepage flow occurs. Hence, for linear Darcy flow we have

$$U = \frac{q}{n} = \frac{K J}{n} = \frac{k g \rho J}{n \mu} \tag{3.59}$$

where q is the Darcy or superficial velocity, n is the porosity, K is the hydraulic conductivity, k is the intrinsic permeability, g is the gravitational acceleration, ρ is the fluid density, and J is the hydraulic gradient. The general expression to the Hazen equation, which mentioned before (Bear, 1972) may written also here for the intrinsic permeability, as

$$k = C_i d^2 \tag{3.60}$$

where C_i, as mentioned before, is experimentally found to be 6.54×10^{-4} for a limit of grain diameter. By substituting Eqs. (3.58 – 3.60) into Eq. (3.57), we obtain the seepage force acting on an individual grain at exit face:

$$F_s = \frac{C_s 3\pi \rho g J d^3}{n} \tag{3.61}$$

where $C_s = C_p \cdot C_i$. The critical hydraulic gradient in the direction of seepage is expressed as a unique function of the slope angle α and the seepage exit angle θ (Howard and Mclane, 1981) as shown in Figure 3.7. The total head difference, Δh across a particular length Δs causes the gradient to be at that exit point. The flow line passing through the exit point will experience the same head difference over the distance Δs, so that the hydraulic gradient is

$$J_{exit} = \frac{\Delta h}{\Delta s} \cdot \mathrm{j} = \frac{\sin\alpha}{\cos(\alpha + \theta)} \cdot \mathrm{j}. \tag{3.62}$$

For nonlinear seepage flow, the hydraulic gradient is expressed by the Forchheimer equation as

$$-J_F = \left(\frac{\nu}{g \cdot k} q + \frac{0.55}{g \cdot \sqrt{k}} q^2 \right). \tag{3.63}$$

The resultant nonlinear seepage force acting on an individual grain can be written as

$$F_s = C_s 3\pi \rho \left(\frac{\nu}{k} q + \frac{0.55}{\sqrt{k}} q^2 \right) d^3 / n. \tag{3.64}$$

From the critical hydraulic gradient at the exit point, the required grain diameter for a stability condition can be obtained from Eq.(3.64). It is important to note that when there is a steep slope, the angle of internal friction is smaller than the slope of the downstream face; hence, the maximum stable slope should be taken into account for the current analysis. The internal friction for several types of soil, based on a stress analysis of embankment slope, is given by Taylor (1948).

4. Mathematical model of the flow (numerical solution)

The solution method used in the commercial program FIDAP 7.6 is the finite element method (FEM). In the FEM the flow region is subdivided into numerous small regions, the finite elements. The partial differential equations of fluid mechanics covering the flow region as a whole are replaced by ordinary differential or algebraic equations for each element. The system of these equations is then solved by sophisticated numerical techniques to determine the velocities, pressures and other unknowns throughout the region.

In the finite element method the problem of continuity is discretize for space and for time. For the time discretization, the time integration command is utilized to obtain the solution which is in time steps. Two models for the flow through porous media are applied in the numerical simulation: the Darcy-Brinkman model and the Forchheimer-Brinkman model the were applied for two dimensional rectilinear and radial flow in confined aquifers. The simulation of the free surface flow is beyond the scope of this study.

Here the governing equations are given in vector notation:

$$\rho_0\left(\frac{\partial \mathbf{u}}{\partial t}+\mathbf{u}\cdot\nabla\mathbf{u}\right)=-\nabla p+\nabla\cdot\tau-\rho_0\left[\beta_T\left(T-T_0\right)+\sum_n \beta_{c_n}c_n\right]\mathbf{g}+\rho_0\mathbf{f} \tag{4.1}$$

The form Eq.(4.1) of the momentum equation is sometimes known as the *stress-divergence* form. In the case that the viscosity is constant, Eq.(4.1) it can be written as

$$\rho_0\left(\frac{\partial \mathbf{u}}{\partial t}+\mathbf{u}\cdot\nabla\mathbf{u}\right)=-\nabla p+\mu\nabla^2\mathbf{u}-\rho_0\left[\beta_T\left(T-T_0\right)+\sum_n \beta_{c_n}c_n\right]\mathbf{g}+\rho_0\mathbf{f} \tag{4.2}$$

or in tensor notation:

$$\rho_0\left(\frac{\partial u_i}{\partial t}+u_i u_{,i}\right)=-p_{,i}+\mu u_{i,jj}-\rho_0\left[\beta_T\left(T-T_0\right)+\sum_n \beta_{c_n}c_n\right]g_i+\rho_0 f_i \tag{4.2a}$$

The form Eq.(4.2) is known as the *Navier-Stokes* form of the momentum equation. Since the porous flow equations are very similar in form to the equations of viscous fluid flow with the exception that the convection terms in the momentum equation are replaced by the Darcy-Forchheimer term in equation (4.2). Thus in case we have isothermal flows the temperature dependence and the buoyancy term is disregarded from the above equation and the obtained equation is Navier-Stokes equation for porous medium flow. The equation solved in FIDAP for porous medium flow is then obtained by replacing the convection term into the Darcy-Forchheimer as follow:

$$\frac{\rho}{n}\frac{\partial u_i}{\partial t} + \left(\frac{\rho\, B}{\sqrt{k_i}} \|u_i\|^m + \frac{A\,\tilde{\mu}}{k_i} \right) u_i = -p_{,i} + \tilde{\mu} u_{i,jj} + \rho f_i \tag{4.3}$$

4.1. Dimension of the flow domain

The governing equations are subject to the boundary conditions associated with the computational domain shown in Figure 4.1 and Figure 4.2, rectilinear and radial flow domain, respectively.

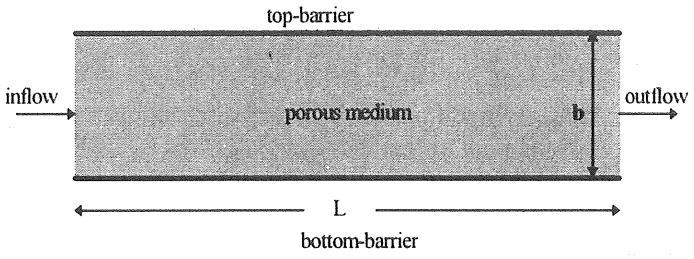

Figure 4.1. Confined aquifer with rectilinear flow

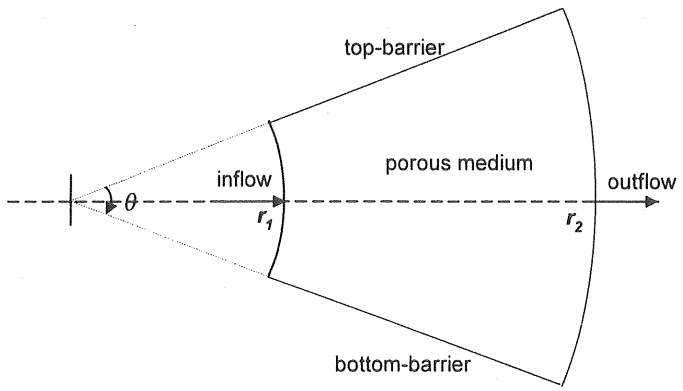

Figure 4.2. Confined aquifer with radial flow

The flow domain is assumed to be homogeneous and isotropic in both confined aquifers. Since we have a two-dimensional flow in a porous medium, we need to define the dimensions of both flow domains. The length of the rectangular flow domain, L, in Figure 4.1, is chosen to be 20 m and the cross-section dimension, b, is 2

m in height. For the radial flow the cylindrical domain of the inner radius, r_1, is 4m and of the outer radius, r_2 is 24m, while the angle of the arch, θ is 60°.

4.2. Initial and boundary conditions

In order to perform a computer simulation of the physical flow problems defined above, it is necessary to specify initial and boundary conditions for the simulation. Initial conditions specify the initial state of the fluid inside the flow domain for the confined problems or, for the free surface simulation, the initial state and the initial position of the free surface. Thus, for a well-posed problem, boundary conditions are required on all boundaries of the computational domain. These boundary conditions are either specified nodal values or specified fluxes across element boundaries for each of the active degrees of freedom in the simulation. For the current numerical simulations, the entity of the "element group boundaries" that is associated with each physical boundary of the confined aquifers is used to define the initial and boundary conditions.

4.2.1. Rectilinear flow

For the *rectilinear* flow with rectangular geometry, the boundary conditions were simple to set in terms of "plot boundary", which means that the velocity component, U_x, is the tangential velocity for the boundary element at the *top* and *bottom barriers*, while the velocity component, U_y, is the normal velocity across the boundary. Hence, the tangential velocity at the *top* and *bottom boundaries* is set to be "free", that is to be computed in the numerical solution, while the normal components of the velocity are set to zero across these boundaries. For the *corners* of the rectangular flow domain no command was needed because the physical normal is consistent with the mathematical normal computed in the numerical solution. For the *inflow* and *outflow* boundaries the tangential component, U_y, of the velocity is set to zero while the normal component, U_x, is kept free. The initial velocity condition in the rectangular domain is then stated as a "linear Stokes solution" which is appropriate for steady state flow in a linear problem. The "Stokes solution" is then applied and this solution is subsequently used as the initial condition for all degrees of freedom (velocity and pressure).

For incompressible flow and Newtonian fluid, the effective viscosity in the program is set to be constant at $\tilde{\mu} = 10^{-20}$ *Pa.s* (cf. Section 3.2.1) in order to reduce the influence of the diffusion term in relation to the Darcy term in the momentum equation. Hence, the value of the associated coefficient, A, in the Darcy term is set to 10^{+17} to compensate for the simulated value of the viscosity for laminar flow as shown in Table 3.1. For turbulent flow with the Forchheimer term, the coefficient, A, is set to another value to compensate for the simulated value of the viscosity, which is changed in relation to the coefficient, B, the inertia coefficient in the Forchheimer

term. Hence A is given the value of one for the viscosity of the 10^{-3} *Pa.s*, and coefficient B is set to be 0.55 (Ward, 1964).

For of flow in saturation and a confined aquifer, there are total head boundary conditions applied at the surfaces of the inflow and outflow sides. The total heads are applied as "constant flux boundary stresses" in Pascal units. At the inflow boundary elements there is a total head of 1.5m water depth which is shown here as

$$P_1 = \rho_w \; g \; h_1 \tag{4.4}$$

while at the outflow boundary, the "boundary stress" is zero, hence $P_2 = 0$.

4.2.2. Radial flow

For a cylindrical domain, the boundary conditions have to be defined in a different way. Because of the shape of the flow domain, the computed normal and tangential components of the velocity are mathematically correct but physically inconsistent, especially at the corner and the edge of the flow domain. Hence, a slip boundary condition needs to be defined for all the boundary element group; then the components of the velocity can be forced to be physically consistent by a correction of the direction of the velocity vector made on the top- and bottom-barrier by using the "normal direction option". Hence, a zero velocity normal component, $U_N = 0$, and a free velocity tangential component is maintained at both the top and bottom barriers, and vice-versa on both the inflow and outflow boundaries.
Also a constant "normal boundary stress", P_{N1}, corresponding to 1.5m water depth, is given in *Pascal* units. and defined on the inflow boundary as:

$$P_{N1} = -\rho_w \; g \; h_1 \tag{4.5}$$

while on the outflow boundary a zero "normal boundary stress", P_{N2} is defined. The other defined boundary conditions are the same as in rectilinear flow, including the initial conditions.

4.3. Discretization of the flow domain

The mesh generated for the flow in a confined porous medium for rectangular and cylindrical domains is shown below in Figure 4.4.

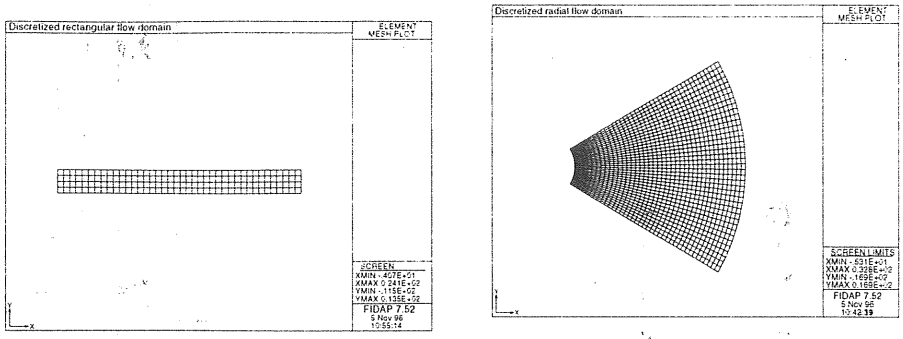

(a) (b)

Figure 4.4. Two-dimensional FEM mesh of: a) Rectangular porous flow domain, and b) Cylindrical porous flow domain.

The number of elements required for the simple rectangular domain was 160, while for the cylindrical one it was 1600 elements. A map mesh was chosen for each flow domain; first, because it offers more simplicity in solving the system of equations obtained from the discretized domain; and second, because the nature of the geometry is not useful with the paved mesh which is not recommended for porous medium simulation (computational theory manual). Quadrilateral 4-node elements were used in generating the mesh. Three degrees of freedom is calculated for each node in the mesh (element grid system); they are the direction and the magnitude of velocity components and the pressure (see Figure 4.6).

The procedure used in solving the discretized domain starts by choosing the interpolation functions, then formulates the equation for each element (local system), couples the elements in nodes and assembles the element equation into an equation system for the whole domain (global system).

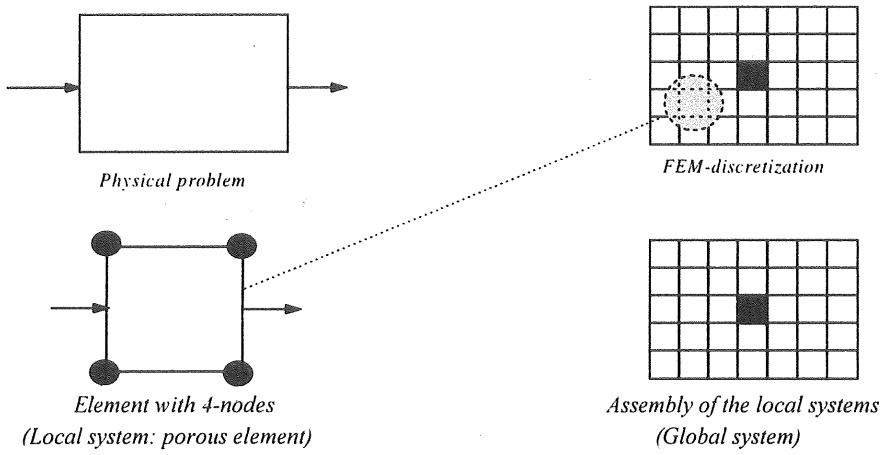

Figure 4.6. Description of the finite element methodology.

4.4. Degree of freedom (parameter effect)

In this section the various parameters that may affect the numerical models applied are elucidated. According to Darcy-Forchheimer terms, there is first the *intrinsic permeability*, k_i, also known as the *physical permeability*, which has the dimension of length squared. It is assumed that k_i is dominated by the saturated flow domain. This coefficient depends on the flow geometry, on the type of porous medium, and on the density, shape and arrangement of the pores. However, it is constant in space when the medium is incompressible and isotropic. Typical values of k_i are given in Table 4.1. The *hydraulic conductivity*, K, is defined by the relation

$$K = \frac{k_i \rho_w g}{\mu}. \tag{4.6}$$

The hydraulic conductivity, K has a unit of velocity, length per time, and, again assuming saturated condition, it is easily seen that it depends on the flow geometry (type of medium and pore) as well as on the fluid specific weight and viscosity. It is also constant for a given fluid at a fixed temperature when the porous medium is incompressible and isotropic. Typical values for a few media with water and other fluids are given in Table 4.1. When the flow occurs in an unsaturated porous medium the values of K differ from those for saturation media; Therefor we need to know of the values of the hydraulic conductivity in different zones or in multiphase flow.
It is reported in the literature that the resistance to flux in an unsaturated porous matrix is greater than the resistance of the same matrix at saturated conditions. This

has two causes: first, a decrease in the water content causes a reduction of the cross-sectional area available for water flow and second, seepage occurs first in larger pores so that the flow in unsaturated conditions is mainly confined to small pores, resulting in an increase in the tortuosity of the flow paths (Bear, 1972). This means that the hydraulic conductivity of a soil decreases as the water content decreases.

Table 4.1: Typical values of hydraulic conductivity for incompressible porous media (Daily, 1966).

Medium	Physical permeability k_i, m^2	Hydraulic conductivity		
		Fluid type	Fluid temperature	K, m/sec
Gravel	$3.0466 \cdot 10^{-7}$ to $3.0466 \cdot 10^{-9}$	Water	15°C	0.914 to $9.14 \cdot 10^{-3}$
Sand	$3.0466 \cdot 10^{-9}$ to $3.0466 \cdot 10^{-12}$	Water	15°C	$9.14 \cdot 10^{-3}$ to $9.14 \cdot 10^{-6}$
Silt	$3.0466 \cdot 10^{-12}$ to $3.0466 \cdot 10^{-16}$	Water	15°C	$9.14 \cdot 10^{-6}$ to $9.14 \cdot 10^{-10}$
Randomly packed uniform spheres (d = diameter)	$(6.15 \cdot 10^{-4})\ d^2$			
Randomly packed uniform spheres ($d = 3.17 \cdot 10^{-3}$ m)	$6.68 \cdot 10^{-8}$	water Atmosp. Air Glycerin Linseed oil	15°C 15°C 20°C 20°C	$5.971 \cdot 10^{-2}$ $4.0824 \cdot 10^{-3}$ $8.8351 \cdot 10^{-5}$ $1.3009 \cdot 10^{-3}$

For saturated flow the hydraulic conductivity is constant, while for free surface flow the hydraulic conductivity should be defined as a function of saturation. Since the simulations are in saturated flow, K is taken as a constant. Laminar and turbulent flow states are assembled and solved for both flow models mentioned before (Darcy and Forchheimer). These states are obtained by changing the properties of the simulated porous medium, represented here by the intrinsic permeability and the porosity, as shown in Table 3.1. Recent works on seepage surface in a porous medium have shown that the hydraulic conductivity is a function of the flow state, hence both turbulent and laminar hydraulic conductivity have been considered in the simulations of flow in granular porous media (Solvik, 1995).

Another parameter that could have an effect on the motion of the fluid through the porous medium is the dynamic viscosity, μ. This fluid property is related to the hydraulic conductivity and at the same time to the Brinkman term in the discretized Navier-Stokes equation. For the current simulation with incompressible Newtonian

fluid, the viscosity is kept constant and the values shown in Table 3.1 are used to compensate for the value of the A coefficient that appears in Eq. (4.3).

For the Forchheimer-Brinkman model an additional coefficient is needed, namely the inertia coefficient, B. The inertia coefficient has been derived from empirical relations and is taken as a constant (Bear, 1972), as shown in Table 3.1. By solving the Navier-Stokes equations for flow through idealized media at different Reynolds number, Stark (1968) has shown that A and B remain essentially constant over a range of Reynolds numbers, therefore and the Forchheimer equation is applicable in real flow problems.
In the literature it can be found from experimental results that the resistance is proportional to the velocity of the power varying between 1 and 2, however but in most cases the power is taken equal to 2 (Volker, 1969). Hence, to approach the Forchheimer model, the power, m, of the nonlinear term in equation (4.3) is set to one in order to get the velocity of the power squared. This term plays a role while the flow state is changing from laminar to turbulent flow; then the inertia force dominates the flow and viscous the effect is negligible.

4.5. Solution method (relaxation, convergence)

The solution procedures employed in the computational program are categorized into two groups depending on whether the steady-state or transient flow equations are to be solved. Furthermore, the solution procedures for the transient equations are sub-divided into two groups depending on whether an implicit or explicit time integration technique is employed. For a steady-state problem or a transient problem employing an implicit time integrator (Backward Euler or Trapezoid rule), a nonlinear matrix system of equations must be solved, once for a steady-state problem or at each time step for the transient problem. The simulation of free surface problems has been treated recently as a moving boundary which means that an initial position of the free surface needs to be defined. This implies a solution made in two stages: first to use a fixed boundary steady-state condition and, then, to use a moving boundary with a transient solution utilizing the results of the fixed boundary simulation as the initial condition. Hence, the free surface simulation must be treated in stages if convergence is to be achieved

The application of the Galerkin finite element procedure to the stationary Navier-Stokes equations, or to the transient Navier-Stokes equations when an implicit time integrator is employed, results in a set of nonlinear algebraic equations that may be represented in matrix form as

$$M\frac{dU}{dt} + \left(K_{D-F}(\mathbf{u}) + K_p\right)U = F \tag{4.7}$$

where $K_{D\text{-}F}(\mathbf{u})$ represents the nonlinear part of equation system (Darcy-Forchheimer term), while K_p is linear part and M is the inertia terms, U is the global vector of the unknowns (velocities, pressures) and F is a vector which includes the effect of the body forces and boundary conditions. For the isothermal problems we have in the current study, all temperature-dependence is absent and the energy equation is not required. In such flows the momentum equation (4.7) is solved with the continuity equation.

At present, in the computational program, there are two different solution methodologies utilized for solving the nonlinear equation systems described above. The resulting algorithms are conceptually quite different. The first approach solves all conservation equations in a simultaneous coupled manner, while the second approach solves each equation separately in a sequentially segregated manner.

The segregated approach is guaranteed to have substantially fewer disk storage requirements than the fully coupled solver. In general this depends on the size of the problem being solved and the number of iterations required to obtain convergence. Due to its sequential and uncoupled nature, the segregated solver requires more iterations than the coupled solver. Before more discussion of the segregated solver chosen, two concepts, which arise repeatedly, will be explained: the radius of the convergence and the rate of the convergence of the particular algorithm. Suppose that an iterative procedure generates a series of iterations $\{\mathbf{u}_i,\ i=1,\ldots,n\}$; then the (asymptotic) rate of convergence is an integer k such that, for sufficiently large i,

$$\left\|\mathbf{u}_{i+1} - \mathbf{u}_i\right\| \le \mathbf{C}\left\|\mathbf{u}_i - \mathbf{u}_{i-1}\right\|^k \tag{4.8}$$

where $\mathbf{C}$ is a constant and $\|\cdot\|$ is an appropriate norm. If $k = 1$, the rate of convergence is linear, if $k = 2$, it is quadratic, etc. When the radius of convergence is referred to, it will usually be in conjunction with a problem parameter, such as the Reynolds number in the current problem is; i.e., given an initial guessed vector, to find the highest Reynolds number for which the iterative algorithm will converge and so on.

The algorithms for the discrete equations arising from steady-state Navier-Stokes equations with a Darcy-Forchheimer term instead of the convection term are considered in this section. The basic structure of the discrete system to be solved is reviewed here. The steady-state Navier-Stokes equation in matrix form is:

$$\left(K_{D\text{-}F}(\mathbf{u}) + K_p\right)U = F. \tag{4.9}$$

The nonlinear part, $K_{D\text{-}F}(\mathbf{u})$, is an unsymmetric matrix and represents the Darcy-Forchheimer matrix which arises from the resistance term of porous medium flow, while and the linear part, K_p is a symmetric matrix and represents the contribution of the diffusion, pressure and continuity terms. There are two ways to approach the solution of the Navier-Stokes equation in FIDAP: the first one is the penalty approach and the other is the mixed approach. If a penalty approach is used, the continuity equation is discarded and the pressure is no longer present in the global vector system

of unknowns, $\mathbf{u}$ and the matrix, K_p, includes the penalty matrix contribution. When the mixed approached is specified the pressure variable is discretized and contributes as an additional degree of freedom to the system of unknowns in the momentum equation to be solve for. Then the momentum equation is solved with the incorporation of the continuity equation, which is also necessarily for flow in porous medium.

For Reynolds numbers much greater than one, the resistance Darcy-Forchheimer term is very important, since it causes the nonlinear character of the equation to become dominant and makes the choice of solution algorithm, its convergence and efficiency, a key issue. The strong nonlinearity of equation (4.9) dictates the use of a type of iterative procedure to reach an accurate solution. The search for suitable iterative methods is complicated by the existence of a multitude of possible procedures and their variants. However the trial solution procedure showed that the full coupled iterative method can be recommended for convergence within a fair range of Reynolds numbers, whereas it is not allowed in the current simulation with the Darcy-Forchheimer resistance term. A trial was made of convergence of the solution of the rectilinear and radial flow by applying the "fixed point iteration" procedure which is also known as successive substitution (S.S.). No effective convergence was reached by this iterative method. Thus, the segregated iterative method is assembled and used in the computer program to solve the problems under consideration.

The segregated solution algorithm has been designed to address large-scale simulations. It is essentially based on the implicit approach and has many features in common with the standard implicit approach also available in the computer program (FIDAP, 7.61). The most important difference is that it avoids the direct formation of the global system matrix. Instead, this matrix is decomposed into smaller sub-matrices, each of which governs the nodal unknowns associated with only one conservation equation. These smaller sub-matrices are then solved in a sequential manner using either direct Gaussian elimination or conjugate gradient type schemes. An important point to realize is that owing to its sequential nature, the segregated algorithm requires more iterations to converge. On the other hand, the computational time required to perform one iteration in the segregated method is substantially less than for one iteration in the fully coupled solver.

A common convergence criterion used by many FEM practitioners requires that the absolute value of the change of solution variables at every node be less than a preset tolerance. However in FIDAP this criterion is not recommended because it does not take into account the values of the solution variables at the node. For example, if the required difference of the velocities at each node between successive iterations is less than 0.001, then if the velocity field is typically of magnitude 10^{-3} at each node this criterion is meaningless. Therefore, two obvious variables for use in designing termination criteria are introduced in the computer program (FIDAP 7.61). They are the solution vector $\mathbf{u}_i$ (at iteration i) and the residual vector $\mathbf{R}(\mathbf{u}_i)$. It is naturally desirable that the solution vector at the end of each iteration be within a certain

tolerance, $\varepsilon_{\mathbf{u}}$, of the true solution vector $\mathbf{u}$. Hence, a realistic convergence criterion, based on relative error, is

$$\frac{\|\Delta \mathbf{u}_i\|}{\|\mathbf{u}\|} \leq \varepsilon_{\mathbf{u}} \quad ; \quad \Delta \mathbf{u}_i = \mathbf{u}_i - \mathbf{u} \tag{4.10}$$

where $\|.\|$ is an appropriate norm, usually the Euclidean norm. However, $\mathbf{u}$ is not known a priori and must be approximated, the obvious choice being for $\|\mathbf{u}_i\|$ $\|\mathbf{u}\|$ and $\mathbf{u}_{i-1}$ for $\mathbf{u}$ in $\Delta \mathbf{u}_i = \mathbf{u}_i - \mathbf{u}_{i-1}$. Although this convergence criterion is quite effective for many algorithms (e.g., Newton-Raphson), a more suitable convergence criterion is also introduced in FIDAP, based on the residual vector which must tend to zero as $\mathbf{u}_i$ tends to $\mathbf{u}$. This criterion requires that

$$\frac{\|\mathbf{R}(\mathbf{u}_i)\|}{\|\mathbf{R}_0\|} \leq \varepsilon_{\mathbf{F}} \tag{4.11}$$

where $\mathbf{R}_0$ is a reference vector, typically $\mathbf{R}(\mathbf{u}_0)$. This shows that a combination of these two criteria provides an effective overall convergence criterion for all possible situations, since both $\Delta\mathbf{u}_i$ and $\mathbf{R}(\mathbf{u}_i)$ tend to zero near the solution. For the problems simulated in the current study, the segregated iterative method is chosen, with 50 iterations. Both velocity convergence tolerance and a residual convergence tolerance of 0.0001 is applied for the steady-state solutions. Note here that a relaxation factor of 0.03 is applied to the solutions; in order to accelerate the convergence rate, this relaxation factor is lower than the default value in FIDAP.

5. Comparison of solutions

In this section analytical and numerical solutions are discussed and illustrated for confined flow (rectilinear and radial flow) and unconfined flow (free surface flow) with the initial and boundary conditions given in Section 4.1. Laminar and turbulent flow states are solved and compared with available numerical solutions applying the linear and nonlinear flow relations (Darcy and Forchheimer).

5.1. Rectilinear flow

For confined laminar flow in a rectangular domain, equations (3.6 - 3.9), obtained in Section 3.3.1 for the linear and nonlinear relations between the hydraulic gradient and flow velocity, are applied with given boundary conditions and illustrated below.
Linear equation (3.6), with $h_1 = 1.5$ m, $h_2 = 0$ m, and $K = 10^{-5}$ m/sec, yields:

$$h_D(x) = 1.5\text{m}\left(1 - \frac{x}{20\text{m}}\right) \tag{5.1}$$

where D denotes the Darcy solution and x varies from 0 m to 20 m.

Equation (3.9) describes the nonlinear relation which yields:

$$h_F(x) = h_1 - \left(\frac{\nu}{g \cdot k}\frac{Q_F}{A_c} + \frac{0.55}{g \cdot \sqrt{k}}\frac{Q_F^2}{A_c^2}\right) \cdot x \tag{5.2}$$

where h_F denotes the Forchheimer solution, ν is the kinematic viscosity, k_i is the intrinsic permeability for laminar flow, and Q_F is the specific discharge per unit width of the flow domain ($Q_F = q \cdot \mathbf{b}$; $\mathbf{b}$ is defined in Fig. 4.1); this can be determined implicitly from Eq.(5.2) with the applied boundary conditions:

$$Q_F = 1.5 \cdot 10^{-6}\,\frac{m^3}{sec \cdot m}. \tag{5.2a}$$

By substituting Q_F in Eq.(5.2) the equation of the falling head was obtained. A comparison of the analytical solution for linear and nonlinear laminar flow is illustrated in Figure 5.1 below

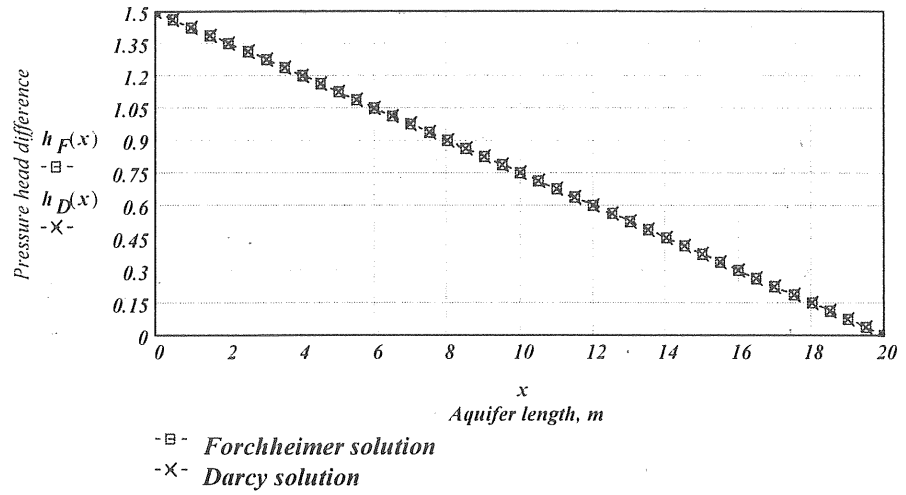

(a)

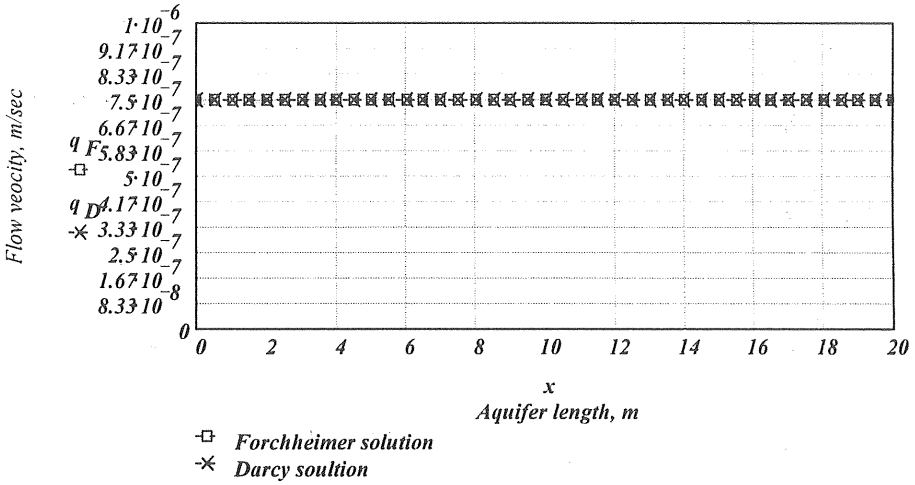

(

b)

Figure 5.1. Laminar confined flow: a) Pressure head difference, and b) Flow velocity

In a turbulent flow state the intrinsic permeability is four orders greater than in laminar flow, which corresponds to coarse gravel as shown in Table (3.1). The solutions of the linear and nonlinear relations in turbulent confined flow are shown in Figure 5.2.

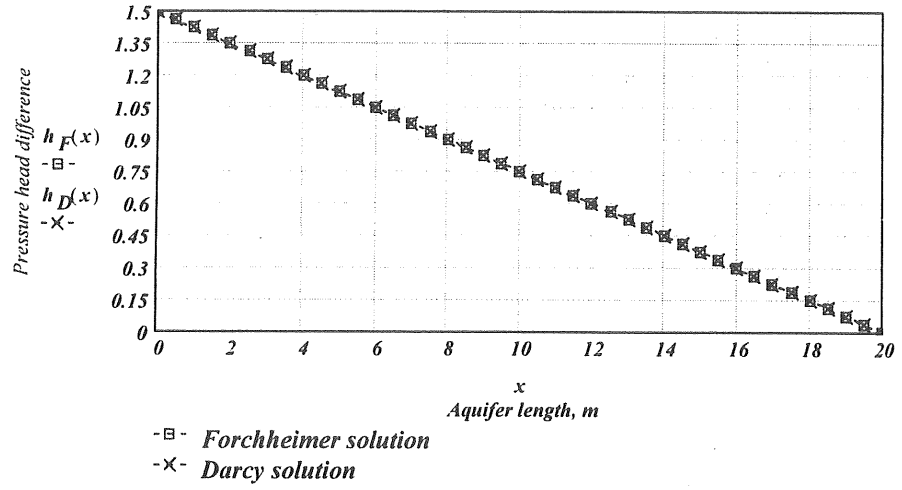

(a)

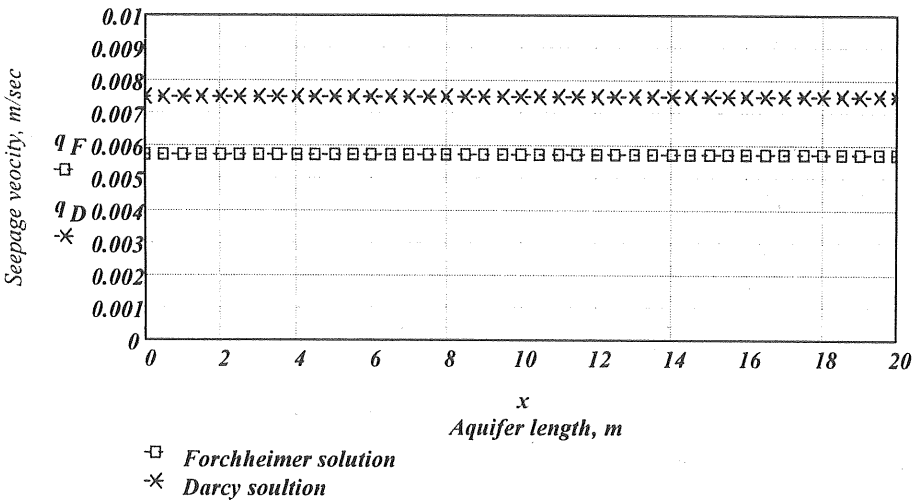

(b)

Figure 5.2. Turbulent confined flow: a) Pressure head difference, and b) Flow velocity

The analytical solutions of the pressure difference in laminar and turbulent states are shown to be similar, since, the hydraulic gradient is constant in both flow states. The results of the flow velocities obtained from linear and nonlinear equations are not similar for turbulent flow, which is reasonable if the squared term dominates the equation.

A velocity vector plot of the FEM solutions for the confined rectilinear flow, with the characteristics specified in Table 3.1, is shown in Figure 5.4

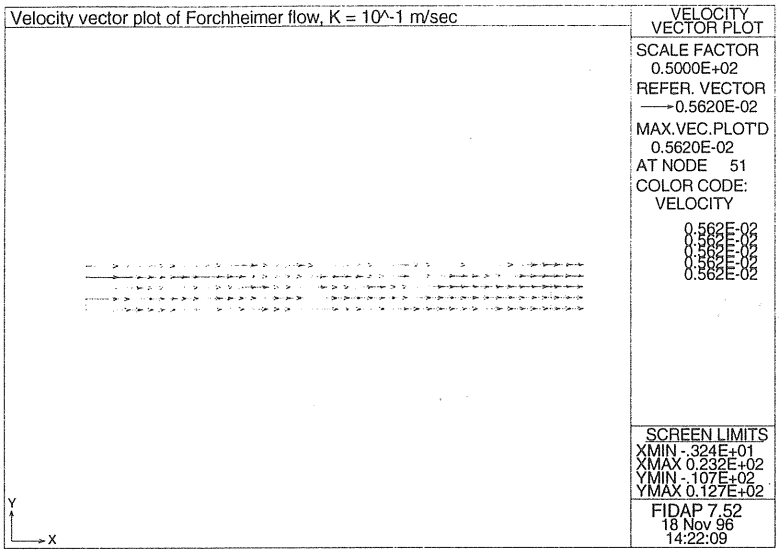

Figure 5.4. Velocity vector plot of rectilinear flow

The results of the velocity vector field by FEM for linear and nonlinear solutions are also the same in laminar flow while in a turbulent flow the velocity vector field obtained when a linear relation is applied is higher than for a nonlinear relation, which agrees with the analytical solutions.
Table 5.1 shows a summary of the analytical solutions and the FEM solution for different degrees of freedom in turbulent and laminar flows.

Table 5.1. A comparison of analytical and numerical solutions for rectilinear flow.

Flow state	Flow model	Flow velocity *m/sec*				Pressure head *m*			
		Analytical solution		*FEM solution FIDAP*		*Analytical solution*		*FEM solution FIDAP*	
		inflow	outflow	inflow	outflow	inflow	outflow	inflow	outflow
Laminar	Darcy	$0.75\cdot10^{-6}$	$0.75\cdot10^{-6}$	$0.736\cdot10^{-6}$	$0.736\cdot10^{-6}$	1.5	0	1.482	0.0187
	Forchheimer	$0.75\cdot10^{-6}$	$0.75\cdot10^{-6}$	$0.736\cdot10^{-6}$	$0.736\cdot10^{-6}$	1.5	0	1.482	0.0187
Turbulent	Darcy	$0.75\cdot10^{-2}$	$0.75\cdot10^{-2}$	$0.736\cdot10^{-2}$	$0.736\cdot10^{-2}$	1.5	0	1.482	0.0187
	Forchheimer	$0.6\cdot10^{-2}$	$0.6\cdot10^{-2}$	$0.562\cdot10^{-2}$	$0.562\cdot10^{-2}$	1.5	0	1.482	0.0187

5.2. Radial flow

The solutions for the linear and nonlinear relations in the symmetric radial flow shown in Figure 4.2 are obtained by a simple integration with the transformation to the spherical coordinate. When the boundary conditions are (cf. Sec. 4.2.2), the linear laminar flow rate per unit width with $K = 10^{-5}$ m/sec., from Eq.(3.15), yields:

$$Q_D = 8.767 \cdot 10^{-6} \frac{m^3}{sec.m} \tag{5.3}$$

and the falling pressure head along the radial distance, from Eq.(3.16), becomes

$$h_D(r) = 1.5\text{m} + C \frac{Q_D}{K} ln\left(\frac{4\text{m}}{r}\right) \tag{5.4}$$

where C is defined (cf. Sec. 3.3.2) as

$$C = \frac{360°}{2\pi\theta} \tag{5.5}$$

where $\theta = 60°$. The subscript D denotes the Darcy solution for radial flow. The radial distance, r, varies between $r_1 = 4$ m and $r_2 = 24$ m.
In the same way, the nonlinear laminar flow rate can be obtained from Eq.(3.21) in which the Forchheimer power is set to $m = 2$ and Eq.(3.21) becomes

$$1.5\text{m} = C_1 ln\left(\frac{24\text{m}}{4\text{m}}\right) + C_2\left(\frac{1}{4\text{m}} - \frac{1}{24\text{m}}\right) \tag{5.6}$$

where C_1 and C_2 are defined as

$$C_1 = C\frac{v}{g\,k} Q_F \quad \text{and} \quad C_2 = C^2 \frac{B}{g\sqrt{k}} Q_F .$$

Solving Eq.(5.6) implicitly for Q_F yields

$$Q_F = 8.767 \cdot 10^{-6} \frac{m^3}{sec.m}. \tag{5.7}$$

The resultant falling pressure head of the nonlinear flow becomes

$$h_F(r) = 1.5\text{m} + C_1 \cdot ln\left(\frac{4\text{m}}{r}\right) + C_2\left(\frac{1}{r} - \frac{1}{4\text{m}}\right) \tag{5.8}$$

where the subscript F denotes the Forchheimer solution.
The resultant flow rate per unit width when applying the linear and nonlinear flow equations is the same for laminar flow with $K = 10^{-5}$ m/sec. The analytical linear and nonlinear solutions for the pressure head difference and the flow velocity at laminar flow are illustrated in Figure 5.5.

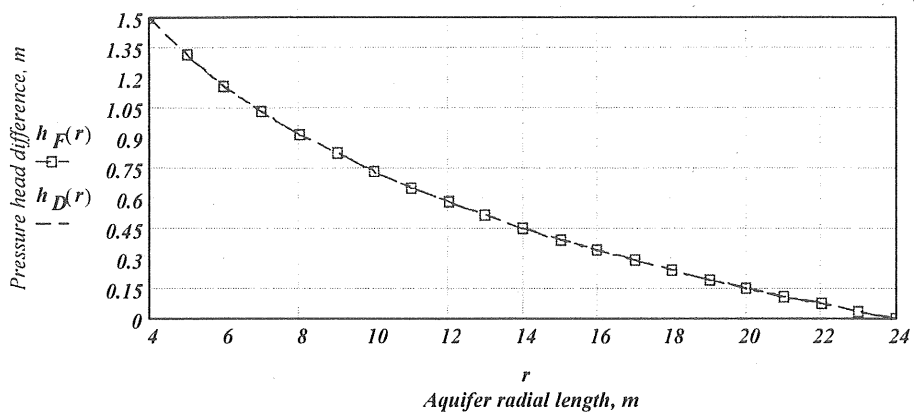

(a)

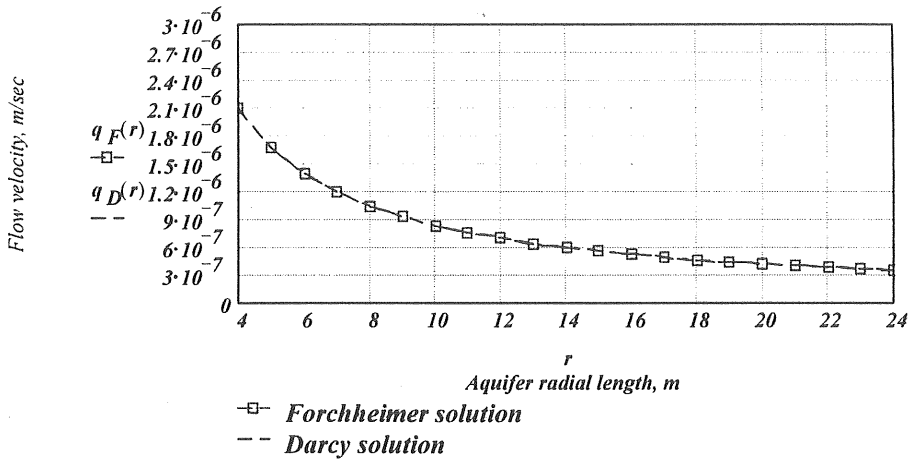

(b)

Figure 5.5. Laminar confined flow: a) Pressure head difference, and b) Flow velocity.

The resultant turbulent flow rate from Eqs. (3.15 and 5.6), in which $K = 10^{-1}$ m/sec. (coarse gravel), see Table 3.1, is different in linear and nonlinear equations:

$$Q_F = 0.0631 \frac{m^3}{sec \cdot m} \quad \text{and} \quad Q_D = 0.08767 \frac{m^3}{sec \cdot m}. \tag{5.9}$$

There are different flow effects for the same boundary conditions where the quadratic term in the nonlinear relation tend to dominate the flow; this is shown by the differences in the flow velocity at the inflow boundary and by the hydraulic gradient from both solutions. The pressure head difference and flow velocity obtained in turbulent flow are shown in Figure 5.6 below.

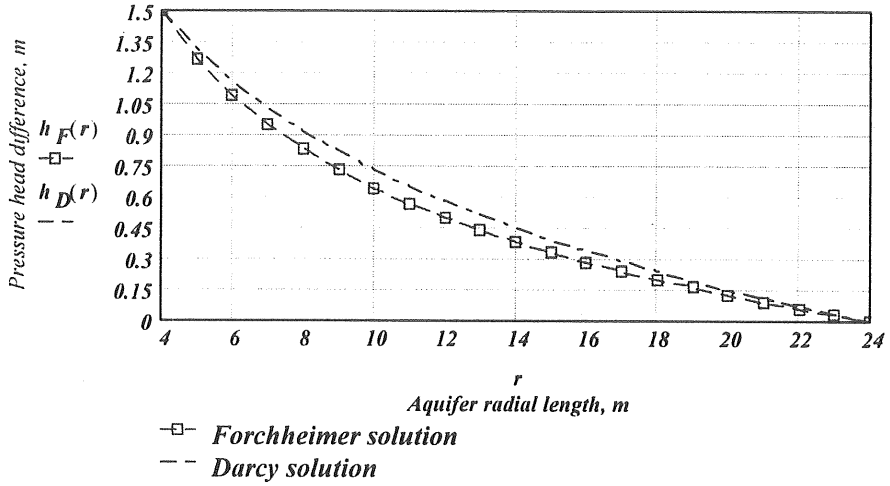

(a)

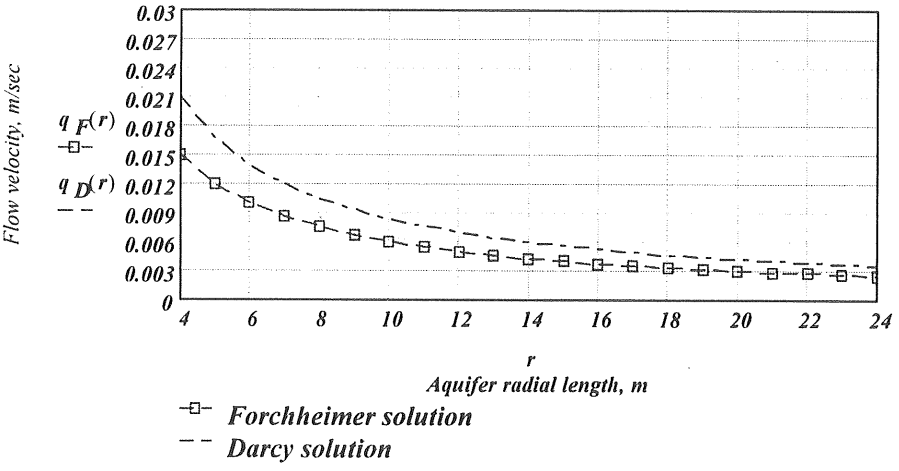

(b)

Figure 5.6. Turbulent confined flow: a) Pressure head difference, and b) Flow velocity

It is obvious that in turbulent radial flow the nonlinear Forchheimer flow gives a higher value of the hydraulic gradient than the linear Darcy flow, as shown in Figure 5.7.

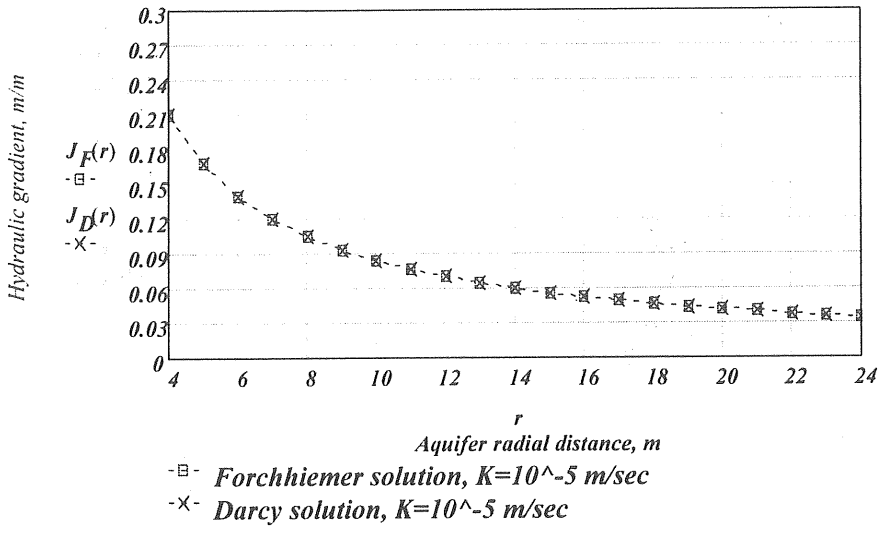

(a)

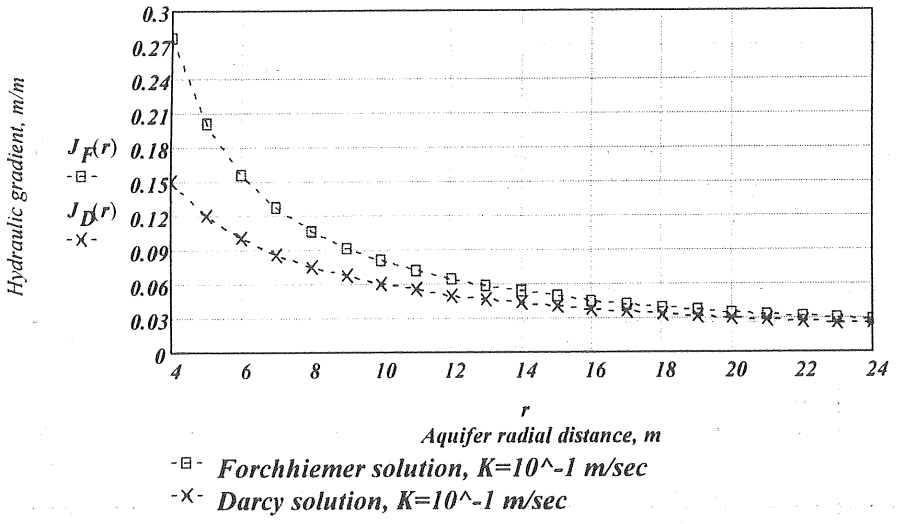

b)

Figure 5.7. The hydraulic gradient in radial flow: a) Laminar flow, and b) Turbulent flow

The numerical solution (FEM) of the velocity vector plot for the radial flow considered is shown in Figure 5.8.

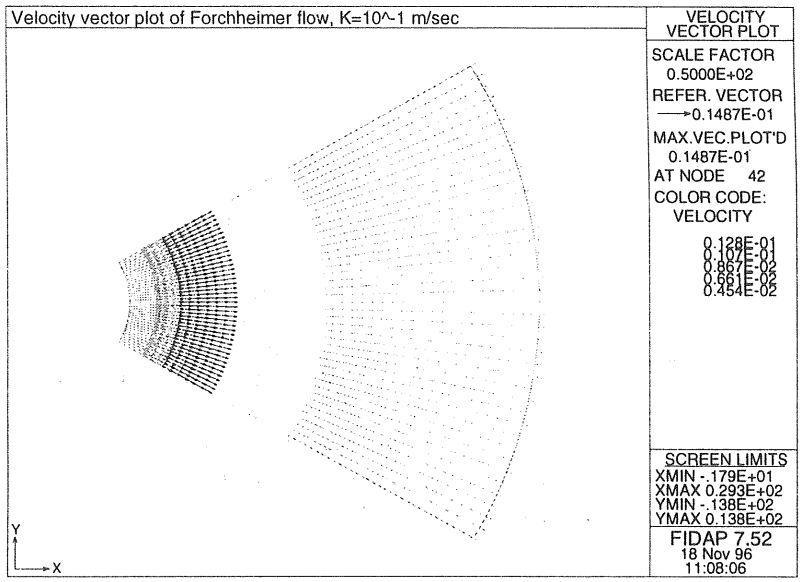

Figure 5.8. Velocity vector plot of radial flow

A summary of the comparison between the FEM solutions and the analytical solutions for different degrees of freedom is illustrated in Table 5.2.

Table 5.2. A comparison of analytical and numerical solutions for radial flow.

Flow State	Flow model	Flow velocity m/sec				Pressure head difference m			
		Analytical solution		*FEM solution FIDAP*		*Analytical solution*		*FEM solution FIDAP*	
		inflow	outflow	inflow	outflow	inflow	outflow	inflow	outflow
Laminar	Darcy	$0.2093 \cdot 10^{-5}$	$0.3488 \cdot 10^{-6}$	$0.20527 \cdot 10^{-5}$	$0.32163 \cdot 10^{-6}$	1.5	0	1.4202	0.00854
	Forchheimer	$0.2093 \cdot 10^{-5}$	$0.3488 \cdot 10^{-6}$	$0.20527 \cdot 10^{-5}$	$0.32163 \cdot 10^{-6}$	1.5	0	1.4202	0.00854
Turbulent	Darcy	$0.21 \cdot 10^{-1}$	$0.3488 \cdot 10^{-2}$	$0.20527 \cdot 10^{-1}$	$0.32163 \cdot 10^{-2}$	1.5	0	1.4202	0.00854
	Forchheimer	$0.178 \cdot 10^{-1}$	$0.3000 \cdot 10^{-2}$	$0.14874 \cdot 10^{-1}$	$0.24751 \cdot 10^{-2}$	1.5	0	1.4202	0.00854

5.3. Free surface flow

For the flow through an earth dam, we are faced with an additional complexity: the uppermost flow line must satisfy the requirement of being everywhere at atmospheric pressure or, in other words, its total must equal its elevation head. The analytical solution is complicated by this condition, but can be obtained by the methods of conformal mapping. The hodograph transformation (cf. Section 3.3.3) of a simple rectangular earth-fill dam, which was first introduced by Polubarinova-Kochina (1951), is applied here for the free surface flow boundary conditions specified in Table 3.1. With the ratio l/h_1 and the ratio h_1/h_2, Given in Figure 5.9, we are seeking the ratio h_0/h_1 together the points coordinates (x,y) of the phreatic line. The parameters α, β, and C of the solutions in equations (3.30 - 3.32) are found implicitly by the integrals, in which K in the above mentioned equations is the complete elliptic integral of the first kind.

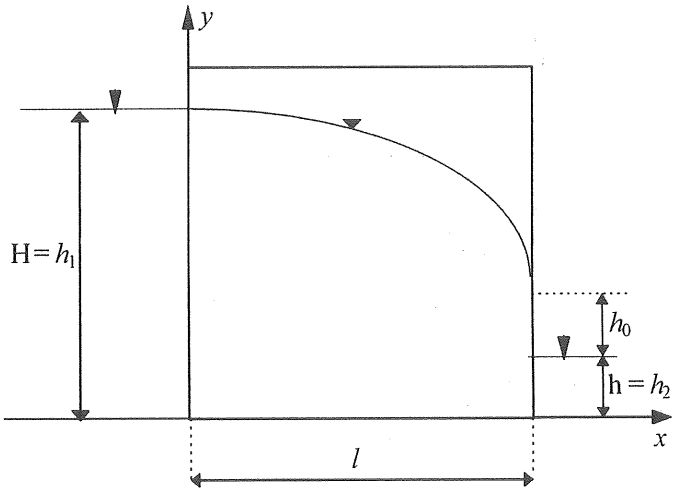

Figure 5.9. Definition of the flow domain dimensions

Hence, for H = 15 m, h = 5 m and l = 20 m, the parameters are

$$\alpha = 0.840079 \qquad \beta = 0.994887 \qquad C = 0.803313. \tag{5.10}$$

By solving the integral in Eq. (3.33) (see Appendix), the height of the separation is h_0 = 0.766 m, while the coordinate points of the phreatic line are found by the integrals in Eqs. (3.33-3.34).

The solution of Polubarinova-Kochina and the solution of the linear Dupuit approximation for flow in a simple rectangular dam are shown in Figure 5.10 below.

It should be noted that the Dupuit approximation is sometimes called the Dupuit-Forchheimer approximation, although it combines Darcy's law with free surface flow. Hence the Dupuit approximation is not applicable when there is extremely nonlinear

free surface flow. In addition, the Dupuit approximation does not give any separation height above the tail water level of the dam. This difference is obvious in Figure 5.10.

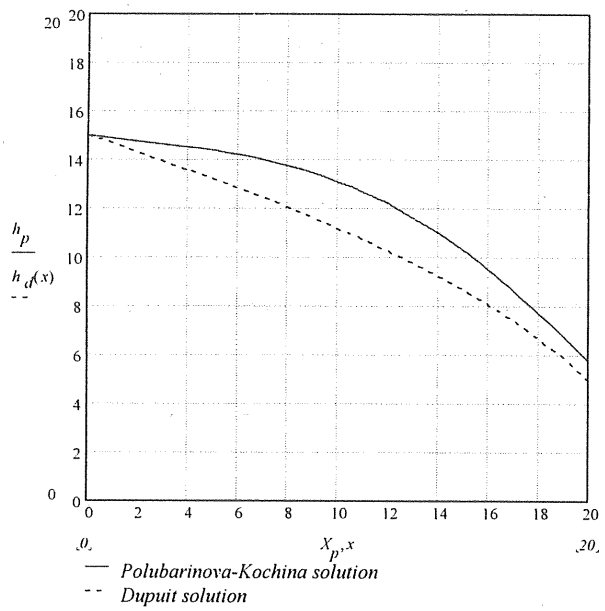

Figure 5.10. Solution of the phreatic line

According to Polubarinova-Kochina solution, the flow rate above the tail water surface at the downstream face can be determined from the following integral formula:

$$Q_{h_0} = K \cdot C \int_0^1 \frac{\boldsymbol{K}(\sin^2\psi)\sin\psi\cos\psi}{\sqrt{(1-\alpha_1\sin^2\psi)(1-\beta_1\sin^2\psi)}}\,d\psi \tag{5.11}$$

where K is the hydraulic conductivity in m/sec, C is as defined above, and $\boldsymbol{K}(\sin^2\psi)$ is the complete elliptic integral of the first kind while $\alpha_1 = 1\text{-}\alpha$ and $\beta_1 = 1\text{-}\beta$. For $K = 10^{-5}$ m/sec, the result is

$$Q_{h_0} = 5.656 \cdot 10^{-6}\, m^3 / \sec \cdot m. \tag{5.12}$$

The mean flow velocity above the tail water level is:

$$U_{h_0} = Q_{h_0} / h_0 = 7.386 \cdot 10^{-6}\, m / sec \tag{5.13}$$

where $h_0 = 0.766$ m (see Appendix).

The total inflow at the upstream face, H=h_1 can be obtained from the integral formula

$$Q_H = K \cdot a_c \int_0^A \frac{K(1-\frac{1}{\xi})}{\sqrt{\xi(\xi-1)(\xi-a)(\xi-b)}} d\xi \tag{5.14}$$

where

$$a = 1/\beta, \qquad b = 1/\alpha, \qquad a_c = \frac{C}{2}\sqrt{a \cdot b} \tag{5.14a}$$

and

$$Q_H = 4.997 \cdot 10^{-5} m^3 / \sec \cdot m. \tag{5.15}$$

The outflow below the tail water level at the downstream face, $h = h_2$, is calculated from the integral formula

$$Q_h = K \cdot C \cdot \sqrt{\alpha} \int_0^{\frac{\pi}{2}} \frac{K(1-\alpha \sin^2 \psi)\sin\psi}{\sqrt{(1-\alpha \sin^2 \psi)(\beta - \alpha \sin^2 \psi)}} d\psi. \tag{5.16}$$

For the same case we have

$$Q_h = 4.431 \cdot 10^{-5} m^3 / \sec \cdot m. \tag{5.17}$$

The vertical mean flow velocity in different sections of the earth dam is shown in Figure 5.11 in comparison with the Dupuit solution.

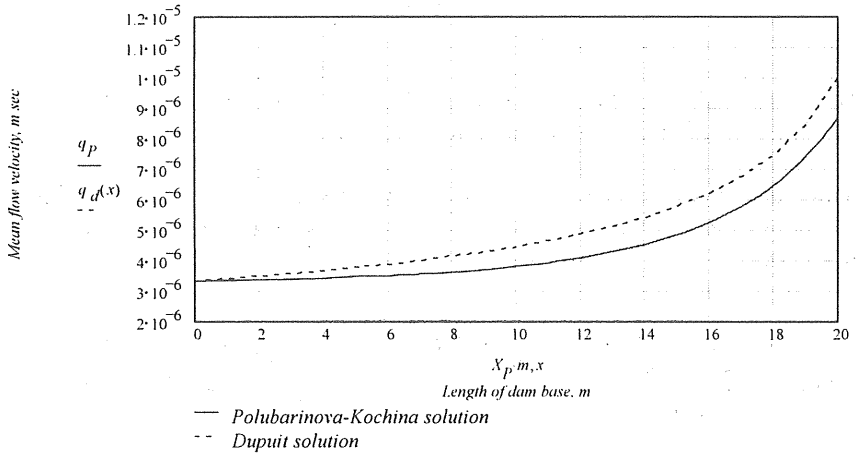

Figure 5.11. Mean flow velocity in the laminar state

For comparison, the vertical mean of the inflow and outflow velocities at laminar and turbulent states according to the Polubarinova-Kochina and Dupuit solutions is illustrated in Table 5.3.

Table 5.3. Vertical mean flow velocity in a simple rectangular earth dam

Flow state	Polubarinova-Kochina solution mean flow velocity m/sec		Dupuit/Darcy solution mean flow velocity m/sec		
	inflow	outflow	inflow		outflow
Laminar $K=10^{-5}$ m/sec	$3.331\cdot10^{-6}$		$8.666\cdot10^{-6}$	$3.333\cdot10^{-6}$	$1\cdot10^{-5}$
Turbulent $K=10^{-1}$ m/sec	0.033		0.087	0.033	0.1

The linear Darcy relation between the hydraulic gradient and the flow velocity was applied for the simple rectangular earth dam above. The analytical solution of the Laplace equation is possible for several other complicated flow geometries. However, for gravity flow with a free surface and nonlinear hydraulic resistance (Forchheimer equation), the nonlinearity in the phreatic line itself and the resulting nonlinear partial differential equation make it difficult to find an analytical solution for complicated geometries. Nevertheless, by using the Dupuit approximation for nonlinear resistance, we can obtain a solution as in Eq.(3.38) (cf. Section 3.3.3); thus we have

$$J_S = -\frac{dh(x)}{dx} = \frac{\nu}{gk}\frac{Q_S}{h(x)} + \frac{\boldsymbol{B}}{g\sqrt{k}}\left(\frac{Q_S}{h(x)}\right)^2 \tag{5.18}$$

where Q is the specific discharge per unit width and $\boldsymbol{B}$ is the inertia coefficient which is equal to 0.55 (Ward, 1964) obtained from experiments.

By solving the above differential equation with respect to x and expanding the solution in Taylor series, the obtained nonlinear equation of the phreatic line (Sharif's equation) be as:

$$h_S(x)=15\text{m}-\frac{Q_S\left(\frac{\nu}{gk}15\text{m}+\frac{\boldsymbol{B}}{g\sqrt{k}}Q_S\right)}{(15\text{m})^2}x-\frac{1}{2}\frac{Q_S^{\,2}\left(\frac{\nu}{gk}15\text{m}+\frac{\boldsymbol{B}}{g\sqrt{k}}Q_S\right)\left(\frac{\nu}{gk}15\text{m}+2\frac{\boldsymbol{B}}{g\sqrt{k}}Q_S\right)}{(15\text{m})^5}x^2. \tag{5.19}$$

The phreatic line obtained by applying Eq. (5.19) for laminar and turbulent flows is illustrated in Figure 5.12.

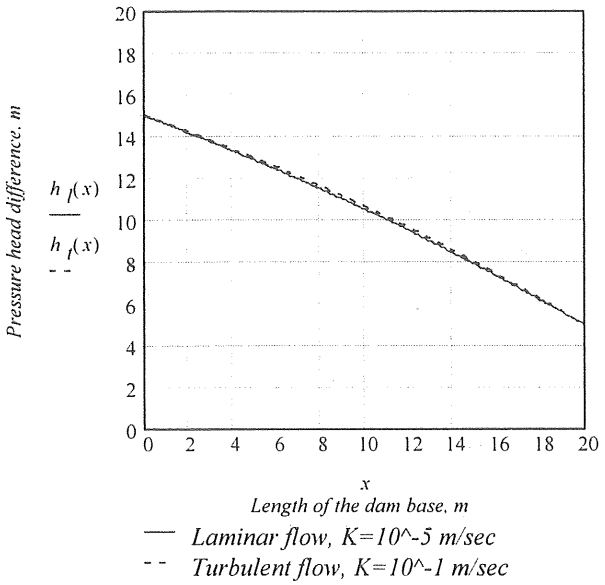

Figure 5.12. Nonlinear flow with the Dupuit approximation in a rectangular earth dam (Sharif's equation)

The Hydraulic gradient related to Eq.(5.19) is shown in Figure 5.13, for both the laminar and turbulent states, while the flow velocity is shown in Figure 5.14.

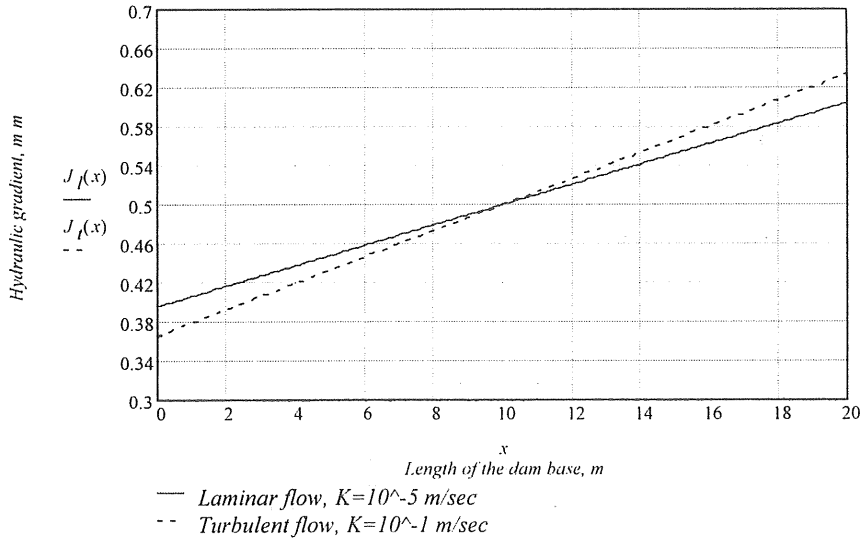

Figure 5.13. Nonlinear hydraulic gradient in a rectangular earth dam

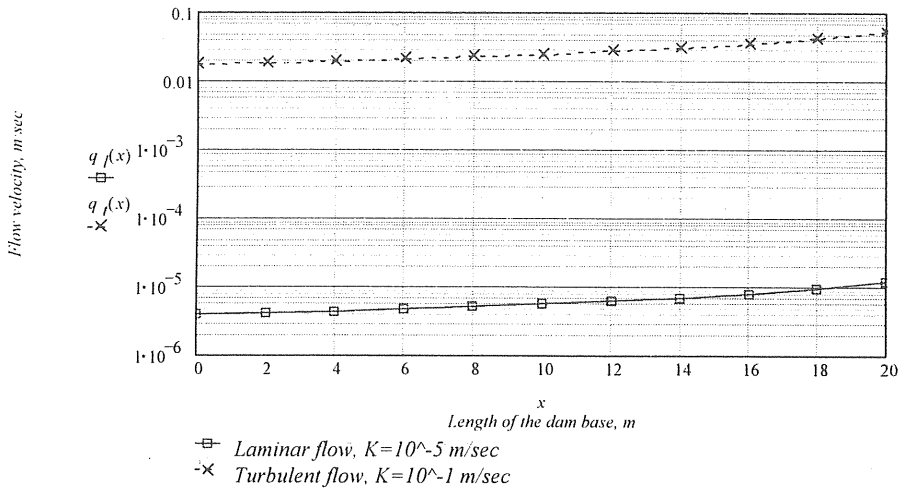

Figure 5.14. Nonlinear flow velocity in a rectangular earth dam

The comparison between the solution with Dupuit's approximation for Forchheimer and Darcy resistance terms is illustrated in Figure 5.15 below.

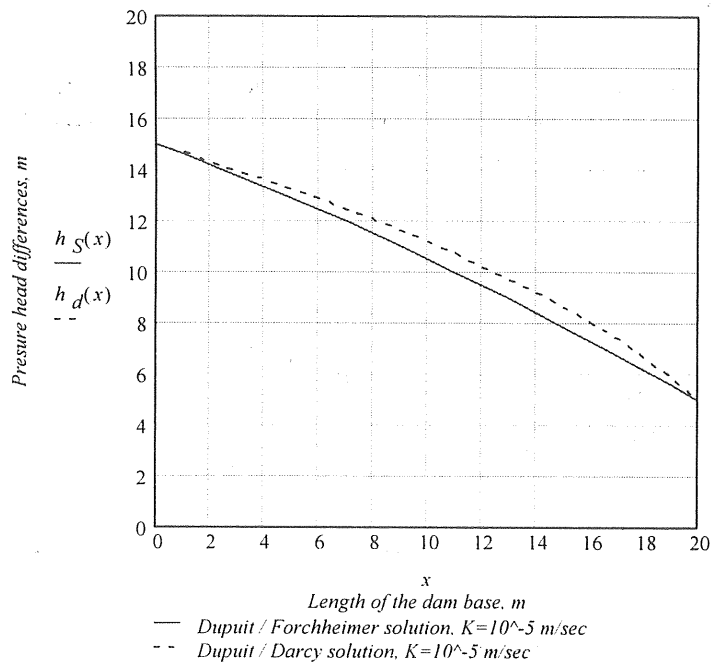

Figure 5.15. Falling head in a simple earth dam

The hydraulic gradient obtained by Dupuit's approximation for Forchheimer (Sharif's equation) and Darcy resistance terms is illustrated in Figure 5.16 below.

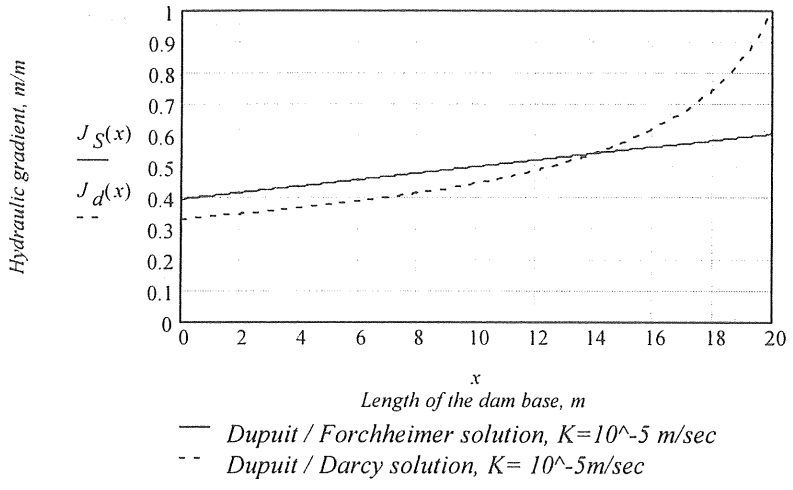

(a)

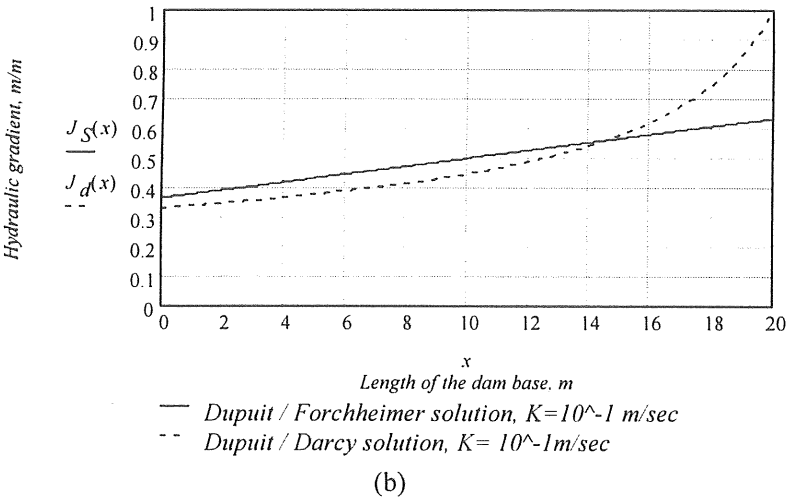

(b)

Figure 5.16. The hydraulic gradient in a simple earth dam: a) Laminar flow, and b) Turbulent flow

For comparison, the vertical mean of the inflow and outflow velocities at laminar and turbulent states according to Dupuit/Forchheimer resistance (Sharif's equation) and Dupuit/Darcy resistance solutions is illustrated in Table 5.4.

Table 5.4. Vertical mean flow velocity in a simple rectangular earth dam

Flow state	Dupuit/Forchheimer solution (Sharif's equation) mean flow velocity m/sec		Dupuit/Darcy solution (linear equation) mean flow velocity m/sec		
	inflow	outflow	inflow		outflow
Laminar $K=10^{-5}$ m/sec	$3.956 \cdot 10^{-6}$		$1.187 \cdot 10^{-5}$	$3.333 \cdot 10^{-6}$	$1 \cdot 10^{-5}$
Turbulent $K=10^{-1}$ m/sec	0.018		0.055	0.033	0.1

6. General discussion

The word seepage has been used to describe water flow phenomena through porous material. Darcy (1856) proposed a semi-empirical linear equation to describe the relation between the flow velocity and the hydraulic gradient in a porous medium. Accurate description of the flow conditions are obtained only in when the flow rate under consideration is in the pre-laminar or creeping regime. For higher flow velocities, it has been recognized since the last century that the Darcy law is not valid. The inertial effects, neglected in Darcy's law, must now be taken into consideration. This inclusion of inertial effect is important in porous media with large grain size. Thus, in a study of flow through rock-fill dams and flow in areas adjacent to a pumping well in a coarse-grained aquifer, it would be better to use a modified version of Darcy's law to describe the relation between the head loss and the velocity in order to obtain realistic solution. Accordingly, the nonlinear Forchheimer law is applied in the current study to include the inertial effect and with the aim of obtaining accurate estimation of seepage in confined and unconfined saturated porous media.

The linear Darcy law when coupled to mass conservation and appropriate boundary conditions, provides an adequate mathematical model from which valuable information may be deduced; it can often give a closed form solution. However, when applying Forchheimer's law, the resultant partial differential equation of the mass is difficult to solve in closed form. Also complicated flow geometry, e.g., when we have a free surface, made the problem too difficult to solve in simple analytical form. Thus, numerical solutions by the finite element method were applied to solve the linear and nonlinear flow equations using the computational flow program FIDAP 7.61 (1996).
Rectangular and cylindrical domains were selected to test the FEM solution. Then the rectilinear and radial velocity vector fields obtained from the FEM solution were compared with the analytical solution proposed in this study, for both linear and nonlinear laws.
The results showed that in the regime of laminar flow, where $K= 10^{-5}$ m/sec, there was no significant difference between the linear and nonlinear laws; however in flow where a turbulent regime occurs, $K= 10^{-1}$ m/sec, there was a deviation between the two laws of about 25%, which is in agreement with recently published work. The numerical results are also verified by the analytical solutions according to the two laws, which have shown a reasonable agreement.
A numerical solution for flow with a free boundary condition was not included in this study due to certain difficulty in obtaining such a free surface flow. However, different analytical solutions were obtained for the linear and nonlinear laws with free surface flow in simple rectangular dam. The Hodograph method and Dupuit approximation were applied to solve the linear law while the nonlinear law was solved by using the Dupuit approximation for the Forchheimer equation and expanding the resultant integrated equation in Taylor series (Sharf's equation).
The Hodograph solution has shown that the exit flow occurs at a separation height above the tail water level at the downstream face, while the Dupuit solution, which is also based on solving the linear law, gives different results by exiting the phreatic line

at the tail water level. In the literature, experimental work has shown that a fountain occurs where there is a free surface flow, which is in good agreement with the hodograph solution. Hence, there is a significant difference between the two solutions.
The nonlinear law solution proposed by the author shows different results from that of Dupuit solution at laminar an turbulent flow states. An obvious deviation between the solutions is obtained in turbulent flow. Hence a nonlinear effect is observed clearly in free surface flow when nonlinear law is used.

The linear and nonlinear laws were utilized in a simple relation between the critical gradient and the required grain diameter of the porous material, in order to satisfy a stability condition in the flow pattern. The stability analysis was based on Terzaghi concepts for defining the force applied on an individual grain at the exit gradient. The obtained simple relation obtained can be used in further work for the case of an inhomogeneous porous medium. The predicted shape of the phreatic line introduces the possibility of obtaining the critical gradient at the downstream face where the velocity is higher. Then a filter structure could be developed in order to reduce the higher gradient at that critical point.

Further work

For the current study, free surface flow simulation with the finite element method in homogenous and non-homogeneous porous media was not available. Hence, the following tasks need to be carried out to continue this research.

1. Application of the linear and nonlinear laws for free surface flow in earth and rock-fill dams with slope embankments should be related to unsaturated conditions.

2. A stability analysis needs to be made of the slope embankments relating to flow models applied in the numerical simulation.

3. A model that relates the nonlinear equation to stability of the core material of an earth dam and the transport process of the porous material.

4. A three-dimensional numerical simulation would be more specific for free surface flow in non-homogeneous porous medium in relation to the linear and nonlinear laws.

5. Experimental work is necessary to verify numerical results.

References

- Arulanandan, K., Sargunam, A., Loganathan, P., Krone, R. B., (1973) "Application of Chemical and Electrical Parameters to Prediction of Erodibility," (Special Report 135 on Soil Erosion, Highway Research Board), Jan. 26, pp. 42-51.

- Arulanandan, K., Loganthan, P., Krone, R. B., (1976)," Clouser to "Pore and Eroding Fluid Influence on the Surface Erosion of a Soil," *J. Geot. Engineering Divi.*, ASCE, Vol. 102, No. GT8, Proc. Paper 11078, Aug., pp. 883-884.

- Arulanandan, K., and Heninzen, R. T., (1977), "Erosion and Solid Matter Transport in Inland Water Symposium," Proceeding, Symposium: United Nations Educational, Scientific and Cultural Organization and IAHS, pp. 75-81.

- Bakker, M., (1997), "Groundwater Flow with Free Boundaries Using the Hodograph Method," *Adva. in Water Resources*, Vol. 20, No. 4, pp. 207-216.

- Bear, J., Zaslavsky, D., and Irmay, S. (1968), "Physical Principles of Water Percolation and Seepage", UNESCO, Paris,.

- Bear, J., (1972), *Dynamics of Fluids in Porous Media*, American Elsevier Publishing Company, Inc., N. Y., New York,

- Bear, J., (1979), *Hydraulics of Ground Water*, McGraw-Hill, Inc. New York.

- Bear, J., and Yavuze C. M., (1987), *Advances in Transport Phenomena in Porous media*, NATO ASI Series, Series E: Applied Sciences-No. 128,.

- Boulton, N. S., (1954), "The Flow Pattern Near a Gravity Well in a Uniform Water-Bearing Medium," *Proceedings*, Institution of Civil Engineers, ,Vol. 36, London, pp. 534.

- Boussinesq, J. (1904), *J. Math.* Vol. 10, No. 5 pp. 363.

- Casamitjana, X., and Roget, E., (1988) " Effect of Suspended Sediment on the Heating Lake Banyoles" *J. Geophys. Res.* 93, pp.9332-9336.

- Courant, R., Hilbert, D. Methoden der Mathematischen Physik (2vols.). Interscience Publ., New York, (1943).

- Carslaw, H.S., Jaeger, J. C., (1959), *Conduction of Heat in Solids*. 2nd ed. Clarendon Press, Oxford.

- Casagrande, A., (1976) Chadwick, W.L., Coombs, H. A., Dow, H.W., Fuik, E. M., Higginson, R. K., Leps, T. M., Peck, R. B., Seed, H. B., and Jansen, R. B., "Failure of Teton Dam," U.S., Department of Interior and State of Idaho, Dec., .

- Cedergren, H. R., Seepage Control of Earth Dams, Embankment Dam Engineering, R. C. Hirshfeld and S. J. Poulos, Eds., John Wiley & Sons, Inc., New York, N.Y., 1973.

- Cedergren, Harry R., (1976), "Evaluation of Seepage Stability," Paper presented at Engineering Foundation Conference on Evaluation of Dam Safety, Pacific Grove, Califo., November 28-December 3, pp. 195-218 of Proceedings A.S.C.E., published in 1977.

- Cedergren, Harry R., (1989), *Seepage, Drainage and Flow Nets,* John Wiley & Sons, New York.

- Ching, S. C. , (1988) "Boundary-Element Analysis for Unconfined Seepage Problems", *J. Geot. Engineering*, Vol. 114, No. 5, May, pp. 556-572.

- Childs, E. C., (1956), Soil Science Prog. No. 174, pp. 208,.

- Crank, J., (1984), *Free and Moving Boundary Problems*, Clarendon Press, Oxford.

- Cryer, C. W., (1976), MRC Techn. Summary Rep. 1657, University of Wisconsin, Madison.

- Daily, J. W., Donald Harleman. R. F., (1966), "*Fluid Dynamics*" Addison-Wesley Publishing Company, INC. .

- Darcy, H., (1856) "*Les Fontaines Publiques de la Ville de Dijon, Dalmont*", Paris.

- Decker, R. S., and Dunningan, L. P., (1976),"Development and Use of the SCS Dispersion Test," American Society of Testing and Materials Symposium on Dispersive Clays, Chicago, I11.,

- Desai, C. S., (1970), "Seepage in Missippi River banks: analysis of transient seepage using viscous flow model and numerical methods", Miscellaneous Paper S-70-3, USA Engineer Waterways Experiment station, Vicksburg, Feb.,

- Desai, C. S., (1971), *Seepage in Porous Media*, In Numerical Method in Geotechnical Engineering, C. S., Desai and J. T. Christian (Eds.), McGraw-Hill, New York.

- Desai, C. S., (1972), "Overview, Trends and Projections: Theory and Applications of the Finite Element Method in Geotechnical Engineering" State of the Art Paper,

Proceedings of Symposium on Application of FEM in Geotechnical Engineering, C. S. Desai (ed.), USA Engineer Waterways Experiment Station, Vicksburg.

- Dupuit, J., (1863), *Études Théoriques et Pratiques sur le Mouvement des Eaux dans les Canaux Découverts et á travers les Terrains permeables*, 2nd ed., Dunod, Paris.
- Dykstra, H., Parsons, R. L., (1951), *Trans. AIME* Vol. 192, pp. 227.
- Emersleben, O. (1924), "Bautecnik" No. 2, pp.73.
- Emersleben, O. (1925), Physikal, Z. No. 26, pp. 601.
- Emerson, W., (1954)"The Determination of the Stability of Soil Crumbs," *Journal of Soil Saturation*, Vol. 5, pp. 233-250.
- Engelund, F., (1953), "On the Laminar and Turbulent Flows of Groundwater through Homogenous Sand," Tech. Univ. of Denmark Bull., No. 4.
- Ergun, S., Oring, A. A., (1949) "Fluid Flow Through Randomly Packed Columns and Fluidised Beds, " *J. Indus. and Engineering Chemistry*, Vol. 41, No. 6, pp. 1179-1183.
- Finn, W. D. L. (1967), "Finite-Element Analysis of Seepage through Dams, " *J. Soil Mech. & Found. Div.* ASCE, Vol. 93, No. SM6, Proc. Paper 5552, Nov., .
- FIDAP, 7.61, (1996), " *FluId Dynamics Analysis Package*", Theory and FIPREP manuals of the program.
- Forchheimer, P. H., (1901), "Wasserbewegung durch boden," Z. Ver. Ing., pp. 1782.
- Forchheimer, P. H., (1930), Hydraulik. B. G. Teubner, Leipzig.
- Florin, V. A., (1948), "Certain Nonlinear Problems on the Consolidation of Water-Saturated Substances of the Earth" (in Russian), *Izv. Akad. Nauk, SSSR, Otdel. Tekh. Nauk* 9, pp. 1389.
- Gardner, W. et al. (1934), Trans. Amer. Geophys. Un. 15, pp. 563.
- Ghislain de Marsily, (1986), "*Quantitative Hydrology*," *Groundwater Hydrology for Engineers*, Academic Press, INC.
- Giriniski, N. K. (1937), "Generalization of Some Solutions for Wells to More Complicated Natural Conditions" (in Russian), Dokl. A.N. U.S.S.R. No. 3, 54.
- Giriniski, N. K. (1941), Stori´zdat, Dokl. 1941.

- Golubeva, O. V., (1950), "Equations of Two-Dimensional Flow of an Ideal Fluid with Curvilinear Surface and their Application in Seepage Theory," Prikl. Mat. Mekh. Vol. XIV, 17, pp. 485.
- Hall, H. N., (1953) "Compressibility of Reservouir Rocks", Trans. A.I.M.E., 198, pp. 309-316
- Hamel, G., (1934) Z. Ang. Math. Mech., Vol. 14, pp. 129.
- Harr, M. E., (1962), "*Groundwater and Seepage*," McGraw-Hill Book Co., Inc., New York.
- Hele-Shaw, H. S., (1899), " Experiments on the Nature of the Surface Resistance in Pipes and on Ships, " *Trans. Inst. Naval Architects* Vol. 39, pp. 145-156.
- Howerd, A. D., and Mclane, C. F. (1981), " Groundwater Sapping in Sediments: Theory and experiments (abstract), " NASA tech. Memo, 84271, pp. 283-285.
- Howerd, A. D., and Mclane, C. F. (1988), " Erosion of Cohensionless Sediment by Groundwater Seepage." *Water Resour. Res.*, 24(10), pp. 1659-1674.
- Hubbert, M. K., (1940), "The Theory of Groundwater Motion," *J. Geol.* Vol. 38, pp. 785-944.
- Hubbert, M. K., (1956), " Darcy Law and the Field Equations of the Flow of Underground Fluids ," Trans., Amer. Inst. Min. Metal Eng. " 207, pp. 222-239.
- Irmay, S., (1946), "On the Motion of Water in Soil, Basic Chapters in Theories of Soil Physics and Mechanics, M. Sitz(ed.) Israel Assn. Eng. Arch; water section, TelAviv, 59-71a.
- Irmay, S., (1947), "Sur Le Mouvement Des Eaux Dans Le Sol", Resvue Universells des Mines, 3, liée, pp. 129-139.
- Irmay, S., (1951), "On the Motion of Capillary Moisture in Soils," Sci. Pub., 4, Hebrew Inst. Tech., Haifa, Israel, pp. 43-90; p. (XII-XIV), (English abstract).
- Irmay, S., (1953)," Saturated Steady Flow in Non-Homogenous Media and its Application to Earth Embankments, wells, drains, *3rd Intern. Conf. Soil Mech. Found. Eng.* , Zurich, 2, pp. 259-263.
- Irmay, S., (1956)," Experiments on the Range of Validity of Darcy's Law and the Appearance of Turbulence in a Filtering Flow, La Houille Blanche, 11, pp. 419-421.

- Irmay, S., (1958), "On the Derivation of Darcy and Forchheimer Formulas " Trans. Amer. Geophys. Union, Vol. 39, No. 4, pp. 702-707.
- Jacob, C. E., (1950) "*Flow of Groundwater*", Engineering Hydraulics, H. Rouse, (ed.) Wiley & Sons.
- John, A. McCorquodale, (1970), "Variational Approach to Non-Darcy Flow" J. Hyd. Divi., ASCE, Vol. 96, No. HY11, Nov., pp. 2265-2278.
- Jeppson, R. W., (1968), "Seepage from Ditches: Solution by Finite Differences," J. Hyd. Divi., ASCE, Vol. 94, No. HY1, Proc. Paper 5763, Jan., pp. 259-283.
- Kozeny, J.,(1927) "Über Kapillare Leitung des Wassers im Boden," Sitz-Ber. Wiener Akad., Abt Iia, 136, pp. 271-306.
- Landu, L. D., and Lifschitz, E. M., (1958), "*Statistic Physics* (English translated by E. Peierls and R. F. Periels), Addison Wesley, Reading, Mass.
- Lamb, T. W., and Whitman, R. V. (1968). "*Soil Mechanics*" John Wiley and Sons, New York, N. Y.
- Laurent, J. (1949), "Review on General Hydraulics", 15, No. 50, 79; No. 51, pp.143.
- Leibenzon, L. S. (1947), " The Flow of Natural Fluids and Gases in Porous Media", (in Russian), Gostekizdat, Moscow.
- Lindquist, E., (1933), "The Flow of Water Through Porous Soil," 1st, Congress on Large Dams, Stockholm.
- Manegold, E., (1937), "Kolloid"-Z. 80, pp. 253
- Manegold, E., (1941), "Z. Ver. Deut. Ing., Beih. Verfarenstech., pp. 44.
- McCorquodale, J., A., (1970), "Variational Approach to Non-Darcy Flow" *J. Hyd. Divi., ASCE*, Vol. 96, No. HY11, Nov., pp. 2265-2278.
- Mendoza, C. and Zhou, D. (1992), " Effect of Porous Bed on Turbulent Stream Flow Above Bed," *J. Hydr. Engineering, ASCE*, 11, pp. 1222-1240.
- Missbach, A., *Listy Cukrova*, Vol.55, pp. 293.
- Muniram, B., and Roger, G., (1996) "Slope Instability from Ground-Water Seepage" J. Hydr. Engineering, ASCE, Vol. 122, No. 7, July, pp. 415-417.
- Muskat, M., (1946), "*The Flow of Homogeneous Fluid Through Porous Media*" 1st , McGraw-Hill, New York.

- Muskat, M., (1949), "*Physical principle of oil production*", McGraw-Hill, New York, pp. 922.
- Neuman, S. P., Witherspoon, P. A., (1971) "Analysis of Unsteady Flow with a Free Surface Using the Finite Element Method" , Water Resources Research, 7, pp. 3-23.
- Oroveanu, J., (1966), "Flow of Multiphase Fluids through Porous media (in Romanian), Edittura Academiei Republicii Socialiste Romania, Bucarest.
- Oden, J. T., (1972), "*Finite Element of Nonlinear Continua*" McGraw-Hill, New York.
- Perry, E. B., (1976)"Dispersion Characteristics of Soil From Teton Dam" Isaho, Report to the Independent panel to Review cause of Teton Dam Failure.
- Polubarinova-Kochina P. Ya., and Falikovich, S. V., (1947), "Theory of seepage in porous media," P M M, Vol. XI, No. 6. pp. 153-225.
- Polubarinova-Kochina P. Ya., (1951), "Theory of Filtration of Liquid in Porous Media," Advance in Applied Mechanics, v. Mises and v. Karman (ed.) Academic press,2, pp. 153-225.
- Polubarinova-Kochina P. Ya., (1962), *Theory of Groundwater Movement*, Princeton University press, Princeton, N.J.
- Remson, G. M. Hornberger and Molz, F. J., *Numerical Methods in Subsurface Hydrology*," Wiley-Interscience, New York, 1971.
- Rideal, E., (1958), Introductory lecture, Proc. 10^{th} Symp. Closten Res. Soc., " The Structure and Properties of Porous Materials" (D. H. Everett and F. S. Stone, Eds.), pp. 1-5, Butterworth, London,.
- Richards L. A., (1931), "Capillary conduction of liquid through porous medium", *Physics* 1, pp. 318-333.
- Risenkampf, B. K., (1940), "Hydraulics of Soil Eaters", Part 3. *Uchen. Zap. Saratovskogo gos. Un-ta* XV, No. 5, Gidravlika, pp. 3-93.
- Rumer, R. R., and Drinker, (1966), "Resistance to Laminar Flow through Porous Media", *J. Hydraul. Div. ASCE*, 92, pp. 155-163.
- Scheidegger, A. E., (1960), *The Physics of Flow through Porous Media*, 2^{nd} ed., University of Toronto Press, Toronto.

- Schneebeli, G, (1955), "Expérience sur la limite de validité de la loi de Darcy et l'apparition de turbulence dans un écoulement de filtration, La Houille Blanche, 9, pp. 141-149.

- Scott, R. F., (1963), *Principle of Soil Mechanics*, Addison Wesley publishing Company, INC., U.S.A.

- Shaw, F. S., and Southwell, R. V., (1941), "Relaxation Methods Applied to Engineering Problems; VII Problems Relating to the Percolation of Fluids through Porous Materials, " Proceedings., Royal Society of London, Vol. 178, August, pp. 1-17.

- Sherard, J. L., (1972), *Embankment Dam Cracking*, Embankment-Dam Engineering, John Wiley & Sons, Inc., New York, N. Y., 1972, pp. 271-354.

- Sherard, J. L., (1974), "Study of Piping Failure and Erosion Damage from Rain in Clay Dams in Oklahoma and Mississippi," Soil Conservation Service, Washington, D. C., Mar.

- Sherard, J. L., ., Dunningan, L. P., and Decker, R. S., (1976), " Identification and nature of Dispersive Soils," Journal of Geotechnical Engineering Division, Vol. 102, No. GT4, Apr., pp. 287-301.

- Sherard, J. L., L. P. Dunnigan, (1985), "Filters and Leakage Control in Embankment Dams," "Seepage and Leakage from Dams and Impoundments," Proceedings of a Symposium, Notional Convention, ASCE. Denver, Colorado, pp. 1-30.

- Shields, A., (1963), "Anwendung der Aen lickei kemechanik und der Tur bulentz Porschung auf die Geschiebebewegung," (Berlin, 1936), translated by W. P. Off, and J. C. Uchelen, California Institute of Technology, Pasadena Calif..

- Slattery, J. C., (1972) *Momentum Energy and Mass Transfer in Continua*, McGraw-Hill, New York.

- Slichter, C. S., (1898), "Theoretical Investigation of the Motion of Groundwater," 19th Annual Report. U. S. Geol. Survey, Part 2, , p.329.

- Smith, W. O., (1932), "Capillary flow through an ideal uniform soil", *Physics*, 3, pp. 139-146.

- Solvik, ø., Sevee, R., (1976) "Flow Condition Criteria and Some Throughflow Problems in Rock-fill" Commission Internationale, Des Grandes Barrages, Mexico, Q.45, R.37, pp. 637-646.

- Staliman, R. W., (1956), "Pup. Assoc. Int. Hydrologie (UGGI) 41, pp. 227-243.

- Stark, K. P., (1968), "Some Aspects of the Nonlinear Laminar Regime of Flow in Porous Media," thesis presented to the Univ. College of Townsville, at Townsville, Australia, in Partial fulfillment of the requirements for the degree of Doctor of Philosophy.

- Stokes, G. G., (1851), "On the Effect of the Internal Friction of Fluids on the Motion of Pendulums," *Trans. Cambridge Phil. Soc.*, 9.

- Streeter, V. L., (1978), "*Fluid Mechanics,*" 5th ed. McGraw-Hill, New York.

- Taylor, D. W., (1948), "*Fundamental of Soil Mechanics*", John Wiley and Sons, Inc. New York, N. Y.

- Taylor, R. L., Brown, C. B., "Darcy Flow Solutions with a Free surface," *J. Hydr. Divi.*, ASCE, Vol. 93, No. HY2, Proc. Paper 5126, March 1967, pp. 25-33.

- Taylor, G. S., Luthin, J. N., (1969), "Computer methods of transient analysis of water table aquifer", Water Resources Research, 15, Feb.

- Taylor, C., France, P. W., Parekh, C. J., Peters, J. C., (1917), "Numerical Analysis of Free Surface Seepage Problems," *J. Irrigation and Drainage Divi. ASCE*, Vol. 97, IR1.

- Thom, A., Apelt, C. J., (1961), *"Field Computations in Engineering and Physics,"* D. Van Nostrand Co., Ltd., London.

- Terzaghi, K., (1922), " Der Grundbruch an Staveverken und Seine Verbutung, Die Wasser-Kraft, Vol. 17 ., pp. 445-449.

- Terzaghi, K., (1925), "Erdbaumechanik auf bodenphysikalischer Grundlage, Franz Deuticke, Leipzig-Wein, pp. 399-412.,

- Trescott, C., Pinder, G. F. and Larson, (1976) "Finite difference model for aquifer simulation in two dimensions with results of numerical experiments," U. S. Geol. Survey, Techniques of Water Resources Investigations, Book 7, Automated Data Processing and Computations, 116 pp.

- Uchida, S., (1952) Proceeding First Japanese National Congress Applied Mechanics, National Commite Theor. Appl. Mech, pp. 437-441.

- Volker, R. E., (1969), "Nonlinear Flow In Porous Media by Finite Elements", *J. Hydraul. Divi., ASCE*, Vol. 95, No.HY6, Novemeber.

- Ward, J. C., (1964), "Turbulent flow in porous media", Proc., ASCE, No. HY5, 90, pp. 1-12.

- Wörman, A., and Olafsdotter, R., (1991), " Interfacial Sediment Transport, Paper No. 1, Erosion in a Granular Medium Interface," Ph.D. thesis, Royal Institute of Technology, Stockholm, Sweden, Bulletin No. TRITA-VBI-152.

- Yu, W. S., Lin, H. T. And Lu, C. S., (1991) "Universal Formulation and Comprehensive Correlations for Non-Darcy Natural Convection and Mixed Convection in Porous media". Inernational Journal of Heat Transfer, 34, pp. 2859-2868.

- Yahara, K., (1954), "Problems in Geophysics" Inst. Kyoto University., 9, No. 2, pp.171-176.

- Zienkiewicz, O. C., Mayer, P., and Cheung, Y. K., (1966), " Solution of Anisotropic Seepage Problems by Finite Elements," Journal of the Engineering Mechanics Division, ASCE, Vol. 92, No. EM1, Proc. Paper 4676., Feb., pp. 111-120.

Appendix

Hodograph transformation

A review is given here of some relevant properties also mentioned by Polubarinova-Kochina for the hypergeometric equation

$$z\cdot(1-z)\cdot\frac{d^2Y}{dz^2}+(c-(a+b+1)\cdot z)\cdot\frac{dY}{dz}-a\cdot b\cdot Y=0 \qquad \text{(A-1)}$$

and its solution in the form of hypergeometric series. Equation (A-1) has three regular singularities at the points z = 0, 1, and ∞. There are three kinds of solutions in the form of power series: (i) a solution in a series of powers of z, center z = 0, and valid within a circle of unit radius; (ii) a solution in a series of powers of 1–z, center z = 1, and valid within a circle of unit radius; (iii) a solution in a series of powers of 1/z, center z = 0, and valid outside a circle of unit radius.

The process of finding the complex velocity w (reviewed by Polubarinova-Kochina, 1958) as a function of ζ consists essentially of a conformal mapping of a circular polygon with n apexes onto a semi-plane. Polubarinova-Kochina supposed that the angles at the apexes, which in the ζ–plane become points a, b, and c of the real axis, are respectively $\pi\alpha$, $\pi\beta$, ..., $\pi\gamma$. The angle has been taken at the apex, which becomes the infinitely remote point:

$$(\zeta=\infty),\ \text{be}\ \pi(\delta-\delta');\ \alpha+\beta+\ldots+\delta+\delta'=n-2.$$

Next, it is assumed that U and V are linearly independent solutions of the following equation in the auxiliary plane:

$$\xi\cdot(1-\xi)\cdot\frac{d^2Y}{d\xi^2}+(1-2\cdot\xi)\cdot\frac{dY}{d\xi}-\frac{1}{4}\cdot Y=0 \qquad \text{(A-2)}$$

Polubarinova-Kochina wrote the following functions:

$$F=\frac{A\cdot U+B\cdot V}{\sqrt{(1-\xi)(\xi-a)(\xi-b)}},\qquad \text{and}\qquad Z=\frac{C\cdot U+D\cdot V}{\sqrt{(1-\xi)(\xi-a)(\xi-b)b}} \qquad \text{(A-3)}$$

Then, about the point $\xi = 0$ the solution U is obtained by putting $a = b = 1/2$, $c = 1$ into the solution of equation (A-1), as follows:

$$U=F\left(\frac{1}{2},\frac{1}{2},1,\xi\right)=1+\left(\frac{1}{2}\right)^2\cdot\xi+\left(\frac{1\cdot3}{2\cdot4}\right)^2\cdot\xi^2+\left(\frac{1\cdot3\cdot5}{2\cdot4\cdot6}\right)^2\cdot\xi^3+\ldots\ldots \qquad \text{(A-4)}$$

Polubarinova-Kochina postulated that this solution is different from the complete elliptic integral of the first kind only by a multiplying constant. Thus, we may write one of the particular solutions of equation (A-2) as

$$U = K(\xi) = \int_0^{\frac{\pi}{2}} \frac{1}{\sqrt{(1-\xi \cdot sin^2(\theta))}} d\theta \tag{A-5}$$

where ξ is equated to the square of the modulus k ($k^2 = \xi$).
Since Eq.(A-2) does not change when substituting 1-ξ for ξ, Polubarinova-Kochina sets ξ as a solution of

$$V = K(1-\xi) = K' \quad \text{and} \quad k'^2 = 1-\xi \tag{A-6}$$

which ξ is regular about $\xi = 1$ but has a logarithmic singularity about $\xi = 0$. Thus $U = K(\xi)$ and $V = K(1-\xi)$ are linearly independent solutions about $\xi = 0$.

From the third kind of solution in the form of a power series (iii) Polubarinova-Kochina found that

$$U_1 = \left(\frac{1}{\sqrt{\xi}}\right) \cdot K\left(\frac{1}{\xi}\right) \quad \text{and} \quad V_1 = \left(\frac{1}{\sqrt{\xi}}\right) \cdot K\left(\frac{1}{\xi}\right) \tag{A-7}$$

which are linearly independent solution of (A-2) convergent for $|\xi| > 1$ and by substituting 1-ξ for ξ they obtained

$$U_1 = \left(\frac{1}{\sqrt{1-\xi}}\right) \cdot K\left(\frac{1}{1-\xi}\right), \quad \text{and} \quad V_1 = \left(\frac{1}{\sqrt{1-\xi}}\right) \cdot K\left(\frac{1}{1-\xi}\right) \tag{A-8}$$

which converges outside a circle of unit radius, center $\xi = 1$. Polubarinova-Kochina tried to relate these various functions to the hodograph function,
$w = qx - iqy$, from the hodograph flow region, shown in Figure 3.2b, which is mapped on to the upper-half ξ–plane in Figure 3.2d, by the relationship

$$w = \frac{A \cdot K(\xi) + B \cdot K(1-\xi)}{C \cdot K(\xi) + D \cdot K(1-\xi)}. \tag{A-9}$$

It should be noted that on the segment (0,1), for ξ, we have for $\xi = 0$, $w = k\,i$ (AB = k), for
$\xi = 1$, $w = 0$, and for $\xi = 0.5$, $w = 0.5\,k + (0.5i)k$, thus we can find that:

$$w = \mathrm{k}\frac{K(1-\xi)}{K(\xi) - i \cdot K(1-\xi)}.$$

By using the relationships

$$K(\xi) - i \cdot K(1-\xi) = \left(\frac{1}{\sqrt{\xi}}\right) \cdot K\left(\frac{1}{\xi}\right) = \frac{-i}{\sqrt{(1-\xi)}} \cdot K\left(\frac{1}{1-\xi}\right) \tag{A-10}$$

$$K(1-\xi) = \left(\frac{1}{\sqrt{\xi}}\right) \cdot K\left(\frac{\xi-1}{-\xi}\right) = \frac{1}{\sqrt{(1-\xi)} \cdot \left(K\left(\frac{1}{1-\xi}\right) - i \cdot K\left(\frac{-\xi}{\xi-1}\right)\right)} \tag{A-11}$$

Polubarinova-Kochina rewrote w for the segment $1 < \xi < \infty$, as

$$w = \mathrm{k}\,\frac{K\left(1-\frac{1}{\xi}\right)}{K\left(\frac{1}{\xi}\right)} \tag{A-12a}$$

and for $-\infty < \xi < 0$

$$w = \mathrm{k} \cdot i \cdot \frac{K\left(\frac{1}{1-\xi}\right) - i \cdot K\left(-\frac{\xi}{1-\xi}\right)}{K\left(\frac{1}{1-\xi}\right)} \tag{A-12b}$$

which satisfies the necessary correspondence between the w- and ξ- planes.
Returning to expressions (A-3) for

$$\mathrm{F} = \frac{d\phi}{d\xi} + i \cdot \frac{d\psi}{d\xi} \qquad \text{and} \qquad Z = \frac{dx}{d\xi} + i \cdot \frac{dy}{d\xi}$$

and inserting the appropriate expressions U_1, V_1, etc. from (A-5) to (A-8) for each segment of the real axis of the ξ–plane (Figure 3.2d) and by applying the local boundary condition for the simple dam on the corresponding boundary segment in the physical plane. Thus for $1 < \xi < a$, which corresponds to the inlet face AF in Figure 3.2a, where x = 0 and ϕ is constant, we write, using (A-7),

$$Z = i\frac{dy}{d\xi} = \frac{-A \cdot i \cdot K\left(\frac{1}{\xi}\right)}{\sqrt{(\xi(\xi-1)(\xi-a)(\xi-b))}} \qquad \text{(A-13a)}$$

$$F = i\frac{d\psi}{d\xi} = \frac{-k \cdot A \cdot i \cdot K\left(1-\frac{1}{\xi}\right)}{\sqrt{(\xi(\xi-1)(\xi-a)(\xi-b))}} \qquad \text{(A-13b)}$$

By integrating (A-13a) with respect to ξ over the range $1 < \xi < a$, we obtain

$$H = A \cdot \int_1^a \frac{K\left(\frac{1}{\xi}\right)}{\sqrt{(\xi(\xi-1)(\xi-a)(\xi-b))}} d\xi \qquad \text{(A-14a)}$$

and similarly (A-13b) gives the flow Q_T, where

$$Q_T = K.A \cdot \int_1^a \frac{K\left(1-\frac{1}{\xi}\right)}{\sqrt{(\xi(\xi-1)(\xi-a)(\xi-b))}} d\xi \qquad \text{(A-14b)}$$

By proceeding similarly for the segment $b < \xi < \infty$, which is BC in Figure 3.2a, we find

$$h = A \cdot \int_b^\infty \frac{K\left(\frac{1}{\xi}\right)}{\sqrt{(\xi(\xi-1)(\xi-a)(\xi-b))}} d\xi$$

and for $a < \xi < b$, i.e. the base AB in Figure 3.2.a,

$$l = A \cdot \int_a^b \frac{K\left(\frac{1}{\xi}\right)}{\sqrt{(\xi(\xi-1)(\xi-a)(\xi-b))}} d\xi$$

the length of the seepage surface, CD in Figure 3.2a, follows by considering the segment $-\infty < \xi < 0$, and is

$$h_0 = A \cdot \int_{-\infty}^{0} \frac{K\left(\frac{1}{1-\xi}\right)}{(1-\xi)\sqrt{((a-\xi)(b-\xi))}} d\xi$$

The following changes of variables were introduced by Polubarinova-Kochina (1962):

$$\alpha = \frac{1}{b}, \qquad \beta = \frac{1}{a}, \qquad 0 \le \alpha \le \beta \le 1, \qquad \tau = \frac{1}{\xi}, \qquad C = \frac{2 \cdot a_c}{\sqrt{a \cdot b}}$$

and

$$\tau = \alpha + (\beta - \alpha)\sin^2(\psi), \quad a < \xi < b; \qquad \tau = \beta + (1-\beta)\sin^2(\psi), \quad 1 < \xi < a;$$

$$\tau = \alpha \sin^2(\psi), \quad a < \xi < b$$

The expressions for l, H, and h become:

$$l = C \cdot \int_0^{\frac{\pi}{2}} \frac{K\left[\alpha + (\beta - \alpha) \cdot \sin^2(\psi)\right]}{\sqrt{(1 - \alpha - (\beta - \alpha) \cdot \sin^2(\psi))}} d\psi \qquad \text{(A-15)}$$

$$\mathrm{H} = C \cdot \int_0^{\frac{\pi}{2}} \frac{K\left[\beta + (1 - \beta) \cdot \sin^2(\psi)\right]}{\sqrt{(\beta - \alpha + (1 - \beta) \cdot \sin^2(\psi))}} d\psi \qquad \text{(A-16)}$$

$$\mathrm{h} = C \cdot \alpha^{\frac{1}{2}} \int_0^{\frac{\pi}{2}} \frac{K\left(\alpha \cdot \sin^2(\psi)\right) \sin(\psi)}{\sqrt{(1 - \alpha \cdot \sin^2(\psi))(\beta - \alpha . \sin^2(\psi))}} d\psi \qquad \text{(A-17)}$$

Crank (1984) put the expressions $1/(1-\xi) = \cos^2\psi$, $\alpha_1 = 1-\alpha$, and $\beta_1 = 1-\beta$ in the integral for h_0 and obtained:

$$h_0 = C \cdot \int_0^{\frac{\pi}{2}} \frac{K\left(\alpha \cdot \cos^2(\psi)\right) \sin(\psi) \cos(\psi)}{\sqrt{(1 - \alpha_1 \cdot \sin^2(\psi))(1 - \beta_1 \cdot \sin^2(\psi))}} d\psi \qquad \text{(A-18)}$$

where the height of the separation point above the dam base is h_s = h + h_0. Cryer (1976) pointed to errors in the expressions (A-16) and (A-15) in Polubarinova-Kochina (1962) and his corrections have been included.

To find the equation of the free surface, we consider the segment $0 < \xi < 1$ and observe that:

$$Z = \frac{dx}{d\xi} + i \cdot \frac{dy}{d\xi} = -A \cdot \frac{K(\xi) - i \cdot K(1-\xi)}{\sqrt{(1-\xi) \cdot (a-\xi) \cdot (b-\xi)}} \qquad \text{(A-19a)}$$

$$F = \frac{d\phi}{d\xi} = \frac{-k \cdot A \cdot K(1-\xi)}{\sqrt{(1-\xi) \cdot (a-\xi) \cdot (b-\xi)}} \qquad \text{(A-19b)}$$

By separating real and imaginary parts in (A-19a) and substituting $\xi = sin^2(\psi)$ we obtain:

$$X = l - C \cdot \int_0^{\psi} \frac{K\left(sin^2(\psi)\right) sin(\psi)}{\sqrt{\left(1 - \alpha \cdot sin^2(\psi)\right)\left(1 - \beta \cdot sin^2(\psi)\right)}} d\psi \qquad \text{(A-20a)}$$

$$Y = h + h_0 + C \cdot \int_0^{\psi} \frac{K\left(cos^2(\psi)\right) sin(\psi)}{\sqrt{\left(1 - \alpha \cdot sin^2(\psi)\right)\left(1 - \beta \cdot sin^2(\psi)\right)}} d\psi \qquad \text{(A-20b)}$$

for

$$0 \le \psi \le \frac{\pi}{2}$$

Publications of the Dept. of Hydraulics, Chalmers

A. Doctoral dissertations

1 **Moberg, G.:** Wave Forces on a Vertical Slender Cylinder. 1988. Report A:16

2 **Nilsdal, J-A:** Bedömning av översvämningsrisken i dagvatten-system. Kontrollberäkning med typregn. 1988. Report A:18

3 **Johansson, M.:** Barrier-type Breakwaters. Transmissions, Reflection and Forces. 1989. Report A:19

4 **Perrusquía, G.:** Bedload Transport in Storm Sewers. Stream Traction in Pipe Channels. 1991. Report A:22

5 **Lei, A., X.:** Dynamic Characteristics of Floating Breakwaters. 1996. Report A:26

B. Licentiate essays

1 Johansson, M.: Transient Motions of Large Floating Structures. 1986. Report A:14

2 Mårtensson, N., Bergdahl, : On the Wave Climate of the Southern Baltic. 1987. Report A:15

3 **Perrusquía, G.:** Part-full Flow in Pipes with a Sediment Bed. Part one: Bedform dimensions. Part two: Flow resistance. 1988. Report A:17

4 **Rankka, W.:** Estimating the Time to Fatigue Failure of Mooring Cables. 1989. Report A:20

5 **Olsson, G.:** Hybridelementmetoden, en metod för beräkning av ett flytande föremåls rörelser. 1990. Report A:21

6 **Berggren, Larry:** Energy Take-out from a Wave Energy Device. A Theoretical Study of the Hydro-dynamics of a Two Body Problem Consisting of a Buoy and a Submerged Plate. 1992. Report A:23

7 **Forsberg, Jan:** Strömning i ett styrbart sidoöverfall, 1995. Report A:24

8 **Gustafsson, L-G:** Utveckling och tillämpning av en konceptuell avrinningsmodell för urban hydrologi 1995. Report A:25

9 **Sharif, N.:** Seepage through Earth-fill Dams and Stability Analysis of Downstream Embankment. 1997 Report A:27.

C. Papers to International Scientific Journals

1 **Berggren, L & Johansson, M.:** Hydrodynamic coefficients of a wave energy device consisting of a buoy and a submerged plate. Applied Ocean Research, Vol. 14, No 1, 1992.

2 **Lyngfelt, S.:** Base catchment modelling in urban runoff simulation. Nordic Hydrology, Vol. 22, No. 3, 1992.

3 **Lyngfelt, S.:** An improved rational method in urban runoff application. Nordic Hydrology, Vol. 22, No. 3, 1992.

4 **Sulisz, W. & Johansson, M.:** Second-order wave diffraction of a surface-piercing horizontal cylinder of substantial draught. Applied Ocean Research, Vol. 14, No. 6, 1992.

5 **Björkenstam, U & Lei, X.:** Wave loading on multiple floating bodies. International Shipbuilding Progress, 38, No. 416, pp. 361-391, 1992.
Perrusquía, G.: An experimental study on the transport of sediment in sewer pipes with a permanent deposit. Water Science and Technology, IAWPRC, Vol. 25, No. 8, 1992.

6 **Berggren, L., & Sjöström, B-O.:** Energy from ocean waves: a review. In Power Generation Technology. The International Review of Primary Power Production. (Ed. David A Jones), Sterling Publ. Ltd., 1994

7 **Sulisz, W.:** Stability analysis for multilayered rubble bases. Journal of Waterway, Port, Coastal, and Ocean Engineering, Vol. 120, No. 3, May June 1994.

8 **Perrusquía, G.:** Influence of sewer sediments on flow friction and bed shear stress distribution",, Water Science and Technology, IAWQ, London, England. (In print.)

9 **Perrusquía, G.:** Hydraulic resistance in part-full pipes with a composite

roughness" (Submitted for review and possible publication to Journal of Hydraulic Engineering, ASCE)

10 **Perrusquía, G., & Mark, O.** Predictions of locations with sediment deposits in sewers, Water Sicence and Technology, IAWQ, U.K. (in print) 1995,

11 **Perrusquía, G., & Nalluri, C.** Modelling of sediment trasport ni pipe channels. Journal of Hydrology and Hydromechanics, Czech Republic, (in print) 1995.

12 **Liu, Y., Bergdahl**, L, Frequency domain dynamic analysis of cables. Journal of Engineering Structures, Vol. 19, No. 6, pp 499-506, 1997.

13 **Liu, Y., Bergdahl, L.** Influence of current and seabed friction on mooring cable response: comparison between time-domain and frequency-domain analysis. Accepted for publication in Journal of Engineering Structures, vol. 19, 1997.

D. Papers at international conferences and workshops

1 **Berggren, L. & Bergdahl, L.:** Forces on a wave energy module. The third symposium on ocean wave energy utilisation, Tokyo, Japan, 1991.

2 **Häggström**, S.: Project oriented and "traditional" education at the School of Civil Engineering at Chalmers University of Technology. Presented at Transfer of Technologies 2000, Prague, Czechoslovakia, Sept. 1991.

3 **Perrusquía, G.:** Bedload transport in storm sewers. First International Workshop on Sewer Sediments, Brussels, Belgium, 4-6 Sept. 1991.

4 **Perrusquía, G.:** Sediment transport in sewer pipes in stream traction. Study Day on Sediment Transport, Katholieke Universiteit, Leuven, Belgium, 3 March, 1992.

5 **Perrusquía, G.:** Physical modelling of sand transport in sewers. International Workshop on Environmental Hydraulics and Sediment Transport. Aalborg University, Denmark, 10 April, 1992.

6 **Lei, X. & Bergdahl, L.:** Hydrodynamic properties of multiple floating and submerged bodies analysed by a panel method. Boundary Elements in Fluid Dynamics; Southampton, U.K., 29-30 April, 1992.

7 **Bergdahl, L.:** Review of research in Sweden. In Energy. Wave Energy R & D. Proceedings of a workshop held at Cork, 1 and 2 October 1992. (Eds. G. Caratti, A T Lewis, D. Howett).(CEC DGXII.E.3)

8 **Sulisz, W.:** Numerical modelling of the stability of rubble bases. Proceedings, 23rd Coastal Engineering Conference, ASCE, New York, pp 1798-1803, 1992.

9 **Häggström, S. & Johansson, G.:** Recent changes in civil engineering education at Chalmers University of Technology. Proceedings of the Conference: Innovation and Change in Civil Engineering Education, Belfast, Northern Ireland, 19-21 April, 1993.

10 **Lei, X., & Bergdahl. L.:** Dynamic response of linked, moored, floating structures. The Eighth International Workshop on Water Waves and Floating Bodies. St. John's, Newfoundland, 23-26 May 1993.

11 **Perrusquía, G.:** "Sediment transport in storm sewers with a permanent deposit", Proceedings, Sixth International Conference on Urban Storm Drainage, Niagara Falls, Canada, 12-17 September 1993.

12 **Sjöström, B-O:** Technocean AB. The past, present and future of hose-pump wave energy converter. Proceedings. 1993 European Wave Energy Symposium. Edinburgh, Scotland, 21-24 July 1993.

13 **Perrusquía, G.:** "Influence of sewer sediments on flow friction and bed shear distribution", specialized International Conference "The Sewer as a Physical, Chemical and Biological Reactor", Aalborg, Denmark, 15-18 May 1994.

14 **Gustafsson, L-G.** Using a 3-D distributed physically based model in urban hydrology. Submitted to WEFTEC'95, 68th Annual Conference & Exposition, Miami Beach, USA, October 21-25. 1995.

15 **Perrusquía, G. & Nalluri, C.** Modelling of bedload transport in pipe channels, Proceedings, 8th International Conference on Transport and Sedimentation of

Solids, Prague, Czech Republic, Jan. 1995.

16 **Bergdahl, L., & Mårtensson, N.** Certification of wave-energy plants - Discussion of existing guidelines, expecially for mooring design, Second European Wave Power Conference, 8-10 Nov., 1995, Lisbon, Portugal.

17 **Nielsen, K., Holmes, B., & Berggren, L.** On the tank testing of off-shore wave power converters. Second European Wave Power Conference, 8-10 Nov., 1995. Lisbon, Portugal.

18 **Berggren, L., & Bergdahl, L.** Time-domain simulation of a single wave-energy converter. Second European Wave Power Conference, 8-10 Nov., 1995, Lisbon, Portugal.

19 **Liu, Y., & Bergdahl, L.** Study of Current and Seabed Friction Effect on Mooring Cable Response. First Asia-Pacific Conference on Offshore Systems: Mobile & Floating Structures, 10-11 Dec. 1996. Kuala Lumpur, Malaysia.

E. Other reports from the Department of Hydraulics

Report Series B

B:53 **Lyngfelt, S.**: Simulering av ytavrinning i dagvattensystem. 1991.

B:54 **Lyngfelt, S.** Two papers on Urban Runoff Modelling. Base catchment modelling in urban runoff simulation and An improved rational method for urban runoff application. 1991.

B:55 **Perrusquía, G.**: Sediment transport in pipe channels. Postdoctoral experimental studies. December 1991 - April 1992.

B:56 Nordisk möte om bölgeenergi, Hanstholm, 8-9 maj, 1992.

B:57 **Perrusquía, G.:** "An experimental study from flume to stream traction in pipe channels", 1993.

B:58 Activity Report 1992

B:59 Activity Report 1994

B:60 **Asztély, M.**; Literature review of energy losses in manholes. 1995.

B:61 **Lindvall, G.**: Energy losses at manholes. Lab. measurements at non-stationary flow. 1996.

B:62 **Bergdahl, L** MODEX User's Manual. Version 3. 1996

Report Series C

C:35 **Johansson, M.**: RECT - A radiation diffraction program for the analysis of floating breakwaters with rectangular cross-section. G-Göteborg, 1991.

C:36 **Johansson, M.**: SHELF - A diffraction program for the analysis of a barrier-type breakwater with rectangular cross-section and a protruding shelf facing the incident waves. Göteborg, 1991.

C:37 **Johansson, M.**: HYB2D - A radiation diffraction program for the analysis of floating breakwaters. Göteborg, 1991.

C:38 **Perrusquía, G.**: Sediment in sewers - 1. Flow capacity of sewers with a sediment bed. 2. Flow resistance in storm sewers. Göteborg, 1991.

C:39 **Lyngfelt, S.**: BASIC-program för beräkning av geometriska parametrar i ledningstvärsnittet med och utan sediment. Göteborg, 1991.

Other Reports:

Rylander, A., & Sjöström, B-O.: Bestämning av motståndskoefficienterna c_d och medsväng-ande vattenmassa för dämpskivor till slangpumpkraftverk (modellförsök i dyktanken UT/CTH), Technocean, Rapport nr 9102.

Claesson, L. & Sjöström, B-O.: Optimal wave power plant spacing in the tropical North Pacific Ocean. Oceans' 91. Hawaii, USA. Technocean, Rapporter, 9106.

Forsberg, J. & Sjöström, B-O: Överföring av slangpumpens ekvationer till frekvensplanet. Technocean, Rapport 9105.

Sjöström, B.O.: Vågenergiforskningen i världen 1990-1991. En lägesraport. Technocean, Rapport 9105.

Lindvall, G.: Energiförluster i ledningsbrunnar. Laboratoriemätningar vid icke-stationär strömning. Geohydrologiska forskningsgruppen, Meddelande nr 94, 1993.

Bergdahl, L. Dynamics of mooring cables, Svensk sjöfartstidning, nr. 40, 7 okt., 1994 (STU8901511)

International User-Group Meeting on Computer Aided Analysis and Operation in Sewage Transport and Treatment Technology (IUGM),. Proceedings. Geohydrological Research Group. Chalmers University of Technology, Göteborg 13-15 June, 1994.

Uppsatser från ledningstekniska forsknings-gruppen, Chalmers tekniska högskola 1995. Geohydrologiska forskningsgruppen, Chalmers tekniska högskola, Meddelande nr 96, Göteborg, 1995.

Diploma Theses (Master of Science Programme)

1991:1 Granstedt, P.: Framtida reparations- och ombyggnadsbehov av våra damm- och kraftanläggningar.
1991:2 Lundén, M.: working conditions of the CONE-SEAL. Experimental investigations.
1991:3 Hellström, I.: Effekter i Göteborgs centrum av en vattenståndshöjning i havet.
1991:4 Appelgren, C., Kullman, M.: Den hydrologiska modellen NAM. Sensivitetsanalys av modellparametrar.
1991:5 Jansson, E.; Sicard, T.: Recharge of groundwater from percolation ponds in South India. Study based on the modelling approach.
1991:6 Lundberg, M., Ekstedt, C.:Kvävefälla i Veselången - teknisk utformning.
1991:7 Herrera, F.: Grafisk presentation av utdata av datorprogrammet MODEX.
1992:1 Andersson, J., Wahlström, R.: A study of water supply at Nkinga Hospital and three villages in Igunga District, Tanzania.
1992:2 Högberg, R.: Att använda randelementprogrammet WAMIT för analys av vågskydd till småbåtshamnar.
1992:3 Nylander, L.: Datorprogram som hjälpmedel vid hamnprojektering.
1992:4 Gustafsson, A-M.: Den hydrologiska modellen NAM. Kalibrerings-periodens inverkan på modellparametrar och verifieringsresultat.
1993:1 Hafsteinn Halldórsson, B.: Natural convection, numerical approach.
1993:2 Bähr, T.:Vågdämpnings-förmåga hos flytande rektangulära vågbrytare.
1994:1 Adamsson, Å, Eriksson K.: Optimisation of the energy take-out from a floating wave energy device, the Mighty Whale. - An experimental study.
1994:2 Bågenholm, C.: Refined spillway design - Flood routing.
1995:1 Eriksson P.: Rörelser hos Safe Gothia.
1995:2 Bryngelsson, A., & Tenstam, A.: Numeriska beräkningar av hydrodynamiska koefficienter för en tvådimensionell platta utsatt för harmoniskt oscillerande tvärströmning.

1995:3 Halldin, A., Arfvidsson, M. Experimental and theoretical study of a wave-energy device.
1995:4 Karlsson, R.I., Nilsson, M.G.: Local scour in front of coastal structures.
1995:5 Tagliaretti, L. (ej godkänt som svenskt exjobb) Wave diffraction in harbours. Validation of a simulation model.
1995:6 Berg, J., Holmqvist, C.: Hydrodynamiska laster på flexibla konstruktioner. En jämförelse av snittkrafter i en fiskodlingsanläggning för tre olika beräkningsmetoder.
1996:1 Malo, M., Styrenius, O.: Studies of the Hydrodynamic Properties in a Stirred Benthic Chamber. I: Development of low pressure sensors.
1996:2 Ekström, P.: Tryckslag i tappvattensystem.
1996:3 Ljungberg, F., Nilsson, J.: The Mighty Whale Airchamber. Experimental and Numerical Study.
1996:4 Johansson, A., Sundberg, F. Three aspects of modern sewer design.
1997:1 Andrén, J. Simulering av tillrinning till reglerade sjömagasin med NAM-modellen.

Diploma Theses (Applied Civil Engineering Programme)

1991:1 Abrahamsson, S.: Analys av vattenledningsnätet i stadsdelen Backa, Göteborg.
1991:2 Grann, M.: Analys av vattenledningsnätet i högzonen kring stadsdelen Slottskogen, Göteborg.
1993:1 Björklund, A.: Flödet och vattenkvalitetens beroende av råvattnets fördelning på produktionslinjer vid Alelyckans vattenverk, Göteborg.
1993:2 Backlund, M.: Undersökning av effektiviteten av luftreningssystemet för Ryaverkets biologiska steg.
1993:3 Johannisson, P.: Datoranalys av problem med flödeskapacitet i avloppsnätet i området Krokängsparken, Göteborg.
1994:1 Schele, K.F.: Flotationsförsök i en pilotanläggning vid Lackarebäcks vattenverk.
1994:2 Bergström, M.:
Renovering av läckande avloppssystem - undersökning av ett problemområde i Långedrag.
1995:1 Enebrand, P., & Pohorela, B.:
Undersökning av flockningskammare vid Göteborgs vattenverk
Claesson, A-S., & Rosenqvist, S.:
Björkdalen . då avfallsdeponi, idag rekreationsområde.
Astgård, J., & Lundqvist, J.:
Datoranalys av Sannegårdens avloppsvattennät med programmet MOUSE.

Current Textbooks

Häggström, S. Hydraulik för V-teknologer. Undervisningsskrift 1988:8, Andra upplagan, 1992

Häggström, S. Uppgifter till Hydraulik för V-teknologer. Undervisningsskrift 1990:5, Tredje upplagan. 1992.

Lyngfelt, S. Kompendium och kursmaterial för kursen Vattenförsörjnings- och avloppsteknik. Undervisnings-skrift 1992:3

Lyngfelt, S. Hydrologi och miljöteknik. 1992.